universität wien

DIPLOMARBEIT / DIPLOMA THESIS

Titel der Diplomarbeit / Title of the Diploma Thesis

„Immunohistochemical evaluation of CD47 surface protein in a xenograft triple-negative breast cancer (TNBC) mouse model“

verfasst von / submitted by

Julia Pichler

angestrebter akademischer Grad / in partial fulfilment of the requirements for the degree of

Magistra der Pharmazie (Mag.pharm.)

Wien, 2019 / Vienna, 2019

Studienkennzahl lt. Studienblatt / degree programme code as it appears on the student record sheet:	A 449
Studienrichtung lt. Studienblatt / degree programme as it appears on the student record sheet:	Diplomstudium Pharmazie
Betreut von / Supervisor:	Univ. Prof. Dipl. Ing. Dr. Manfred Ogris
Mitbetreut von / Co-Supervisor:	Dr. Haider Sami

Danksagung

An dieser Stelle möchte ich die Gelegenheit nutzen und mich bei all jenen bedanken, die zum Entstehen dieser Arbeit beigetragen und mich während des gesamten Studiums unterstützt haben.

Zuerst gilt mein Dank Univ. Prof. Dipl. Ing. Dr. Manfred Ogris für die Bereitstellung dieser Diplomarbeitsstelle im Labor für „Macromolecular Cancer Therapeutics“ am Department für Pharmazeutische Chemie und für die Möglichkeit, im Bereich der Krebsforschung sehr viel Neues zu lernen.

Ganz besonders möchte ich mich auch bei MSc. Magdalena Billerhart bedanken, die meine Arbeit betreut und begutachtet hat und mir immer viel Geduld und Hilfsbereitschaft entgegengebracht hat. Bei Fragen oder Schwierigkeiten ist sie stets die richtige Ansprechperson gewesen und das nicht nur auf der Uni, sondern manchmal auch in ihrer Freizeit.

Ein herzliches Dankeschön gilt auch Dr. Haider Sami für seine Unterstützung und sein offenes Ohr für jedes Anliegen.

Ebenfalls danke ich allen Laborkollegen/Innen des Departments für ihre stetige Hilfsbereitschaft, Motivation und gute Gruppengemeinschaft. Es war mir eine Freude, ein Semester meines Studiums am MMCT zu verbringen. Ich bin außerdem sehr glücklich darüber, viele neue Freunde gewonnen und sehr viel für meine berufliche Zukunft gelernt zu haben.

Ich danke auch all meinen Freunden/Innen und Studienkollegen/Innen, ohne die mir das Studium sicherlich viel schwerer gefallen wäre.

Abschließend möchte ich meiner Familie ganz besonders danken, die mir mein Studium durch ihre finanzielle und persönliche Unterstützung ermöglicht hat.

Table of contents

1. Abbreviations

AB	Antibody
ABC	Avidin-Biotin-complex
ADCC	Antibody-dependent cell-mediated cytotoxicity
BLI	Bioluminescence imaging
BMDMs	Bone marrow-derived macrophages
BSA	Bovine serum albumin
CDC	Complement-dependent cytotoxicity
CD47	Cluster of differentiation 47
DAB	Diaminobenzidine
ECM	Extracellular matrix
ER	Estrogen receptor
EtOH	Ethanol
FFPE	Formalin fixed - paraffin embedded
H&E	Hematoxylin & Eosin
HER 2	Human epidermal growth factor receptor 2
HIER	Heat induced epitope retrieval
HRP	Horse radish peroxidase
IAP	Integrin associated protein
IHC	Immunohistochemistry
LN	Lymph node
Luc	Luciferase

mAB	Monoclonal antibody
ME	Mesentery
MMS-domain	Multiple membrane-spanning domain
NK cells	Natural killer cells
pAB	Primary antibody
PBS	Phosphate Buffered Saline
PE	Peritoneum
PR	Progesterone receptor
RT	Room temperature
RTU	Ready to use
sAB	Secondary antibody
SCID	Severe combined immunodeficiency
SHP1 /SHP2	Src homology 2 domain tyrosine phosphatase 1 and 2
SIN vector	Self-inactivating vector
SIRPα	Signal regulatory protein alpha
TAMs	Tumor-associated macrophages
TEM	Transmission electron microscopy
TNBC	Triple-negative breast cancer
TSP1	Thrombospondin 1
TU LE	Tumor left
TU RI	Tumor right
WEK	Demineralized water

2. Aim of the thesis

The main aim of this thesis was to develop an optimal staining protocol for i) the immunohistochemical (IHC) detection of CD47 surface protein in a human xenograft tumor model and ii) to optimize the IHC staining procedure to detect the reporter enzyme luciferase in tumor tissue derived from luciferase transduced tumor cells. In the third aim of this work these protocols were applied to analyze the expression of CD47, luciferase and transgenic human IgG-Fc in tumor tissue after an immunogene therapy approach. Within this therapy, tumors cells were transfected ex vivo and in vivo using a plasmid encoding for a CD47- binding SIRPα-Fc fusion protein. Here, the potential blockade of CD47 and the expression of the Fc-part of the fusion protein in the tumor tissue were analyzed. This should verify by means of IHC if the fusion protein was bound to CD47 at different time points of the therapy.

3. Abstract

The CD47 glycoprotein, overexpressed on the cell surface of tumor cells, is a very important target in cancer immunotherapy. Several tumor cells overexpress this protein to evade the immune system sending out a “don’t eat me signal” to the macrophages by the interaction of CD47 with SIRPα, a membrane glycoprotein expressed on macrophages. Accordingly, the blocking of CD47, e.g. with a SIRPα analogue/variant, is a vital option in the development of anti-cancer drugs to enhance tumor eradication by phagocytosis.

This work focused on the histological evaluation of human triple-negative breast cancer (TNBC) xenografts implanted in immune compromised SCID mice. The effect of SIRPα-Fc fusion protein expression of ex vivo or in vivo transduced tumors on tumor morphology and CD47 receptor accessibility was studied by means of histological methods. First, a staining protocol for immunohistochemical detection of CD47 surface protein was developed. Secondly, tumor cells genetically marked with firefly luciferase were identified by immunohistochemistry using anti-luciferase antibodies. The third aim was the immunohistochemical evaluation of tumors expressing the SIRPα-Fc fusion protein through the detection of the Fc-part in the tumor tissue.

The results demonstrated that CD47 is overexpressed on the TNBC breast cancer cell line MDA-MB-231 LM2-4. Furthermore, a partial blockade of CD47 was observed in a tissue sample 24 hours after the intratumoral treatment with a plasmid encoding for SIRPα-Fc.

4. Zusammenfassung

CD47 ist ein Glykoprotein, das von vielen Tumorentitäten als Transmembranprotein an der Zelloberfläche überexprimiert wird. Damit ist es möglich, der Eliminierung durch das Immunsystem zu entgehen, indem ein sog. “Friss mich nicht” - Signal an Makrophagen ausgesendet wird. Dies erfolgt nachdem CD47 an das Membran-Glykoprotein SIRPα, welches an der Oberfläche der Makrophagen exprimiert ist, gebunden hat. Dementsprechend ist die Blockade von CD47 mit einer SIRPα-Variante ein potenziell vielversprechender Ansatz in der Krebsforschung, um das Tumorwachstum durch die dann verstärkte Phagozytose zu stoppen oder Tumore sogar zu eliminieren.

Diese Diplomarbeit fokussierte sich auf die histologische Auswertung von drei in vivo Experimenten, die an SCID Mäusen durchgeführt wurden, um die Wirkung des Fusionsproteins SIRPα-Fc an einem Xenograft triple-negative breast cancer (TNBC) Mausmodell zu testen. Eine zentrale Aufgabe dieser Diplomarbeit war der immunhistochemische Nachweis von CD47. Dabei wurde das Färbeprotokoll für FFPE (formalin fixed paraffin embedded) Gewebe optimiert. Ein weiteres Ziel der Arbeit war der immunhistochemische Nachweis von Luciferase, ein Reportergen und Enzym, welches ebenfalls vom Tumor exprimiert wird, da die Krebszelllinie in vitro mit dem Luc-Gen transduziert wurde. Der abschließende Teil befasste sich mit dem Nachweis des Fc-Teils des Fusionsproteins, um feststellen zu können, ob SIRPα-Fc zu bestimmten Zeiten nach Therapiebeginn tatsächlich im Gewebe aufzufinden ist, indem es an CD47 gebunden hat und dieses blockiert.

Die Ergebnisse zeigten, dass CD47 von der getesteten humanen TNBC Brustkrebszelllinie MDA-MB-231 LM2-4 überexprimiert wird. Ebenso konnte das Luciferase Protein erfolgreich in den Luc-transduzierten Tumorzellen immunhistochemisch nachgewiesen werden. Weiterhin konnte histologisch gezeigt werden, dass das Fusionsprotein 24 Stunden nach einer intratumoralen Behandlung mit einem Plasmid, das für SIRPα-Fc kodiert, noch teilweise an CD47 gebunden war und das Protein somit blockiert war.

5. Introduction

5.1. CD47 surface protein

Cluster of differentiation 47 (CD47) is a ~50 kDa glycosylated transmembrane protein of the immunoglobulin family (Liu et al. 2017) ubiquitously expressed on the cell surface acting as a checkpoint for the innate and adaptive immune system (Kauder et al. 2018). CD47 is also called integrin-associated protein (IAP), because originally it was known as a plasma membrane molecule interacting with integrin αvβ3 (Brown 1990; Lindberg et al. 1994; Brown 2001). Lindberg et al. could demonstrate with the first anti-CD47 antibody that CD47 and IAP are the same protein. Is has been clarified that it also interacts with other integrins and has different functions, such as cell adhesion and migration, and it also has its own extracellular ligands. (Lindberg et al. 1994; Brown 2001).

5.1.1. Structure

CD47 consists of a heavily glycosylated extracellular domain (IgV), which forms the N-terminus and 5 highly hydrophobic transmembrane segments (multiple membrane-spanning domain (MMS-domain)) which a cytoplasmatic tail (Fig. 1). Due to four alternative splice options, four different isoforms of the protein can be distinguished. The length of the cytoplasmatic C-terminus ranges from 3-36 amino acids (Lindberg 1993; Brown 2001). Human, rat, bovine and mouse CD47 have been cloned and the results showed that 70 % of the amino acids are identical (Brown 2001).

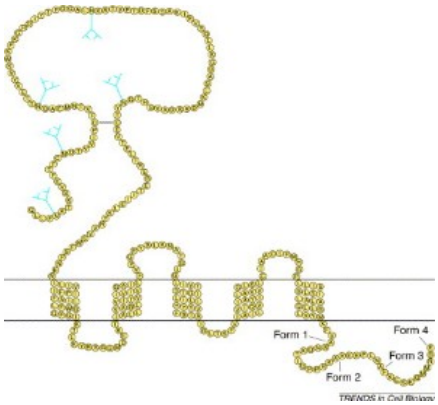

Figure 1 *Structure of the CD47 protein (Brown 2001)*

5.1.2. CD47-SIRPα interaction in cancer therapy

Many solid and hematologic cancers try to 'trick' the immune system with the overexpression of CD47 to evade immunological eradication (Liu et al. 2017). CD47 protein prevents immunoclearance by binding to its ligand Signal Regulatory Protein alpha (SIRPα), which is expressed also on immune cells such as dendritic cells and macrophages (Oldenborg 2000). The CD47-SIRPα-interaction triggers a "don't eat me" signal to phagocytic cells *via* initiating a signaling cascade in the cytoplasm of macrophages (Brown 2001). The docking of CD47 to SIRPα causes phosphorylation of the cytoplasmatic tyrosine-based inhibition motifs receptor of SIRPα and the recruitment of Src homology 2 domain containing tyrosine phosphatases SHP-1 and SHP-2 (Oldenborg 2000; Willingham et al. 2012).

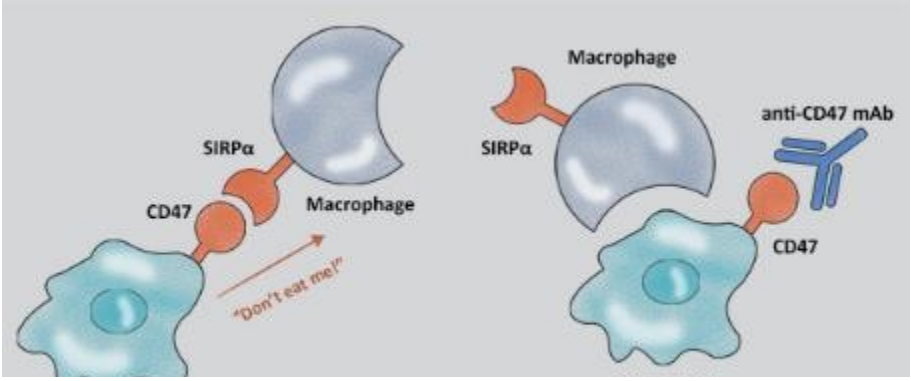

Figure 2 *Representation of the emitted "don't eat me" signal via interaction of CD47 protein on cancer cells and SIRPα expressed on the surface of macrophages. On the right side a monoclonal anti-CD47 antibody blocks CD47 and enables tumour elimination by phagocytosis. (ACROBiosystems 2017)*

Besides binding to its ligand SIRPα, CD47 is a receptor for thrombospondin (e.g. TSP1) and, as mentioned above, a component of a supramolecular plasma membrane complex containing specific integrins (αvβ3), cholesterol or heterotrimeric G proteins. It is known that CD47 modulates a wide range of cell activities including cell motility and adhesion, platelet activation and leukocyte migration as well as phagocytosis (Brown 2001). Furthermore, CD47 plays a role as a "marker of self" in the host cells of the organism as well. It is ubiquitously expressed on many cells in our organism such as red blood cells and protects them from clearance from the bloodstream by macrophages (Oldenborg 2000).

Similar effect is observed with hematopoietic stem cells: during inflammation-mediated mobilization, the upregulation of CD47 protects normal hematopoietic stem cells (Jaiswal et al. 2009).

Analysis of tumor tissue and adjacent normal tissue displayed the overexpression of CD47 on cancer cells. The levels of CD47 mRNA expression correlates with lower chance of survival for various cancer types (Willingham et al. 2012).

The CD47-SIRPα interaction has been discovered as a new target for cancer treatment *via* immunotherapy and its disruption has promised great therapeutic effects. Indeed, many antibodies have been developed against CD47 to decrease the size of primary tumors and metastases in various pre-clinical tests (Liu et al. 2017). Monoclonal antibodies against this protein enabled phagocytosis of solid cancer cells in vitro and inhibited tumor growth and metastasis in xenotransplantation models of human tumors in immunodeficient mice concomitant with increased survival time. The therapy was evaluated on larger and on smaller tumors. On larger tumors, growth was inhibited and metastasis prevented; on smaller tumors the therapy was even curative (Willingham et al. 2012).

The problem is that not every patient responds to this therapy and various side effects occur, e.g. autoimmune reactions against host cells or tissue. As CD47 is expressed on erythrocytes, anemia is a considerable side effect. The challenge is now to make the therapy specific to the tumor. Various combinations of different immune-based therapies or immune therapy combined with chemotherapy or radiotherapy may have synergistic effects in anticancer treatment (Krebsinformationsdienst 2018). A blockade of both CD47 on tumor cells and a SIRPα knockdown may have a synergistic effect in cancer therapy combined with immune checkpoint inhibitors which target the adaptive immune response. Moreover it has been shown that the blockade of CD47 increases the stimulation of tumor-specific cytotoxic T-cells (Murata et al. 2018).

CD47 does not only play a significant role in cancer treatment, but also in other diseases such as cardiovascular dysfunctions. Studies have shown that thrombospondin 1 (TSP1) is upregulated in cardiovascular diseases including cardiac infarction, peripheral arterial disease, pulmonary hypertension or stroke. Due to its interaction with CD47, TSP1 inhibits NO, cAMP, cGMP and VEGF signaling to promote thrombosis, limit blood flow and decreases cellular and further tissue survival. Blocking this interaction can reach success in the therapy of cardiovascular diseases (Rogers et al. 2014).

Research data showed that CD47 and SIRPα may be also involved in bone resorption, which means that a treatment based on these two proteins may prevent osteoporosis. However, this signaling system in the bone tissue seems to be more complex and further research is needed (Maile et al. 2011; Oldenborg 2013). Of note, scientists at the University of Stanford were able to cure lung fibrosis in mice by using an anti-CD47 antibody, since they found out that fibrotic diseases are associated with a signaling pathway including the CD47 protein (Stanford Medicine News center 2017).

5.2. Tumor microenvironment

The major components of the tumor microenvironment are fibroblasts, leukocytes, vascular endothelial cells and immune cells including macrophages. Immune cells surrounding the cancer tissue can influence tumor initiation, - growth and metastasis (Teng et al. 2016; Yang und Zhang 2017). Within tumor tissue, two different types of macrophages, M1 and M2, can be distinguished. The M1-polarized macrophages are activated by cytokines (e.g. interferon-γ), produce immunostimulatory and proinflammatory cytokines (IL-12, IL-23) and play an important role in T helper cell responses and in protection against bacteria. M2-macrophages are activated by cytokines such as IL-4, IL-10 or IL-13 which belong to the group of Th2-cytokines and are causally related to tissue repair. Tumor associated macrophages (TAMs), which are typically M2-activated, are “protumoral macrophages” and promote metastasis, invasion and proliferation of cancer cells and are capable to inhibit antitumor immune responses caused by T cells. Furthermore, they stimulate angiogenesis and tumor progression (Grivennikov et al. 2010; Yang und Zhang 2017). Lin et al. demonstrated that SIRPα plays a role in macrophage polarization. Overexpression of SIRPα in bone marrow-derived macrophages (BMDMs) enhanced M2 polarization, which might be related to the interaction of SIRPα and CD47 and the intracellular SHP1 signaling pathway. In contrast, a knockdown of SIRPα promoted M1 polarization (Lin et al. 2018).

5.3. Triple-negative breast cancer

Breast cancer is the most frequently diagnosed cancer in women and has the second highest incidence of all cancer types overall. In 2018, more than 2 million new cases were registered worldwide (Bray et al. 2018; World Cancer Research Fund International 2018). Major risks are being female, the age, genetic factors, high breast

tissue density and medical procedures such as high-dose radiation or biopsy confirmed hyperplasia. Further it was observed that a long menstrual history, use of oral contraceptives, overweight, daily consumption of alcohol, never having children or having the first child after age 30 are some potential factors that increase the risk for breast cancer. Persistent physical activity, a healthy body weight and breast feeding are associated with a lower risk (Vilma Cokkinides 2007).
It is known that breast cancer can be divided into distinct subtypes. Most of the breast cancer cells have the expression of the estrogen receptor (ER), progesterone receptor (PR) and the amplification of human epidermal growth factor receptor 2 (HER-2) such as the healthy cells of the breast. About 20-30 % of breast cancers have a higher expression of the HER-2 receptor, which leads to a stimulation of their growth, because this receptor receives signals that enhances its growth. Then there are cancer cells (about 10-20 %) which do not express ER, PR and do not have the HER-2 amplification (Breastcancer.org 2018). This group is called as triple-negative breast cancer (TNBC) and belongs to the basal subtype (Holliday und Speirs 2011). TNBC is more frequently diagnosed in younger, premenopausal women.

Patients with TNBC have a poor prognosis compared to the other subtypes, because they do not respond to a hormone therapy or a medication that targets the HER-2 receptor, but initially often respond well to chemotherapy, although most patients relapse. It is now of big interest to find new and better therapies than hormone-, chemo- or radiation therapy. In addition, TNBC is also more aggressive than the other subtypes leading to metastases mainly in lung and bone (Breastcancer.org 2018).

The tissues histologically processed in this thesis derived from 3 in vivo experiments performed by Magdalena Billerhart at the MMCT lab. Magdalena Billerhart used human breast cancer cells for her experiments (MDA-MB-231 LM2-4 EGFP Luc) and injected them into SCID mice. MDA-MB-231 is a human triple negative breast cancer cell line that belongs to the claudin-low subtype of breast cancer and shows all the characteristics from the basal type (triple negative). LM 2-4 is the metastatic variant of the human TNBC cell line which originates from a metastasis found in a breast cancer patient. The cell line MDA-MB-231 LM2-4 is regarded as high invasive in vitro and through rounds of selections it also shows metastasis in vivo (Kang et al. 2003; Holliday und Speirs 2011).

5.4. Marking tumor cells with reporter genes

To monitor tumor growth and to unambiguously identify tumor cells in transplantable tumor models, tumor cells can be stably marked with reporter genes prior to implantation. Luciferases, for examples, are enzymes which catalyze the emission of visible light during the conversion of the substrate to its product. In this thesis, MDA-MB-231 LM2-4 cells were stably marked with a fusion protein of firefly luciferase and EGFP using a self-inactivating lentiviral vector (SIN) (Su et al. 2013). The expression of firefly luciferase can be analyzed by several means, e.g. performing a luciferase reporter assay, during in vivo imaging or using Immunohistochemistry (IHC).

5.5. Human xenograft TNBC mouse model

In the three histological evaluated in vivo experiments of this thesis, a human xenograft tumor model in immunodeficient mice was consulted. This model is used to investigate invasion and metastasis of the tumor as well as to verify the response to the therapy. In this most widely used model, human cancer cells are transplanted, either into the organ type from the originated tumor or under the skin of immunodeficient mice which do not reject the foreign cells, for example athymic nude mice or severely compromised immunodeficient (SCID) mice (Morton und Houghton 2007; Richmond und Su 2008). The in vivo experiments were performed on SCID mice. Macrophages and natural killer (NK) cells in SCID mice show normal or even enhanced activity, in contrast to T and B lymphocytes which are totally missing (Tournoy et al. 2000). The advantage of this model is a rapid analysis of the response to a therapeutic treatment and it can predict the response to this drug in a human cancer patient. On the other hand, it has the big disadvantage that the tumor microenvironment is not realistic in immunocompromised mice. Depending on the number of the injected cells or the size of the transplanted tumor, the tumor in general will develop over 1-8 weeks, or in some cases longer (1-4 months) and the response to the tested therapy can be studied in vivo. (Richmond und Su 2008).

5.6. Cancer immunogene therapy

Gene therapy is a possibility to treat or prevent diseases by altering the genetic instructions (Dana-Farber Cancer Institute 2018). To transfer genetic material into a cell, viral and non-viral vectors can be used. Manipulation of the tumor microenvironment for better recognition by the immune cells or immunomodulation of

the cancer cells or the immune system of the host organism are also included in the field of gene therapy. Cancer therapy based on gene delivery has the big advantage of providing individual therapeutic effects by considering the host immune status, genomic constituents and individual tumor specifics (Amer 2014). Due to long-term effects, low influence on physiological processes in the organism and relatively low side effects in comparison to a systemically antibody therapy, gene therapy is already established in the modern cancer treatment and will certainly get more attention in the future (Deutsches Ärzteblatt).

5.6.1. SIRPα-Fc gene therapy

The aim of the in vivo experiments was to test the therapeutic effect of cancer immunogene therapy on a human breast cancer cell line using the fusion protein SIRPα-Fc (IL2-P-Fc, P encodes for SIRPα) encoded on a therapeutic vector and expressed into intercellular space blocking CD47 on MDA-MB-231 LM2-4 cancer cells. The IL2- sequence is necessary for the secretion of the SIRPα protein to the outside of the cell. The Fc-region is a human IgG1 enabling to activate both the antibody-dependent cell-mediated cytotoxicity (ADCC) and complement-dependent cytotoxicity (CDC) due to a single point mutation. In between of these sequences a high affinity SIRPα variant was inserted (Fig.3) (Richards et al. 2008; Aminah Kassem 2017).

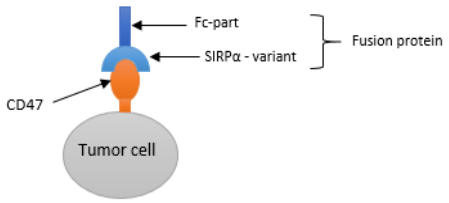

Figure 3 *Schematic illustration of fusion protein and its target receptor CD47 on cancer cells*

In the first animal experiment, the in vitro transfected human breast cancer cells were orthotopically implanted into the 4th pair of inguinal nipples 48 hours after the transfection. In this experiment three groups (IL2-P-Fc, bb-mCherry and untransfected) of 3 mice each (bearing 2 tumor sides each, n=6) were included. Tumor growth was followed *via* 2D bioluminescence imaging (BLI) after a subcutaneous injection of K-Luciferin (30 mg/kg) on an IVIS Spectrum-CT imaging system (PerkinElmer).

The IL2-P-Fc group bearing cancer cells were transfected with the IL2-P-Fc vector: pCpG-hCMV-SCEP-IL2-P-Fc. The bb-mCherry group was used as transfection control, transfected with the pCpG-hCMV-SCEP-mCherry plasmid in vitro. This plasmid encodes for the fluorescent reporter mCherry in place of the IL-2-P-Fc sequence and contains the same backbone as all the plasmids used during the experiments (Aminah Kassem 2017). In the untransfected growth control group, untransfected tumor cells were injected. After 34 days of BLI evaluated tumor growth, mice were euthanized and the tumors dissected, fixed, embedded and sectioned (Fig. 4).

The idea behind the second in vivo experiment with four groups of mice was to investigate the influence of the Fc-part, whether there is a difference in clearance between the IL2-P-Fc and the IL-P fusion protein without the Fc-part. The experiment was performed exactly as the first in vivo experiment with the additional IL2-P group and a different endpoint of the experiment already 25 days after implantation (Fig. 4). The additional IL2-P group was injected with cancer cells which were in vitro transfected with the pCpG-hCMV-SCEP-IL2-P plasmid. The Fc-part is known to interact with the innate and adaptive immune system and therefore it provides specificity to a big range of innate effector cells such as natural killer cells, macrophages or granulocytes. (Ackerman und Nimmerjahn 2013).

The third in vivo experiment differs from the other two experiments, because the tumor treatment was performed *via* an intratumoral injection. Untransfected tumor cells were implanted into the mice. After 13 days the tumors were treated by intratumoral injection of polyplexes including either the IL2-P-Fc plasmid encoding for SIRPα fusion protein, the bb-mCherry plasmid as a transfection control or only buffer as negative control. Tumors were dissected 24 h, 48 h or 72 h after treatment to see at which time point macrophages infiltration occurs, if at all. The experiment was performed with 1 mouse (2 tumor sides, n=2) per group.

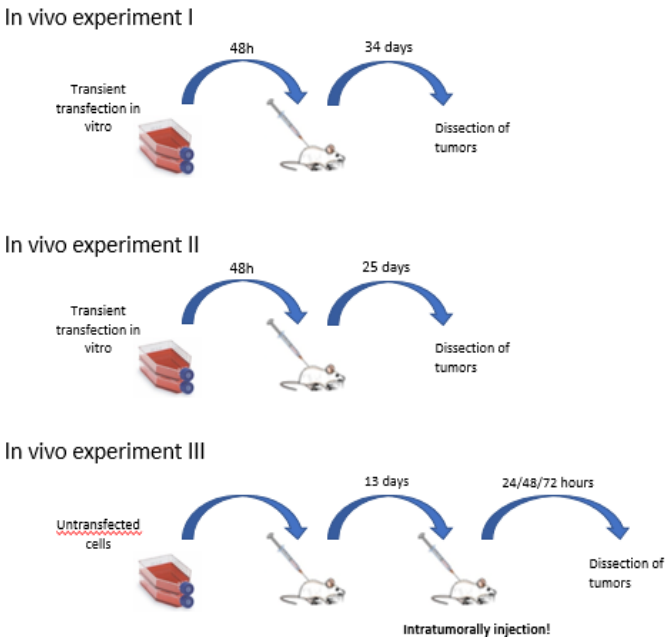

Figure 4 *Schematic overview of the animal experiments (Thermo Fisher Scientific; Fredrick Griffith)*

5.7. Histology

The study of the tissue biology, also called histology, is an important method in cancer research and clinical diagnostics. Histology has a focus on different cell structures and arrangement of the cells to form a tissue and in further consequence to constitute the organ with different functions. Tissues consist of two interacting components: the cells and the extracellular matrix (ECM). In the ECM many kinds of macromolecules which form collagen fibrils and other complex structures are found. It is important that the cells and the ECM work together in a well-coordinated manner, because the ECM contains also fluids transporting all the necessary nutrients and oxygen to the cells and carries away their metabolites. Because of the small size of the cells and the matrix components, histology is dependent on the usage of microscopes and furthermore a procedure of tissue preparation such as fixation, embedding, sectioning et cetera is necessary (Mescher 2018).

Fixation is required to preserve not only the cellular morphology, but also proteins or other biological structure in their relationship to the cell and to harden the tissue specimen (Thavarajah et al. 2012). There are a lot of different fixation methods, e.g. mechanisms including heat effects, effect of acids, dehydration or cross linking which contain various advantages and disadvantages. Shrinkage or swelling of the tissue, qualitative variations of histochemical staining, modification of the cellular organelles

or specific molecules retained in the specimen are known problems. There is no ideal fixation method, but in general many antigens can be detected in Formalin fixed paraffin embedded (FFPE) sections, for this reason formalin is routinely used in clinical histology and in research (IHC world).

Fixation is a complex physico-chemical reaction. Formaldehyde diffuses into the tissue and reacts with primary amines, amides, alcoholic hydroxyl groups or other moieties of proteins and causes protein cross linking (Thavarajah et al. 2012). One of the biggest problems which occur with formaldehyde fixation is the loss of the antigen immunorecognition due to protein cross-linking. To avoid this problem, a method of antigen retrieval is necessary before the immunohistochemical staining (Eltoum et al. 2001). Masked epitopes can be recovered using either enzymatic/proteolytic antigen retrieval, or heat-induced antigen retrieval methods. According to the evaluation of different methods by Manuela Simlinger in our lab (Manuela Simlinger 2018), only the heat induced antigen retrieval (HIER) was used for further experiments.

The embedding process with paraffin is important for long term storage and to make sectioning with the microtome possible. After fixation and embedding in paraffin, the tissue must be cut into very thin sections of about 2 µm thickness using a microtome before performing either a Hematoxylin and Eosin (H&E) or an IHC staining.

5.7.1. Hematoxylin and Eosin staining

The H&E staining is the standard method to stain various cell structures allowing rapid tissue differentiation. The simple combination of hematoxylin as the basic dye component and eosin as the acidic substance is most commonly used. Cell components which are anionic (negatively charged) like the nucleic acids in the nuclei are basophilic, which means they have an affinity for basic dyes. On the other hand, cationic components (positively charged), e.g. proteins with many amino groups, are acidophilic and react more readily with acidic dyes. The DNA in the cell nucleus and RNA-rich components in the cytoplasm are stained with hematoxylin in a dark blue or purple color. In contrast, the cytoplasm and collagen are stained pink due to Eosin (Mescher 2018).

5.7.2. Immunohistochemistry

Immunohistochemistry (IHC) uses antibodies to detect the protein of interest and is commonly used in histology. The specific binding of the paratope on the antibody (AB) and the epitope on the target allows in principle the unambiguous identification of antigens in tissue. Whereas polyclonal antibodies raised in host animals (e.g. rabbit, goat, etc.) bind to different epitopes of an antigen, monoclonal antibodies, generated with hybridoma technology, bind to only one epitope of the protein to be detected. The advantage of using a monoclonal antibody (mAB) is that it is highly specific and binds strongly to the protein of interest with less nonspecific binding to other proteins that are similar (Mescher 2018).

IHC uses thin tissue sections which contain the protein that needs to be detected and a solution containing the antibody. Besides FFPE sections, which were used for this thesis, the other possibility is to stain fresh frozen tissue (cryo sections). The cryo method is much faster and better for molecular analysis, including RNA or DNA, of the tissue. For immunohistochemical stainings and morphological analysis, FFPE samples are recommended with the big advantage that they can be stored at room temperature (RT) (Biocompare 2014).

After protein demasking and incubation with the AB solution and following other steps from the staining protocol such as washing steps, the protein's location in the cells can be seen with either electron, light microscopy or transmission electron microscopy (TEM) visualizing the antibody. The antibodies are linked to fluorescent compounds or to an enzyme like peroxidase or alkaline phosphatase that gives a color reaction with the appropriate substrate.

As illustrated in figure 5 there are two different methods in immunohistochemistry, the direct and indirect technique. The direct method uses a primary antibody (pAB) which is directly labelled with a fluorescent compound or a peroxidase. This AB binds to the protein against which it is produced and can be visualized by different methods. The indirect immunohistochemistry uses two antibodies, the pAB which binds to the protein x and then a secondary antibody (sAB) which is directed to the primary AB and is produced in another species than the pAB. The secondary AB is labelled and binds specific to the primary AB, hence indirectly labelling the protein of interest within the

tissue. Signal amplification can be achieved, because more than one secondary AB can bind to one primary AB. This high sensitivity is the reason why this indirect method is more widely used in tissue pathology and research. Another opportunity to obtain an amplification of the detection signal is to use the Avidin-Biotin complex (see also section 6.3.2.1) (Mescher 2018).

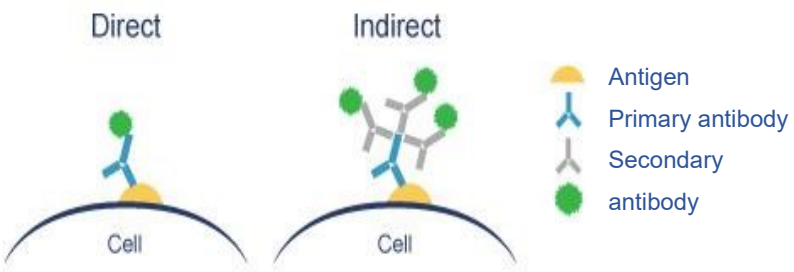

Figure 5 *Direct vs. indirect detection in immunohistochemistry (abcam)*

6. Materials and Methods

Materials

Reagents, materials and devices which were applied for immunohistochemical working steps are listed below in Table 1, 2 and 3.

Table 1 Reagents

NAME	PRODUCT NO.	LOT NO.	SUPPLIER, LOCATION
Acetic acid glacial	20104.334	14A160513	VWR Chemicals, Radnor, PA, USA
Ammonium hydroxide solution	221228	SZBD3180V	Sigma-Aldrich, St. Louis, MO, USA
Avidin-Biotin blocking reagent	BUF016	170515, 146543	BIO-RAD, Hercules, CA, USA
Bovine Serum Albumin	A9647	SLBK9148V	Sigma-Aldrich, St. Louis, MO, USA
3,3'- Diaminobenzidine tetrahydrochloride	D5905	SLBS4779	Sigma-Aldrich, St. Louis, MO, USA
Dulbecco's Phosphate Buffered Saline	D8537	RNBG5563	Sigma-Aldrich, St. Louis, MO, USA
Entellan® new	107961	HX69157261	Merck, Darmstadt, Germany
Eosin Y solution	318906	MKBQ9365V	Sigma-Aldrich, St. Louis, MO, USA
Ethanol denaturated >99,8%	K928.2	068267476	Carl Roth, Karlsruhe, Germany
Ethylenediaminetetraacetic acid	E6758	SLBR6878V	Sigma-Aldrich, St. Louis, MO, USA
Hematoxylin solution acc. to Harris	X903.3	037253899	Carl Roth, Karlsruhe, Germany
HEPES	A3724	7IO15011	AppliChem, Darmstadt, Germany
Hydrogene peroxide 35 %	9683.1	295231751	Carl Roth, Karlsruhe, Germany
Hydrochloric acid	30721	STBG8626	Sigma-Aldrich, St. Louis, MO, USA
MilliQ-Water			

Sodium chloride	1.06400	K49776800805	Merck, Darmstadt, Germany
Sodium chloride	S/3161/60	1726048	Thermo Fisher Scientific, Waltham, USA
di-Sodium hydrogen phosphate dodecahydrate	A3906	3P009818	AppliChem, Darmstadt, Germany
tri-Sodium citrate dihydrate	27833.237	13|170003	VWR Chemicals, Radnor, PA, USA
Paraformaldehyde	A3813	R014578	AppliChem, Darmstadt, Germany
Paraplast®	P3558	SLBN3818V	Sigma-Aldrich, St. Louis, MO, USA
Potassium chloride	A2939	3R007818	AppliChem, Darmstadt, Germany
Potassium phosphate monobasic	P5655	SLBJ7258V	Sigma-Aldrich, St. Louis, MO, USA
Triton X-100	X-100	SLBM3864V	Sigma-Aldrich, St. Louis, MO, USA
Trizma® base	T1503	SLBW7403	Sigma-Aldrich, St. Louis, MO, USA
Tween® 20	A4974	4G009367	AppliChem, Darmstadt, Germany
Vectastain® ABC kit	PK-4001	290617	Vector Laboratories, Burlingame, CA, USA
VitroView™ IHC/DAB kit anti- goat	VB-6026D	0320VB18, 0726VB18	VitroVivo Biotech, Maryland, USA
VitroView™ IHC/DAB kit anti-Mouse & Rabbit Ig	VB-6023D	0326VB18	VitroVivo Biotech, Rockville, MD, USA
Xylene	9713.4	048266714	Carl Roth, Karlsruhe, Germany

Table 2 Materials

NAME	SUPPLIER
coverslip 18x18	Carl Roth, Karlsruhe, Germany
Elite PAP pen	CLSG80125, Cedarlane Laboratories, Ontario, Canada
microscope slide SUPERFROST®	Carl Roth, Karlsruhe, Germany
microscope slide SUPERFROST® PLUS	Thermo Fisher Scientific, Waltham, MA, USA

Table 3 Devices

NAME	SUPPLIER
cellSens Standard	Olympus, Shinjuku, Tokyo, Japan
Embedding station MPS/P1	Slee medical GmbH, Mainz, Germany
Microtome (CUT 5062)	Slee medical GmbH, Mainz, Germany
Olympus BX53 light microscope	Olympus, Shinjuku, Tokyo, Japan
Para cooler model A	Ralf W. Weinkauf, Hallerndorf, Germany
SLEE MTP embedding carousel	SLEE medical GmbH, Mainz, Germany

Methods

6.1. Tissue preparation

6.1.1. Fixation

The fixation solution was prepared by dissolving paraformaldehyde (final concentration 4% w/v) in HBS buffer (20 mM HEPES pH 7.4, 150 mM NaCl) on a magnetic stirrer at 60°C. After cooling to RT, pH was adjusted to 7.4 and the solution filtered into a glass bottle with screw cap. After sacrificing the mice, dissected tumors and other MDA-MB-231 LM 2-4 infiltrated organs (Table 9-11) were fixed for 22 hours at RT. Thereafter, formalin was removed, and the organs placed into labelled embedding cassettes. Organs too big to be placed into the cassettes (e.g. liver or tumors bigger than 1 cm in diameter) were prior cut. Cassettes were stored in a beaker filled with 70 % EtOH to avoid drying out of the organs. To get rid of the water in the tissue and for clearing the tissue, further processing was performed with the embedding carousel SLEE MTP which consists of various containers with increasing concentrations of

ethanol (70 %, 96 %, 100 %) and Xylene. The last two beakers of the carousel contain paraffin (Paraplast®) to infiltrate the tissue. The overall duration of this process is 13 hours.

6.1.2. Embedding

Devices which were utilized were the Embedding station MPS/P1 and the Para cooler model A. To obtain a paraffin block, a prewarmed metal mold was partially filled with a small amount of hot paraffin and the organ was added immediately and pushed down with forceps until the paraffin solidified on the cool spot. Next, the bottom of the cassette was placed onto the mold, the mold filled up with hot, liquid paraffin and the filled mold with the cassette on top transferred to the cooling plate for total paraffin solidification. When paraffin was totally solidified, the block was carefully removed from the mold. Absence of air bubbles in the block was key, otherwise the organ had to be re-embedded.

6.1.3. Sectioning

A semi-automatic precision microtome (CUT 5062) was used to obtain sections of 2 µm thickness. Best results were obtained with a paraffin block cooled down below room temperature. For this reason, the Para cooler model A was used for cooling the blocks. Sections were transferred carefully into a warm water bath filled with distilled water (45-50°C) to let them unfold and afterwards picked up with a labelled microscope slide. For IHC stainings, Superfrost Plus™ Adhesion Microscope Slides and for H&E stainings Superfrost® slides were used.

6.2. Hematoxylin and Eosin stain

H&E staining was performed to demonstrate various normal or abnormal cell structures and to compare it with the CD47 and luciferase staining. The paraffin sections were prewarmed in the drying chamber at 55 °C for at least 2 hours using a slide holder, before they were passed through 3 containers filled with Xylene for 5 minutes each to remove paraffin. Re-hydration and removal of Xylene was achieved by transferring slides through an alcohol row, starting with three times 100 % ethanol for 30 seconds, followed by 3 times 96 % and 3 times 70 % EtOH 30 seconds each. Before starting with the staining, the sections were incubated 1 minute in distilled water. Hydration of

the tissue is indispensable, because the staining reagents are water soluble. For Hematoxylin staining, the slide holder was placed for 4 minutes into a bottle with Hematoxylin solution (3:1) which was made by a mixture of 160 ml Harris Hematoxylin solution and 80 ml WEK water. Hematoxylin needs to be filtered before use to eliminate crystals. For Eosin staining, sections were rinsed in tap water for 20 seconds and incubated in a dilution of 10 drops Ammonium solution 32 % in 250 ml Aqua dest. for further 20 seconds. Afterwards the slides were rinsed in tap water for 1 minute, put into the Eosin staining solution (25 ml Eosin Y solution, 200 ml Aqua destillata and 0.125 ml glacial acetic acid) for 3 minutes and finally rinsed for 10 seconds in water. For tissue dehydration, slides were put in 70 % ethanol 3 times for one second followed by 96 % EtOH and 100 % EtOH the same way and in the end in Xylene 3 times, 1 minute in the first container and 2 minutes each in the other 2 containers. To preserve and support stained sections for light microscopy, the sections were mounted in Entellan®new and coverslipped.

6.3. Immunohistochemistry

6.3.1. Deparaffinization and HIER

Prior to IHC staining, sections underwent deparaffinization and heat induced epitope retrieval (HIER).

Appropriate sections were selected and labelled according to the staining plan. They were prewarmed for 2 hours at 55°C in the drying chamber followed by deparaffinization and hydration using Xylene (3 x 5 minutes) and different concentrations of EtOH (70 %, 96 %, 100 %) for 30 seconds (for each concentration 3 treatments). To finalize hydration, sections were incubated in Aqua dest. for 30 seconds. Afterwards, slides were transferred into a jar with buffer to perform heat mediated antigen retrieval. Depending on the primary antibody used, either 10mM sodium citrate buffer (10 mM Tri-sodium citrate in MiliQ-water, 0.05 % Tween 20 w/v, adjusted to pH 6 with HCl) (IHC world) or Tris-EDTA Buffer (10 mM Tris Base, 1 mM EDTA, in MiliQ-water, adjusted to pH 9 with NaOH, 0.05 % Tween 20 w/v) (IHC world) was utilized. The samples were boiled for 30 minutes in a silicon oil bath at approximately 125-130°C and cooled down for about 30 minutes to reach RT again.

6.3.2. CD47 staining

The main part of this diploma thesis was to detect the surface protein CD47 by IHC and to confirm its overexpression on MDA-MB-231 LM2-4 cells. Further we wanted to see, if the blocking with the fusion protein SIRPα-Fc worked out. For this type of staining, 2 kits with different detection systems, the Vectastain®ABC Peroxidase rabbit IgG kit and VitroViewTM® Universal 1-step Polymer-Based IHC/DAB kit (Anti-Mouse/Rabbit IgG) apart from a lot of different primary antibodies and isotypes were tested.

6.3.2.1. Vectastain® ABC kit

After Deparaffinization and HIER slides were washed 3 times in PBS (1370 mM NaCl, 27 mM KCl, 54 mM $Na_2HPO_4 \cdot 12\ H_2O$, 18 mM KH_2PO_4), drained, and sections were encircled with a PAP pen to create a hydrophobic area around the section preventing that the reagents leak out. Then the slides were placed into a humid chamber and incubated with blocking serum (normal goat serum ready to use (RTU) from Vectastain® kit) for 30 minutes and washed again 3 times with PBS. A 200 µl Eppendorf® pipette was used for carefully pipetting the reagents onto the sections. Next, endogenous Avidin and Biotin were blocked, achieved by an incubation with 1-2 drops of the RTU Avidin solution for 15 minutes, followed by 3 washing steps with PBS and 15 minutes incubation with 1-2 drops of RTU Biotin solution. After 3 further washing steps, sections were incubated with primary antibody or isotype diluted in AB dilution buffer (2 % Bovine serum albumin (BSA) w/v in PBS (0,45 µm filtered)) or only buffer overnight at 4°C.

Table 4 *Primary antibodies used for CD47 stainings*

Anti CT47 antibody	reactivity	product number	LOT number	Retrieval buffer	Tested dilutions
polyclonal rabbit primary antibody	Human, mouse, rat	ab175388	GR3188232-2	citrate buffer pH 6	1:50 = 1:100 of GR3208102-1
polyclonal rabbit primary antibody	Human, mouse, rat	ab175388	GR3208102-1	citrate buffer pH 6	**1:100** 1:200
Monoclonal mouse primary antibody azide free	human	ab213079	GR298233-1	citrate buffer pH 6	1:500 1:1000
rabbit monoclonal antiCD47 antibody	human	ab218810	GR3216895-1	Tris-EDTA Buffer (+0,05% Tween 20, pH 9)	1:1000 **1:2000**

Table 5 *Isotypes used for CD47 stainings*

Isotype control	product number	LOT
Rabbit IgG isotype control	bs-0295P	AH03127265
Mouse IgG isotype control	BD Pharmingen, 557273	6146632
Rabbit IgG [EPR25A] isotype control	ab 172730	GR3179509-11

The next day, slides were drained and washed 3 times with PBS before they were incubated with 0.3 % H_2O_2 for 15 minutes to block endogenous peroxidase and then washed again briefly 3 times with PBS. Afterwards, the secondary antibody or dilution buffer alone was added and drained again after 30 minutes incubation at RT. The tissues were washed 3 times with PBS and incubated 30 minutes with the ABC (Avidin-Biotin-complex) reagent to form the detection complex. After the washing steps, the sections were incubated with DAB (Diaminobenzidine) solution (3,3'- Diaminobenzidine tetrahydrochloride 10 mg (1 tablet) in 15 ml in PBS + 75 µl TritonX-100) where 10.3 µl fresh 35 % H_2O_2 (0.024%) where added before usage. The horseradish peroxidase (HRP) reacts with its substrate DAB in presence of H_2O_2 which leads to a brown color development. If the staining was intense enough, the reaction was stopped with WEK water, otherwise DAB solution was added again for a short period of time. Counterstaining was performed with Hematoxylin.

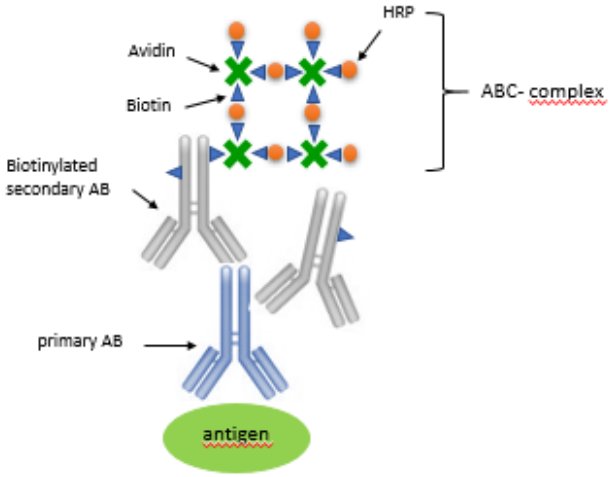

Figure 6 Detection system using the Avidin and Biotin complex. *1) primary AB binds specific to the protein of interest 2) biotinylated secondary AB reacts with the primary AB 3) ABC complex formulation (Avidin/Biotinylated Enzyme complex was added, Avidin forms a strong chemical bond to Biotin, while the enzyme HRP is conjugated with Biotin in the ABC complex 4) Brown staining is caused by the reaction of HRP with its substrate DAB in presence of hydrogenperoxide (Krebsinformationsdienst 2017)*

6.3.2.2. VitroView™ Universal 1-step Polymer-Based IHC/DAB kit

The staining process with this kit is the same as with the Vectastain ABC kit, apart from the detection system, which is different.

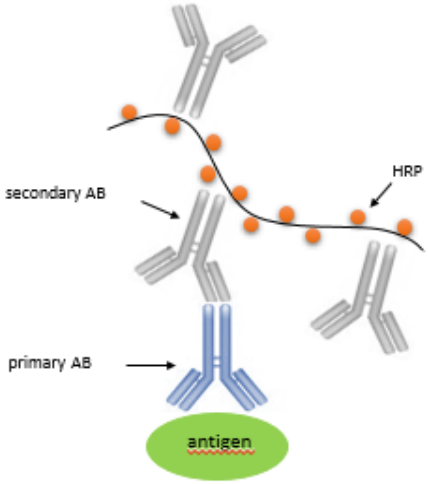

Figure 7 Polymer based detection system
(Krebsinformationsdienst 2017)

The VitroVivo Biotech detection system is based on a polymer of the HRP linked to the secondary antibody. As shown in figure 7, the secondary AB binds to a primary AB which is targeted against the protein of interest, in our case CD47 or luciferase. The

polymer increases the amount of HRP and is necessary to enhance the signal by converting a higher amount of substrate into precipitate (VitroVivo Biotech). The advantage of this method is that it is Avidin and Biotin free and therefore unspecific staining caused by endogenous Biotin or other chemical compounds with high affinity for avidin is reduced and a blocking step is not necessary (Nikiel et al. 2009).

6.3.3. Firefly luciferase staining

As mentioned in the Introduction part, luciferase is expressed by MDA-MB-231 LM2-4 EGFP Luc cells and its detection proves that the sample concerns to tumor tissue and allows us to distinguish between human tumor cells and other (murine) tissue. To detect firefly luciferase, the goat pAB to firefly luciferase (ab181640), goat IgG isotype control (bs-0294P) and VitroView™ Universal 1-step Anti-Goat Polymer-Based IHC DAB kit for detection were used in the optimized staining protocol.

Table 6 *Primary antibodies used for luciferase stainings*

antibody	product number	LOT number	Retrieval buffer	Tested dilutions
goat pAB to firefly luciferase	ab181640	LOT: GR257345-31	1mM EDTA + 0,05 % Tween20 pH 8	1:1000
rabbit polyclonal anti-luciferase AB	ab21176	LOT:GR3192295-1	citrate buffer pH 6	1:200 1:1000
rabbit polyclonal anti-luciferase AB	bs-8539R	LOT: AC12254541	citrate buffer pH 6	1:200
rabbit polyclonal anti-luciferase AB	27986-1-AP	-	Tris-EDTA Buffer (+0,05% Tween 20, pH 9)	1:200 1:500

Table 7 *Isotype controls used for firefly luciferase stainings*

Isotype control	product number	LOT
Goat igG isotype control	bs-0294P	AE091001
Rabbit IgG isotype monoclonal [EPR25A] control	ab172730	GR3179509-11

Selected sections were labelled according to the staining plan and prewarmed for 2 hours at 55°C in the drying chamber. Deparaffinization and antigen retrieval were performed as described in “Deparaffinization and HIER”. Due to usage of the goat primary AB (ab181640), the slides were incubated with a mixture of 1 mM EDTA + 0.05 % Tween20 for antigen retrieval and boiling time was about 15-20 minutes. To make the cell layer more permeable, sections were rinsed in PBS-Triton X-100 (0.025 %) for 2 minutes and afterwards 2 minutes in a jar only with PBS washing buffer. Afterwards slides were incubated with a few drops of RTU normal horse serum for 30 minutes to block non-specific binding of immunoglobulin. Before adding primary antibody, isotype or buffer, 3 short washing steps with PBS washing buffer were performed and then the slides were incubated overnight at 4°C in the cooling room.

Next day, primary AB was drained, followed by 3 washing steps, and the sections were incubated 15 minutes with 0.3 % H_2O_2 to block unspecific staining caused by endogenous peroxidase, washed again 3 times and finally incubated with RTU secondary antibody or buffer for 30 minutes at room temperature. Secondary antibody solution was washed off with PBS washing buffer and ~ 200 µl of DAB solution which was prepared with RTU reagents from the kit, were added to each section and removed after color development gets visible (2-8 minutes). To check the staining intensity under the microscope, slides were put back into the jar with PBS in the meantime, and if the staining was too less, a second incubation time with DAB was necessary. In the other case, if the staining was intense enough, the reaction was stopped by putting the slides into a jar with WEK water. Following steps were counterstaining with Hematoxylin to stain the nuclei blue, dehydration through 70 %, 96 % and 100 % ethanol, clearing in Xylene and mounting in Entellan®.

6.3.4. Staining to detect the Fc-part of the fusion protein

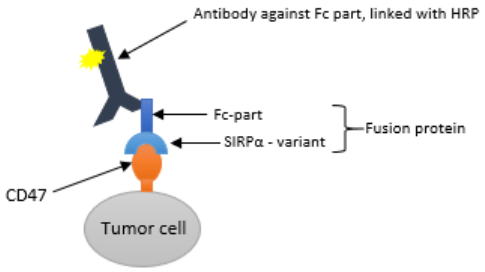

Figure 8 *Staining with AB against Fc-part*

Finally, it was interesting to see if there is fusion protein left in the tissue binding to the CD47 protein. Considering that, the goat anti-human IgG Fc (HRP) preadsorbed (ab98624) primary antibody which binds specific to the Fc-part (tested dilutions: 1:200; 1:500), the goat IgG isotype control (bs-0294P) and the VitroView™ Universal 1-step Anti-Goat Polymer-Based IHC DAB kit as detection system were consulted. For this experiment we chose different samples from the three in vivo experiments, always at least one sample from the IL2-P-Fc group and the other one from the bb-mCherry group or buffer control group to have a negative control (Table 8).

Table 8 *overview of samples tested to detect the Fc-part*

in vivo experiment I.	**in vivo experiment II.**	**in vivo experiment III.**
MCT-0046 IL2-P-Fc TU RI	MCT-115 IL2-P-Fc TU LE	MCT-0209 TU LE IL2-P-Fc
AGE-0482 bb-mCherry TU RI	SGE-0051 bb-mCherry TU LE	MCT-0208 TU LE IL2-P-Fc
		MCT-0210 TU LE IL2-P-Fc
		MCT-204 TU RI bb-mCherry
		MCT-182 TU RI buffer control

After deparaffinization and HIER with Tris-EDTA Buffer (+0.05% Tween 20, pH 9), 3 washing steps with PBS washing buffer were performed. Incubation with Triton X was omitted, because no permeabilization process of the cell membrane is necessary to detect the Fc-part of the fusion protein, since the fusion protein is binding to the cell surface. Afterwards the sections were incubated with 3-4 drops of RTU normal horse serum for 30 minutes to block non-specific binding of immunoglobulin before incubation with the primary AB in the dilution 1:200, isotype control in the same concentration as the primary antibody, or buffer overnight in the cooling room.

An incubation step with the secondary AB was not necessary, because the pAB was already preabsorbed with HRP. Subsequently a peroxidase blocking step was performed and then the substrate DAB was added onto the sections.

Altogether three stainings were performed to detect the Fc-part. Two of them were realized such as described above. The third one was done with an altered protocol, where the sections were incubated with the antibody in the dilution 1:500 in contrast to 1:200 and incubation time was about 2 hours at RT.

6.3.5. Microscopic analysis

Staining results were analyzed by light microscopy (Olympus BX53) using the Olympus cellSens Standard software and pictures were taken at different magnifications with an Olympus DP-73 color camera. Objectives used were: 2x: PLAPON2X/0,08 Plan Apo Objektiv; 4x: UPLSAPO4X/0,16 U Plan S Apo; 10x: UPLSAPO10X2 U Plan S Apo; 20x: UPLSAPO20X/0.75 U Plan S Apo; 40x: UPLSAPO40X2 U Plan S Apo.

Table 9 Overview in vivo experiment 1
(samples highlighted in blue were included in further stainings)

Treatment groups	Mouse number	Pathology date	Embedding date	Organ
untransfected	MCT-0041 (Mouse 1)	7.3.18	13.3.18	**TU LE** **TU RI** ME
	MCT-0042 (Mouse 2)			**TU LE** **TU RI** **LN** **LN (upper axil)**
	MCT-0043 (Mouse 3)			**TU LE** TU RI **visceral Fat//pancreas** **sentinel LN** **LE**
IL2-P-Fc	MCT-0044 (Mouse 4)	7.3.18	13.3.18	**TU RI** **LN** **PE**
	MCT-0045 (Mouse 5)			TU RI **LN**
	MCT-0046 (Mouse 6)			**TU LE** **TU RI** PE
bb-mCherry	AGE-0481 (Mouse 7)	7.3.18	13.3.18	TU LE TU RI **LN or other tissue**
	AGE-0482 (Mouse 8)			**TU LE** **TU RI** Fat tissue + ME **Fat tissue near uterus**
	AGE-0483 (Mouse 9)			TU LE **TU RI** **ME** Fat, ME RI PE (upper right)

Table 10 Overview in vivo experiment 2
(samples highlighted in blue were included in further stainings)

Treatment groups	Mouse number	Pathology date	Embedding date	Organ
untransfected	MCT-124	30.7.18	31.7.18	**TU LE** **TU RI** **sent. LN LE** **sent. LN RI**
	MCT-125			**TU LE** **TU RI** **sent. LN LE**
	AGE-0352			**TU LE** **TU RI** **sent. LN LE** **axil. LN LE** **pancreas/fat**
IL2-P-Fc	MCT-114	30.7.18	31.7.18	**TU LE** **TU RI**
	MCT-115			**TU LE**
	MCT-117			**TU LE** **tissue chest**
IL2-P	MCT-118	30.7.18	31.7.18	**TU LE** **TU RI** **sent. LN?**
	MCT-119			**TU LE** **TU RI** **sent. LN RI?** **axil. LN RI**
	MCT-120			**TU LE** **TU RI**
bb-mCherry	MCT-121	30.7.18	31.7.18	**TU LE** **TU RI** **sent. LN RI**
	MCT-122			**TU LE** **TU RI**
	MCT-123			**TU LE** **TU RI**
	SGE-0051			**TU LE** **TU RI** **sent. LN RI** **axil. LN LE** **axil. LN RI**

Table 11 Overview in vivo experiment 3
(samples highlighted in blue were included in further stainings)

Treatment groups	Mouse number	Pathology date	Embedding date	Organ
buffer control backup mouse	MCT-182	10.10.18 24h after injection	15.10.18	**TU LE** **TU RI**
IL2-P-Fc	MCT-0210	12.10.18 72h after inj.	15.10.18	**TU LE** **TU RI**
	MCT-0208	11.10.18 48h after inj.		**TU LE** **TU RI**
	MCT-0209	10.10.18 24h after inj.		**TU LE** **TU RI**
bb-mCherry	MCT-0203	12.10.18 72h after inj.	15.10.18	**TU LE** **TU RI**
	MCT-113	11.10.18 48h after inj.		**TU LE** **TU RI**
	MCT-204	10.10.18 24h after inj.		**TU LE** **TU RI**

7. Results

7.1. Overview of histologically analyzed tumors

During the in vivo experiments, tumor growth was analyzed from four different groups of mice, bearing tumor cells transfected with IL2-P-Fc, IL2-P, bb-mCherry or untransfected cells as shown in the figures below.

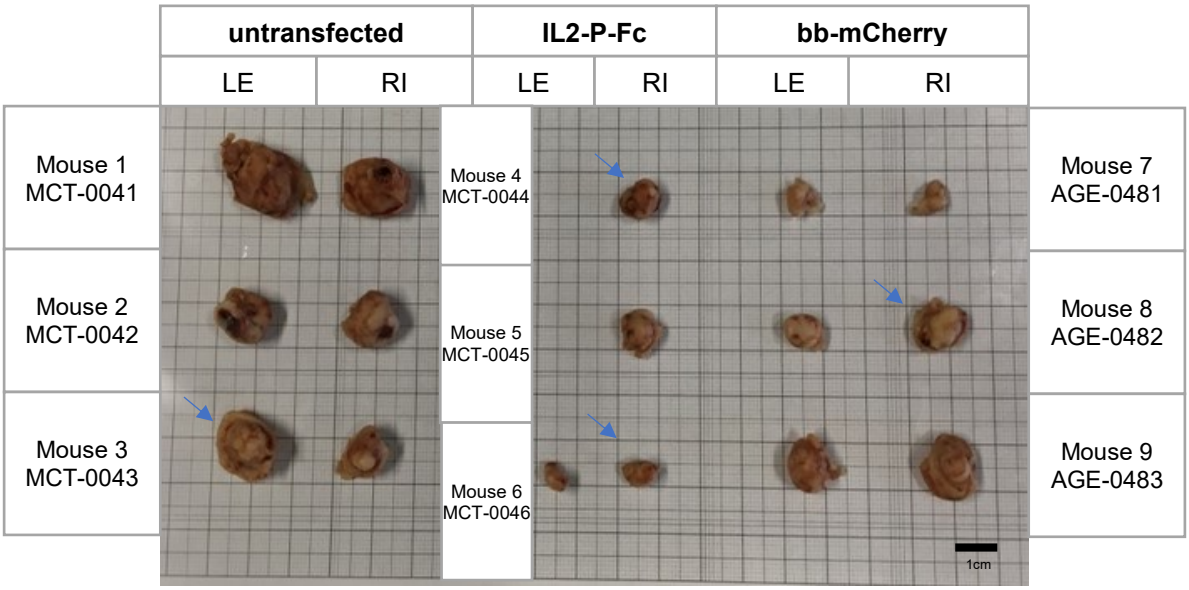

Figure 9 Comparison of tumor size of samples from in vivo experiment 1. *(Blue arrows show tumors which were obtained for further immunohistochemical evaluation)*

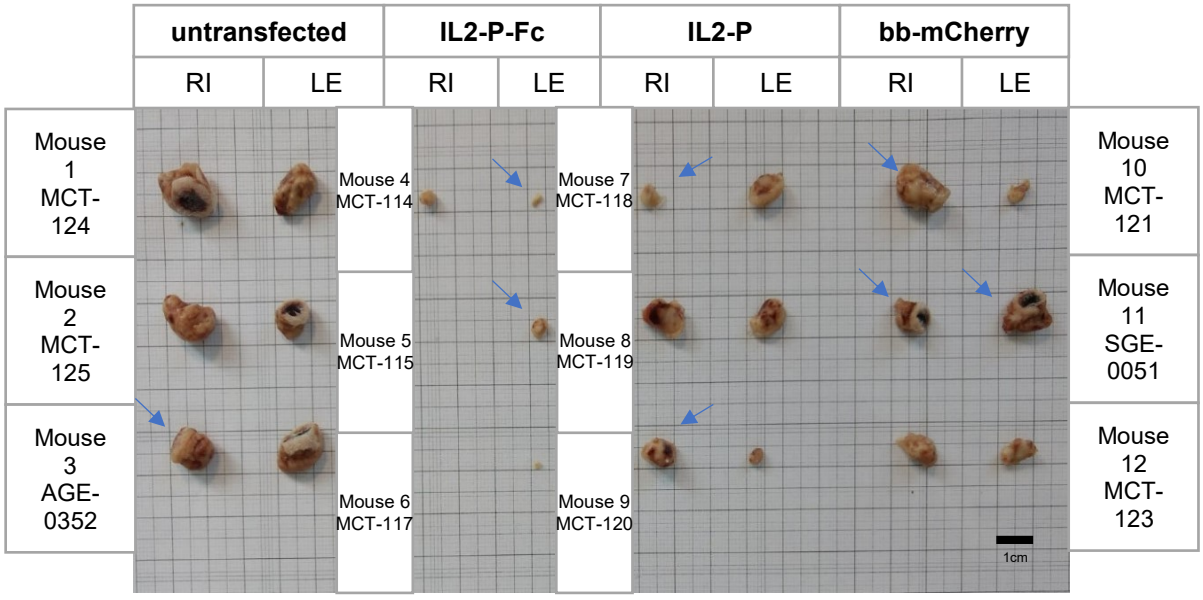

Figure 10 Comparison of tumor size of samples from in vivo experiment 2. *Blue arrows show tumors which were obtained for further immunohistochemical evaluation.*

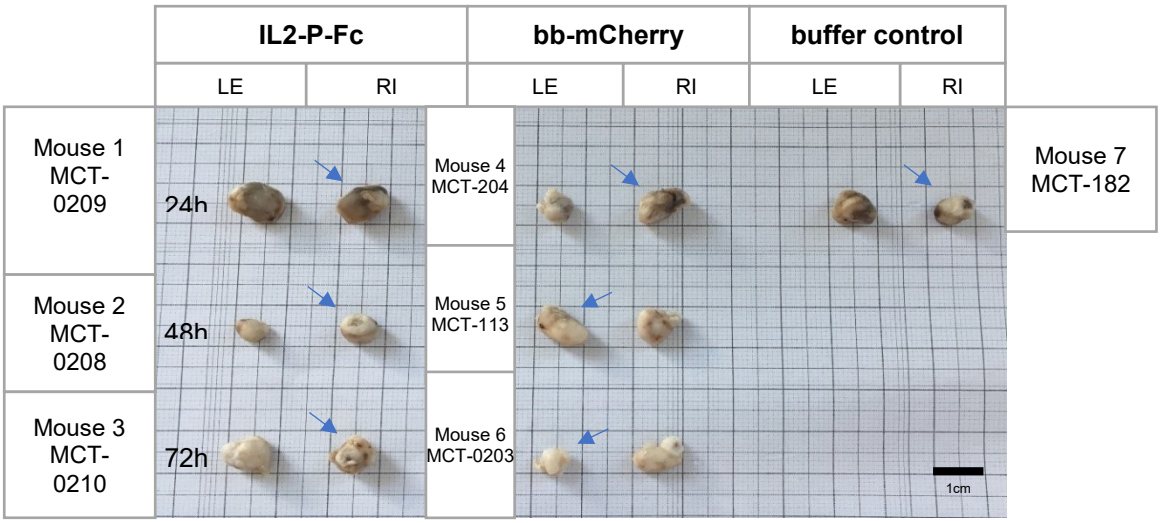

Figure 11 Comparison of tumor size of samples from in vivo experiment 3. *Blue arrows show tumors which were obtained for further immunohistochemical evaluation.*

The setup in the first and second experiment was the same except for a different endpoint (34 days vs. 25 days post injection of in vitro transfected tumor cells). The untransfected group showed constant growth of the tumor and metastasis, whereas the treated group IL2-P-Fc was characterized by very small tumors or even total regression. There was a difference between the IL2-P-Fc and the IL2-P group noticeable. The tumor size was clearly bigger in the IL2-P than in the IL2-P-Fc group. As expected, the transfection itself influences the cells somehow, which might be the reason why the tumors from the control group bb-mCherry are also a little bit smaller compared to the untransfected group.

The results from the third in vivo experiment differed from the other two experiments, since the tumor size looks very similar in all 3 groups as expected. The tumor size did not change a lot, cause the treatment was performed for a short time period (24h/48h/72h) on 13 days old tumors with the same size. The aim was to see if the injection of polyplexes containing the plasmid encoding for IL2-P-Fc blocks the “don’t eat me signal” and if it causes a tumor infiltration by macrophages as a consequence, which was expected between 24 and 72 hours after gene delivery.

7.2. Optimization of staining protocols

From each group (IL2-P-Fc, IL2-P, bb-mCherry or untransfected cells) at least one or two samples were chosen for the histological evaluation. The aim was to detect the CD47 surface protein and luciferase, expressed by the injected tumor cells. Further, an H&E staining and a staining to detect the Fc-part of the SIRPα fusion protein were performed to complete the results. Besides, certain samples were sent to the "Krebsforschungsinstitut Wien" where they were stained for macrophages in the tissue.

7.2.1. Optimization of the CD47 staining protocol

In all the tumor samples a positive CD47 staining was visible as illustrated in the figures below. Brown staining shows positive CD47 signal caused by the reaction of DAB. Positive staining was expected, because after approximately one month (34 days in first and 25 days in second experiment) the CD47 receptor should not be blocked anymore by the fusion protein due to a transient transfection of the tumor cells. The 40x magnification illustrates that mainly the cell membrane, is stained, which was expected as CD47 is a surface protein. Almost all tumor cells were intensely stained dark brown which points out an overexpression of CD47 by these cells. Isotype controls were included to reveal unspecific staining due to cross reaction between the Fc-part of the primary antibody and unknown epitopes in the murine tissue which causes high background staining. To exclude a reaction between the secondary antibody and parts of the tissue, a secondary antibody control was included in every staining protocol. A further negative control was the buffer control which was only treated with buffer to compare the positive tissue with the untreated tissue. These four groups were included in every experiment and compared below.

First of all, an optimized working protocol was necessary to detect the CD47 surface protein. For this reason, many different antibodies, isotype controls and detection methods were tested. At first, two aliquots (frozen vs. stored at 4°) and 2 different dilutions (1:100 and 1:200) of the primary polyclonal AB (ab175388) were tested.

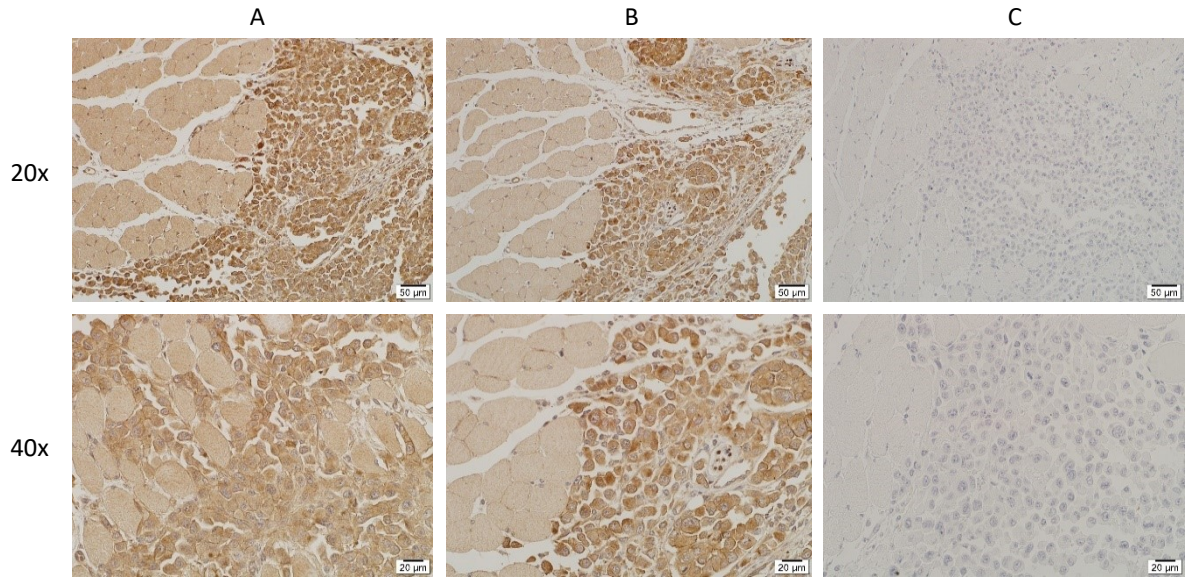

Figure 12 Staining to test frozen aliquot of the anti-CD47 primary polyclonal AB (ab175388) in comparison to an aliquot, stored at 4°C on positive control tumor tissue (M116). *(A) the primary AB stored at -20°C was used in the dilution* ***1:100*** *(B) staining was performed with the same primary AB stored at 4°C in the dilution 1:100 (C) secondary control shows negative staining. Scale bar: 50 µm, 20 µm; Magnification: 20x, 40x*

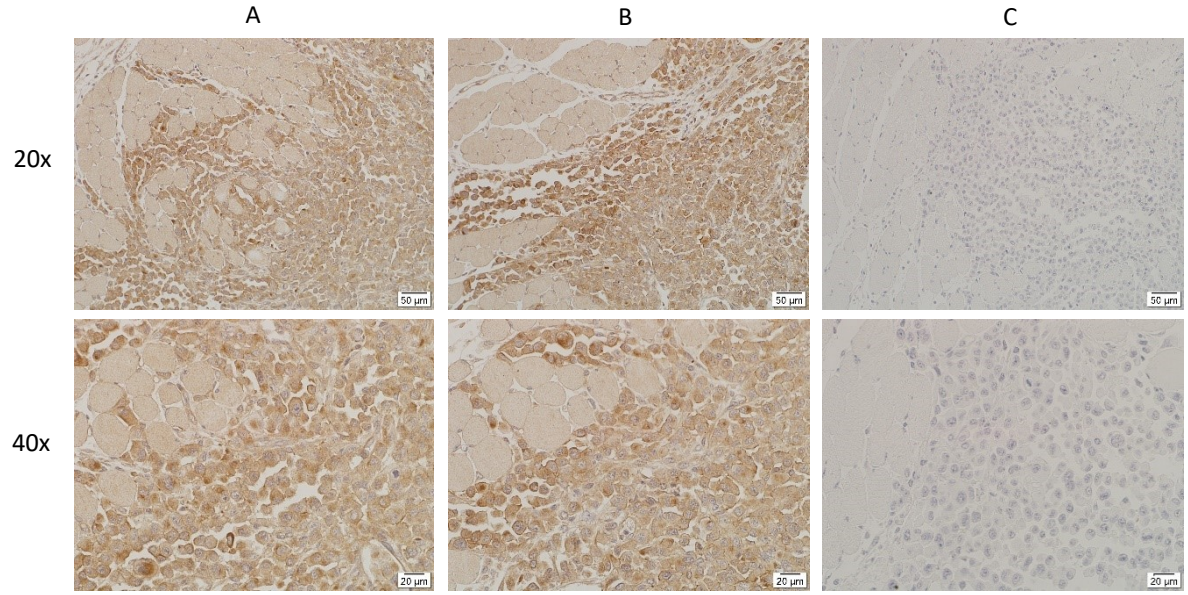

Figure 13 Staining to test frozen aliquot of the anti-CD47 primary polyclonal AB (ab175388) in comparison to an aliquot, stored at 4°C on positive control tissue (M116). *(A) on these sections the primary AB which was stored at -20°C was added in the dilution* ***1:200*** *(B) staining was performed with the prim. antibody stored in the fridge and the same dilution was used (C) secondary control. Scale bar: 50 µm, 20 µm; Magnification: 20x, 40x*

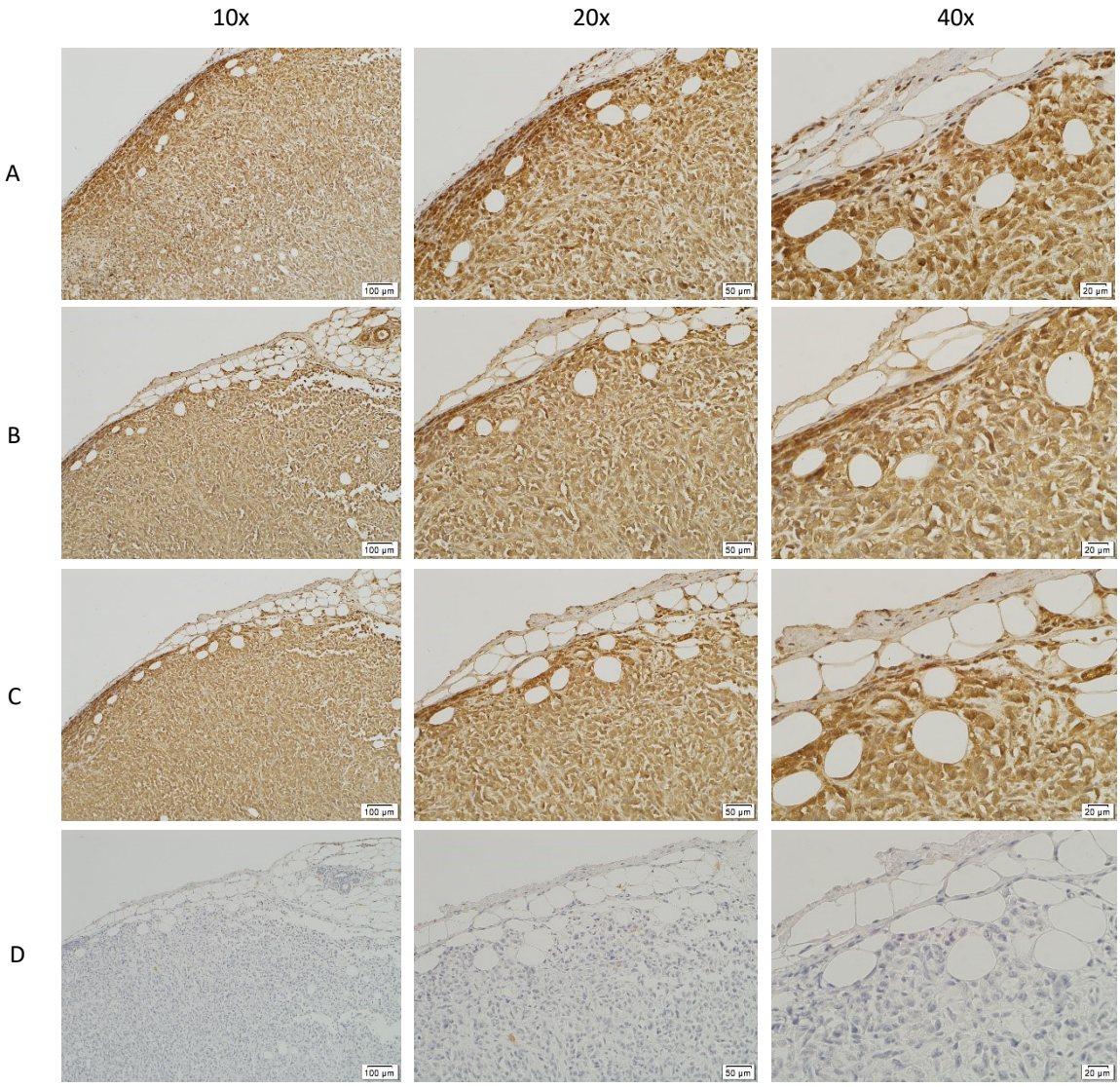

Figure 14 Testing of different batches of primary rabbit polyclonal anti-CD47 AB (ab175388) in the dilution 1:100 on untransfected tissue from in vivo experiment 1. Vectastain ABC kit was used as detection system *(A) aliquot of the AB which was 10 months old and 7 months frozen was utilized (B) 1 month frozen, and altogether 3 months old aliquot was used (C) the last aliquot contained a one-month old AB, which was frozen on the same day of delivery (D) rabbit IgG isotype control (ab172730). Scale bar: 100 µm, 50 µm, 20 µm; Magnification: 10x, 20x, 40x*

The first results showed that the staining quality is the same using a frozen aliquot or an aliquot stored at 4°C of the same antibody (Fig. 12). In addition, storage time up to a year does not have an essential influence on the quality of the antibody, if it is frozen at -20°C. The immunohistochemical staining results looked comparable as shown in figure 14. Moreover, the antibody can be stored a few weeks in the fridge before freezing. The best way is probably to freeze the antibody not later than 2-3 weeks to guarantee its proper function. Figure 13 illustrates that the staining is less intense with the dilution 1:200 of the rabbit primary AB (ab175388), therefore the dilution 1:100 is

recommended to use. All these results were obtained with the Vectastain ABC kit and the polyclonal primary AB (ab175388), which has the big disadvantage of unspecific staining, because it reacts to human and mouse CD47.

In this work two different detection systems were tested. They showed similar results (Fig. 15), except for the color intensity. The Avidin-Biotin based kit stains the cells in a very intense brown color compared to the polymer-based kit. The isotype control showed positive staining too. Because of high background staining (not only the cell membrane but the whole cell was stained) of the polyclonal rabbit primary AB (ab175388), we decided to test a monoclonal one. As shown in figure 16, we got no CD47 signal with the mouse monoclonal AB.

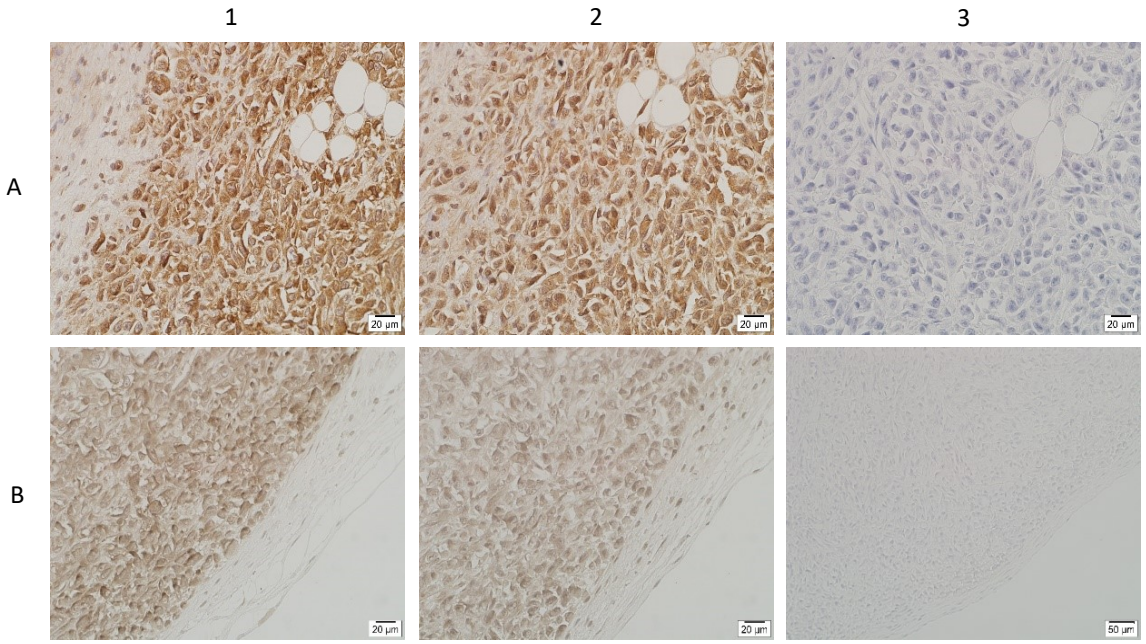

Figure 15 Anti-CD47 staining with two different detection systems (*A) Vectastain ABC kit (B) polymer- based VitroVivo Biotech kit (1) sections treated with primary (rabbit, ab175388) + secondary AB (2) isotype control (Rabbit IgG isotype control bs-0295P) (3) secondary control. Scale bar: 20 µm; Magnification: 40x*

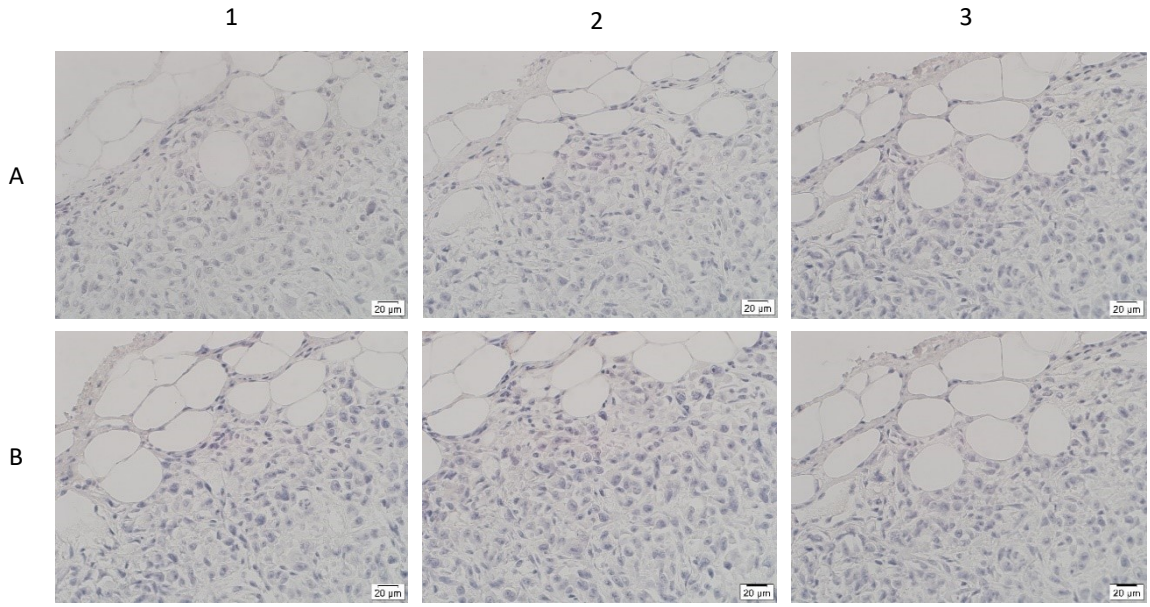

Figure 16 Anti-CD47 staining with mouse monoclonal AB (ab213079), mouse IgG isotype control and a polymer-based detection system *(A1) primary AB in the dilution 1:1000 was used (B1) 1:500 dilution of the antibody (2) isotype control (3) secondary control. Scale bar: 20 µm; Magnification: 40x*

Next, the rabbit isotype control (ab172730) was tested. As shown in figure 17, the isotype control was negative this time.

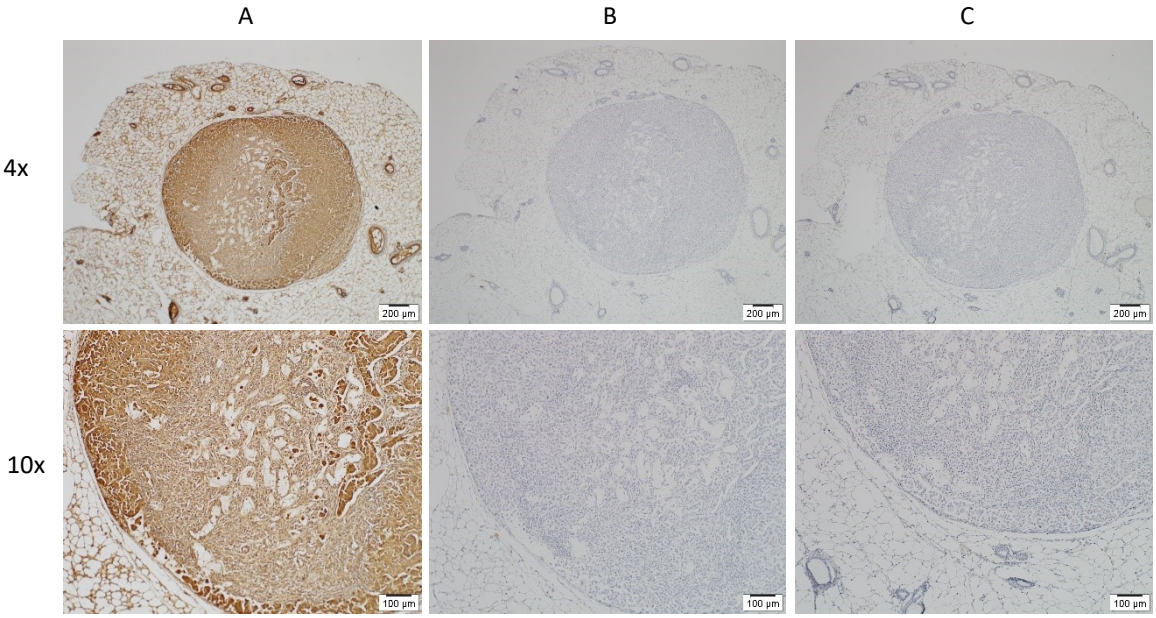

Figure 17 Anti-CD47 staining of a LN with rabbit isotype control (ab172730), primary polyclonal AB (ab175388) and Vectastain ABC kit. *(A) Positive CD47 signal with high background staining is visible (B) isotype control is negative (C) secondary control is negative. Scale bar: 200 µm, 100 µm; Magnification: 4x, 10x*

Best results were obtained with the **rabbit monoclonal anti-CD47 AB (ab218810)** in the dilution **1:2000** (Batch concentration: 0,52 mg/ml, reacts to: human) and rabbit IgG isotype monoclonal [EPR25A] control (ab172730) in same concentration as pAB, which were applied for further CD47 stainings (Fig. 18). The Vectastain ABC kit was used as detection system.

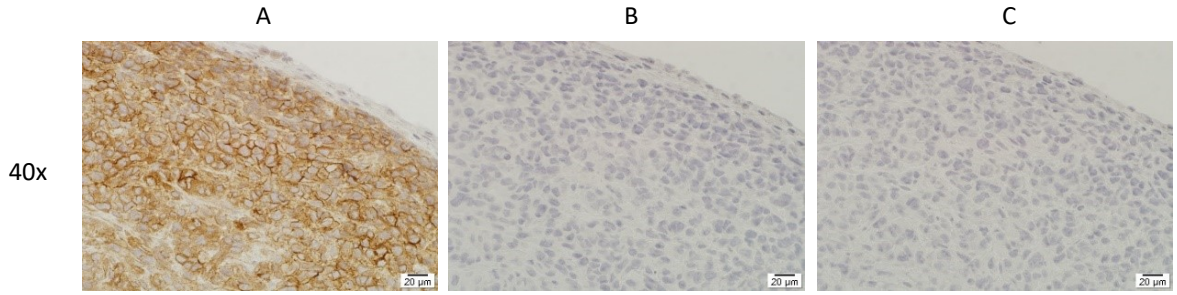

Figure 18 Anti-CD47 staining of a tumor from the in vivo experiment 1 from the treated IL2-P-Fc group (MCT-0044 TU RI) using the rabbit monoclonal anti-CD47 AB (ab218810) in the dilution 1:2000. *(A) brown staining shows positive and specific CD47 signal on the cell membrane of the human tumor cells, tumor capsule and connective tissue of the mouse are not stained, because this antibody only reacts with human CD47 (B) isotype control is negative (C) secondary control shows negative staining. Scale bar: 20 µm; Magnification: 40x*

7.2.2. Optimization of the luciferase staining protocol

In this thesis four different anti-luciferase antibodies were tested (Fig. 19) and with one out of four we got specific staining results (goat pAB ab181640). The others showed cross-reactivity with e.g. muscle tissue. Finally, the **goat primary AB to firefly luciferase (ab181640)** in the dilution **1:1000** (stock concentration: 1mg/ml) and goat IgG isotype control (bs-0294P) were used for the detection of luciferase. As detection system we chose the Avidin-Biotin free VitroVivo Biotech polymer-based kit (1-step Anti-Goat Polymer-Based IHC DAB kit).

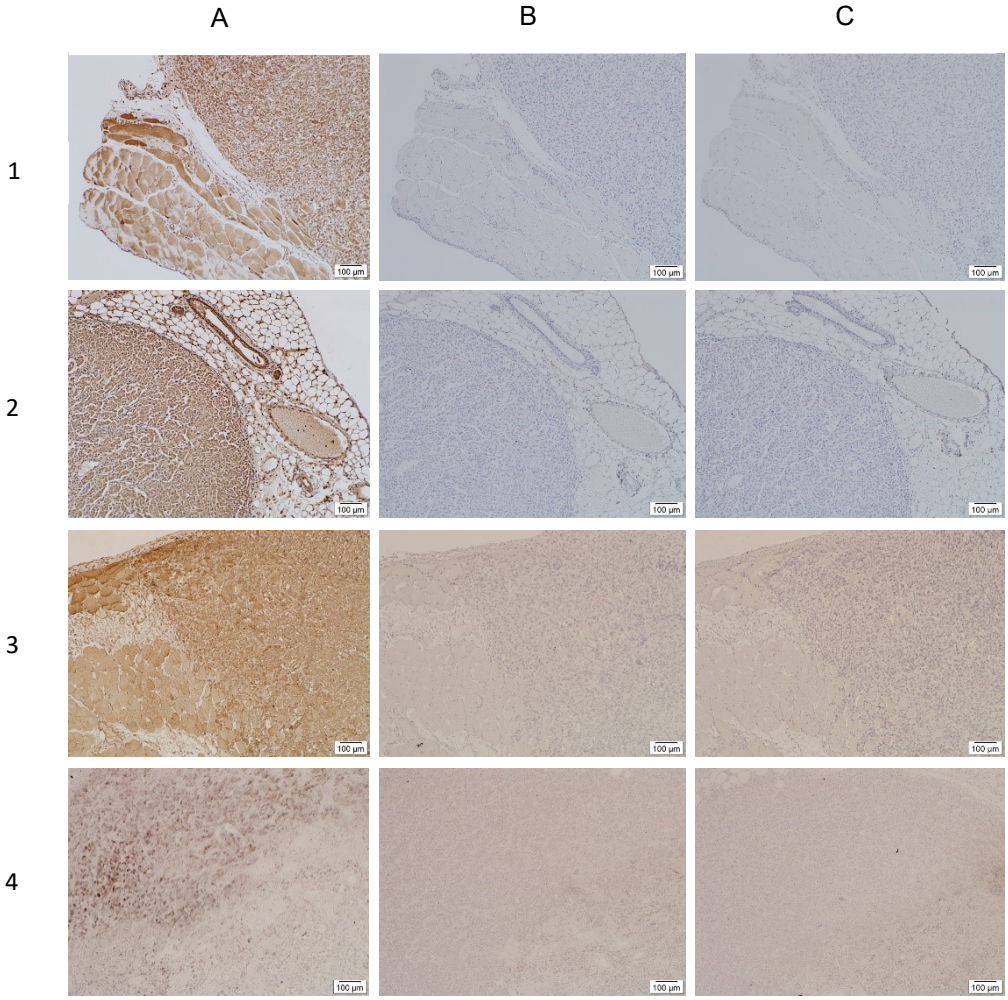

Figure 19 Testing of different anti-luciferase antibodies. *(A) sections incubated with primary and secondary AB (B) isotype control (C) Secondary control (1) rabbit polyclonal primary AB (ab21176) (2) rabbit polyclonal primary AB (bs-8539R) (3) rabbit polyclonal primary AB (27986-1-AP) (4) goat polyclonal primary AB (ab181640). Scale bar: 100 µm; Magnification: 10x*

Compared to the CD47 staining, the luciferase staining is not that intense in brown color. This depends on the one hand on the detection kit which was used and on the other hand luciferase might not be that highly expressed such as CD47. The tumor cells were transduced with the Luc gene and only around 70-80 % of the cells were positive from the beginning. It was observed that the necrotic parts of the tumor were mainly negative for luciferase. In summary, the areas which are stained are comparable with the CD47 staining, which means that the antibodies are specific. Especially the organs or lymph nodes which show metastasis (Fig. 20) allow a comparison between these two stainings.

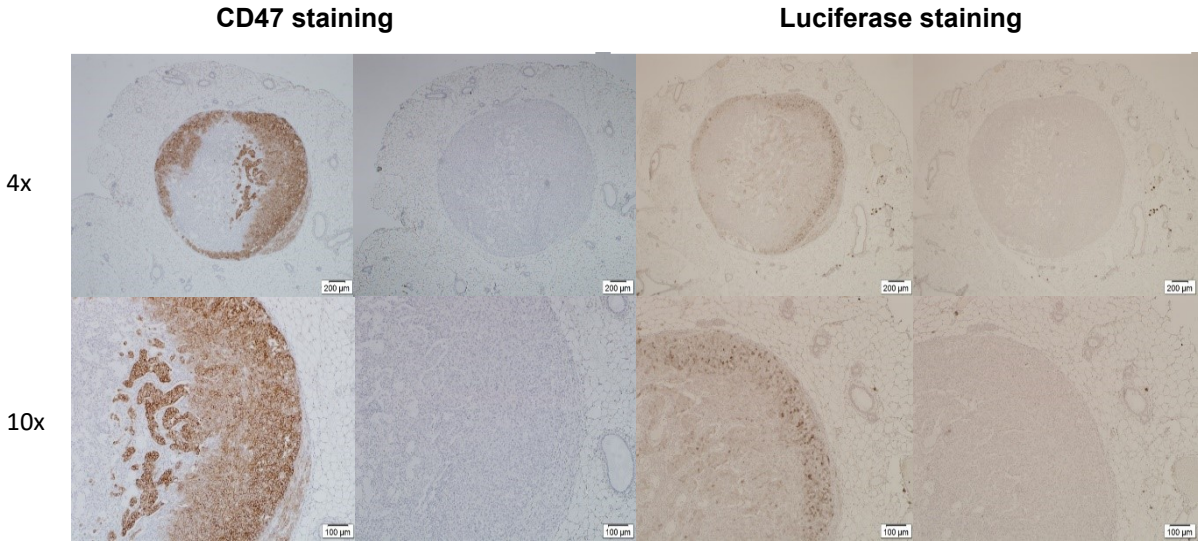

Figure 20 Positive CD47-areas *(rabbit monoclonal anti-CD47 AB (ab218810))* ***compared with luciferase staining*** *(goat polyclonal primary AB (ab181640)). Scale bar: 200 µm,100 µm; Magnification: 4x, 10x*

7.3. Histological examination of ex vivo transfected tumors 34 days after transfection

7.3.1. CD47 staining

All the groups showed positive CD47 staining with the rabbit monoclonal anti-CD47 AB (ab218810) at a 1:2000 dilution and rabbit IgG isotype monoclonal control (ab172730), which was expected. Of course, the tumor grows and 34 days after the transfection, no fusion protein is left in the tissue. That's why CD47 cannot be blocked anymore and can be detected completely in the IL2-P-Fc group. The bb-mCherry and untransfected group do not express the fusion protein. Accordingly, the CD47 staining should look similar in all the samples as shown in the figures below.

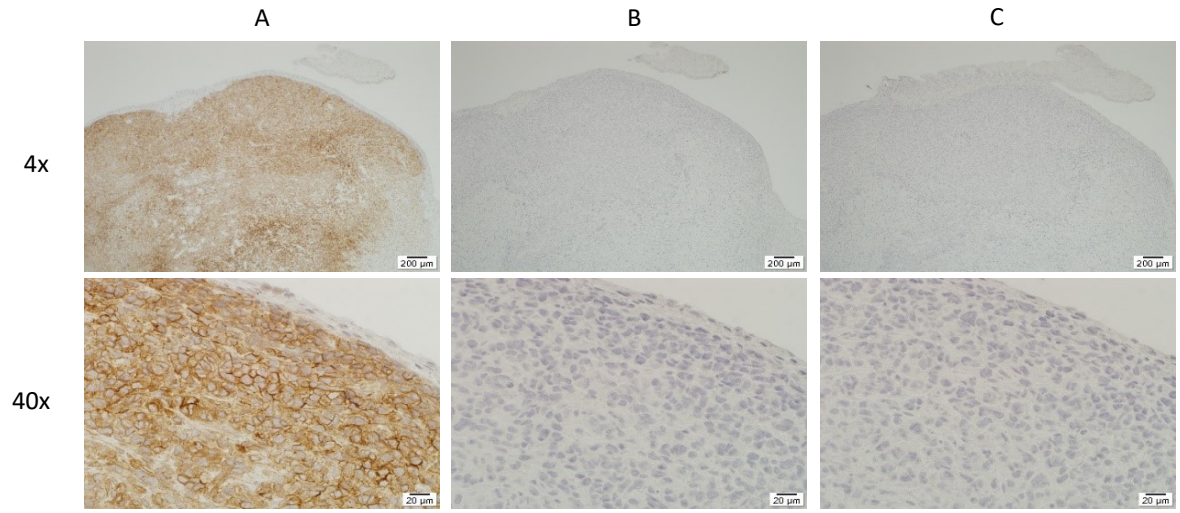

Figure 21 CD47 staining of a tumor from the treated IL2-P-Fc group (MCT-0044 TU RI). *(A) brown staining shows positive CD47 signal on the cell membrane of the tumour cells (B) isotype control (C) secondary control. Scale bar: 200µm and 20 µm; Magnification: 4x, 40x*

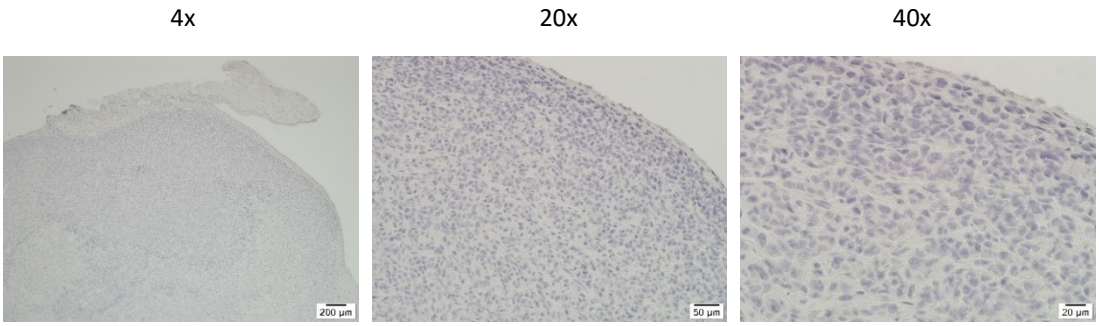

Figure 22 Buffer control from CD47 staining on tissue from IL2-P-Fc group (MCT-0044 TU RI). *Scale bar: 200 µm, 50 µm, 20 µm; Magnification: 4x, 20x, 40x*

The results of the buffer control were negative like the secondary control or isotype control. Concerning this reason and a lack of space only the tissue treated with primary AB and secondary AB, the isotype control and the secondary control are shown below.

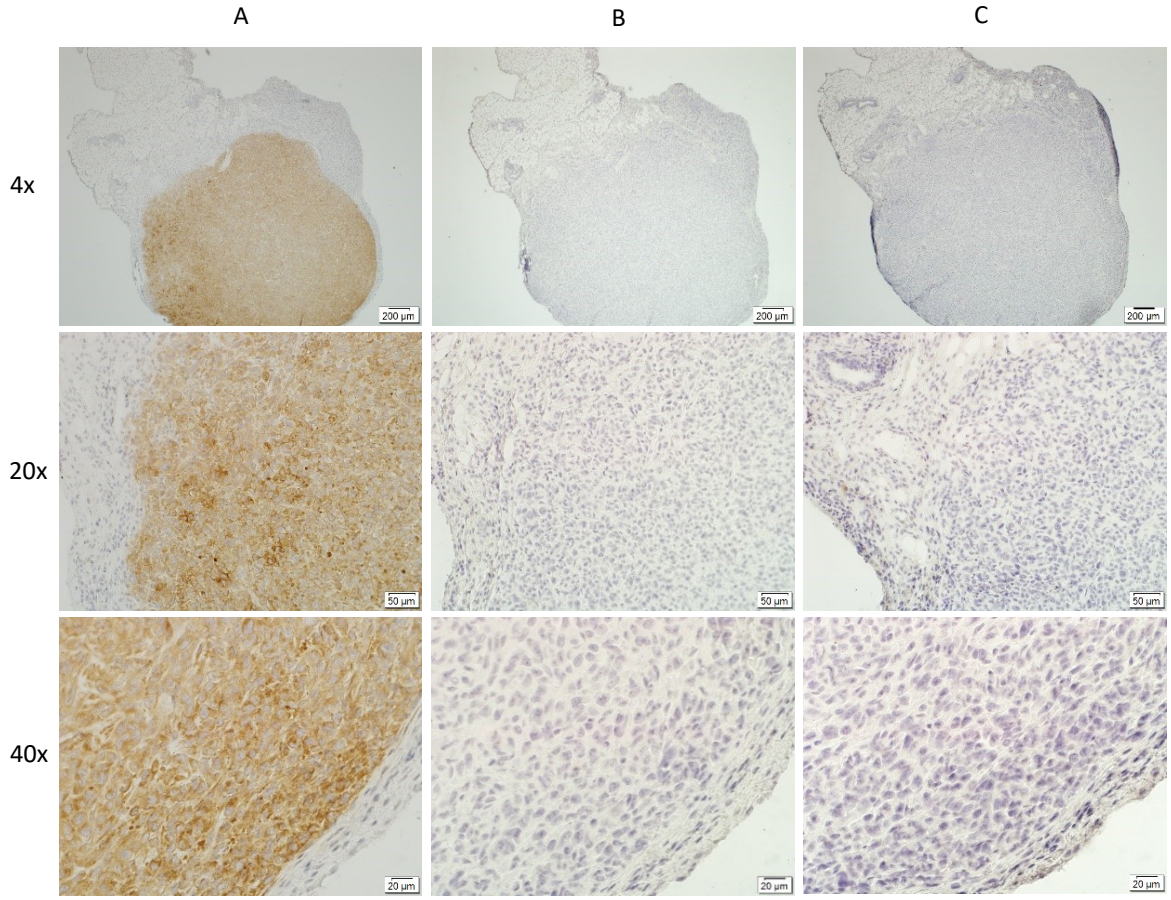

Figure 23 CD47 staining of another sample from the treated IL2-P-Fc group (MCT-0046 TU RI). *(A) brown staining shows positive CD47 signal caused by the reaction of DAB (B) isotype control (C) secondary control. Scale bar: 200µm, 50 µm and 20 µm; Magnification: 4x, 20x, 40x*

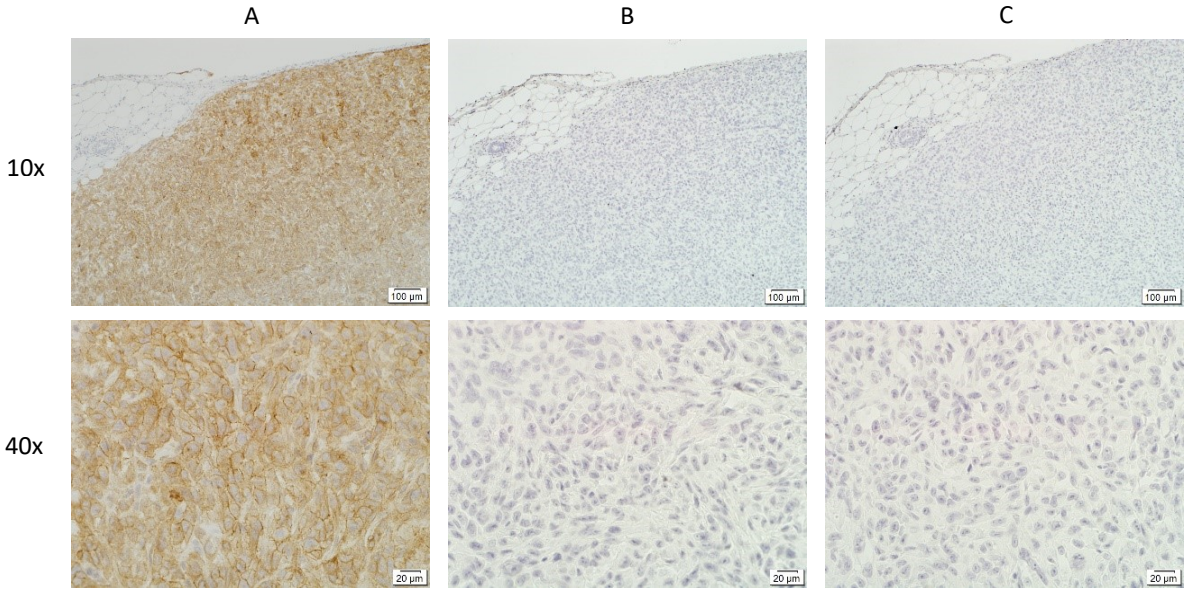

Figure 24 CD47 staining of a tumor from the bb-mCherry group (AGE-0482 TU RI). *(A) positive CD47 staining (B) isotype is negative (C) no brown staining with secondary control. Scale bar: 100 µm and 20 µm; Magnification: 10x, 40x*

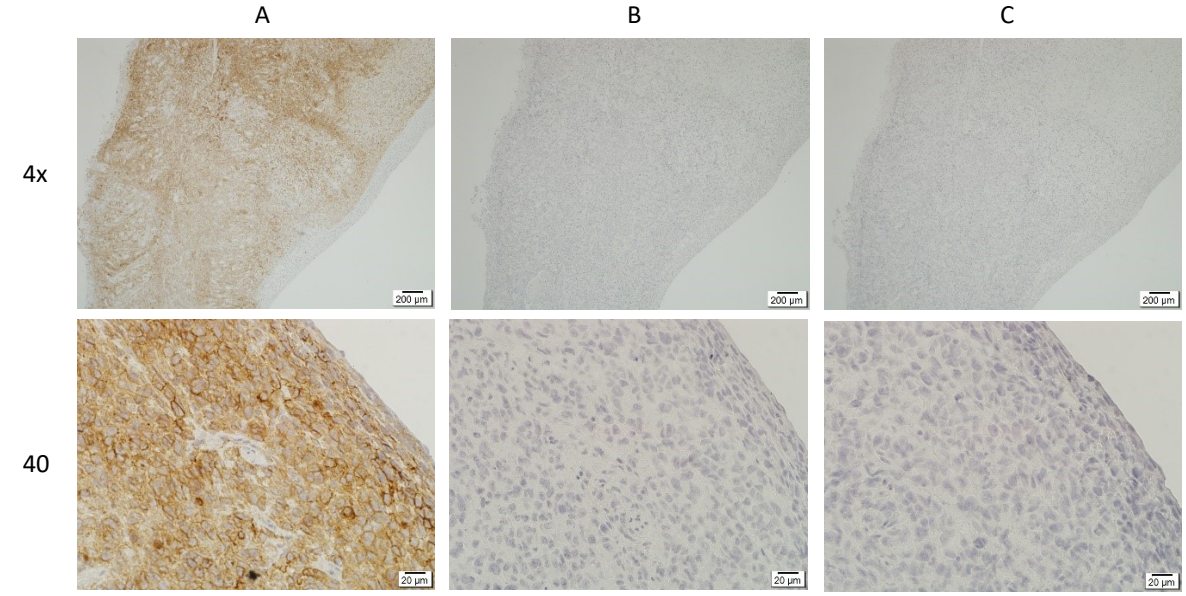

Figure 25 CD47 staining of a tumor from the untransfected group (MCT-0043 TU LE). *(A) brown staining shows positive CD47 signal, (B) isotype control (C) secondary control. Scale bar: 200µm and 20 µm; Magnification: 4x, 40x*

During in vivo imaging, metastasis in other organs such as lymph nodes or pancreas were observed. These organs or lymph nodes with positive signal monitored *via* 2D BLI were harvested and histologically analyzed 34 days after implantation (Fig. 26-27). Especially in the untransfected group metastases could be found. The antibody which was used for the CD47 IHC stainings is directed to human tissue, which ensures that the tumor cells in the infiltrated areas really derived from the injected human cancer cells.

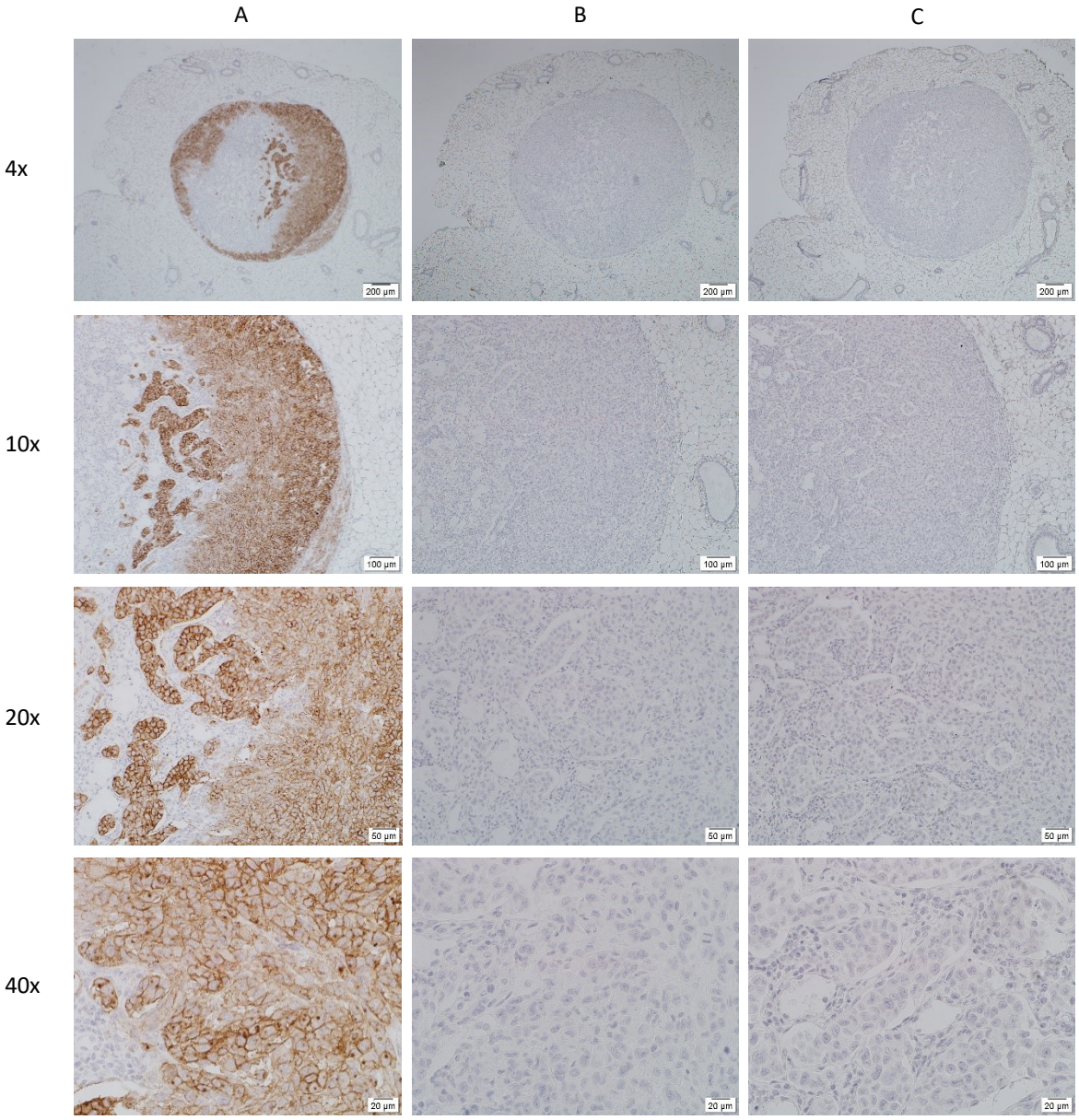

Figure 26 CD47 staining of a metastasized lymphnode from the untransfected group (MCT-0042). *(A) brown staining shows tumor infiltration in the lymph node (B) isotype control (C) secondary control. Scale bar: 200µm, 100 µm, 50 µm and 20 µm; Magnification: 4x, 10x, 20x, 40x*

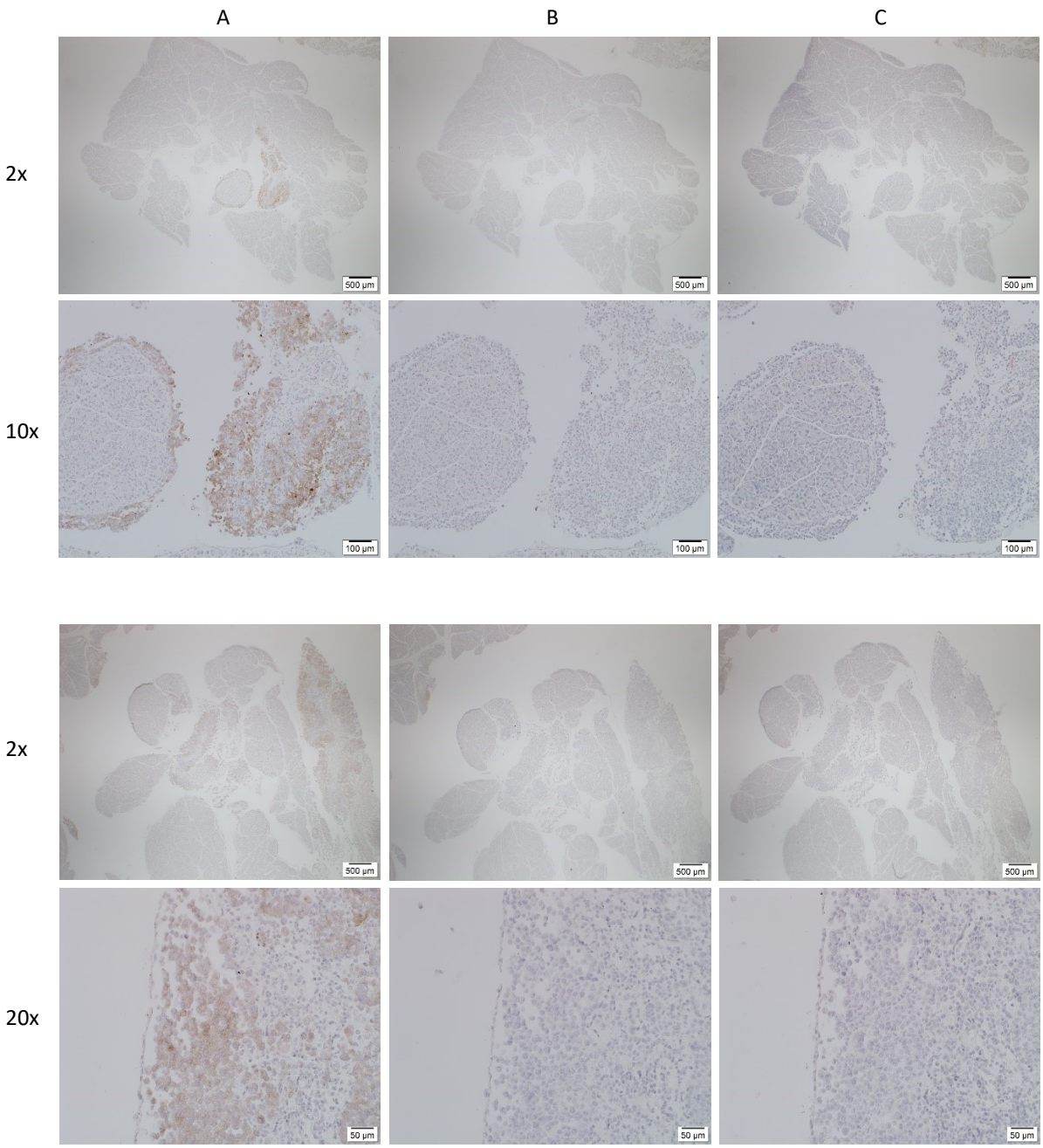

Figure 27 CD47 staining of pancreas surrounded by visceral fat tissue which belongs to the untransfected group (MCT-0043). *(A) different parts of the pancreas which are stained in brown color are infiltrated with cancer cells (B) isotype control (C) secondary control. Scale bar: 500µm, 100µm, 50 µm; Magnification: 2x, 10x, 20x*

7.3.2. Luciferase staining

All the samples were afterwards stained to detect luciferase using the primary goat anti-firefly luciferase AB (ab181640) at a 1:1000 dilution and the goat IgG isotype control (bs-0294P). Brown staining was observed in every tissue and there were no significant differences noticeable between the groups.

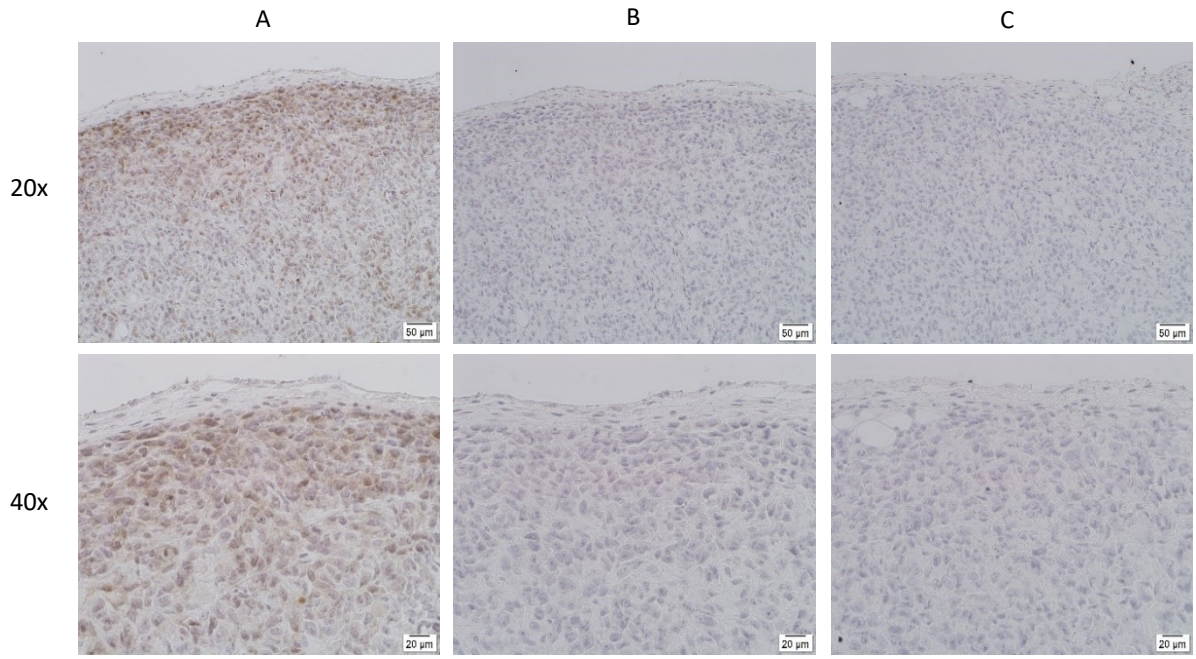

Figure 28 Positive luciferase signal in tissue from IL2-P-Fc group (MCT-0046 TU RI). *(A) sections treated with primary and secondary AB (B) no unspecific reaction between the tissue and the isotype control (C) secondary control. Scale bar: 50 µm and 20 µm; Magnification: 20x, 40x*

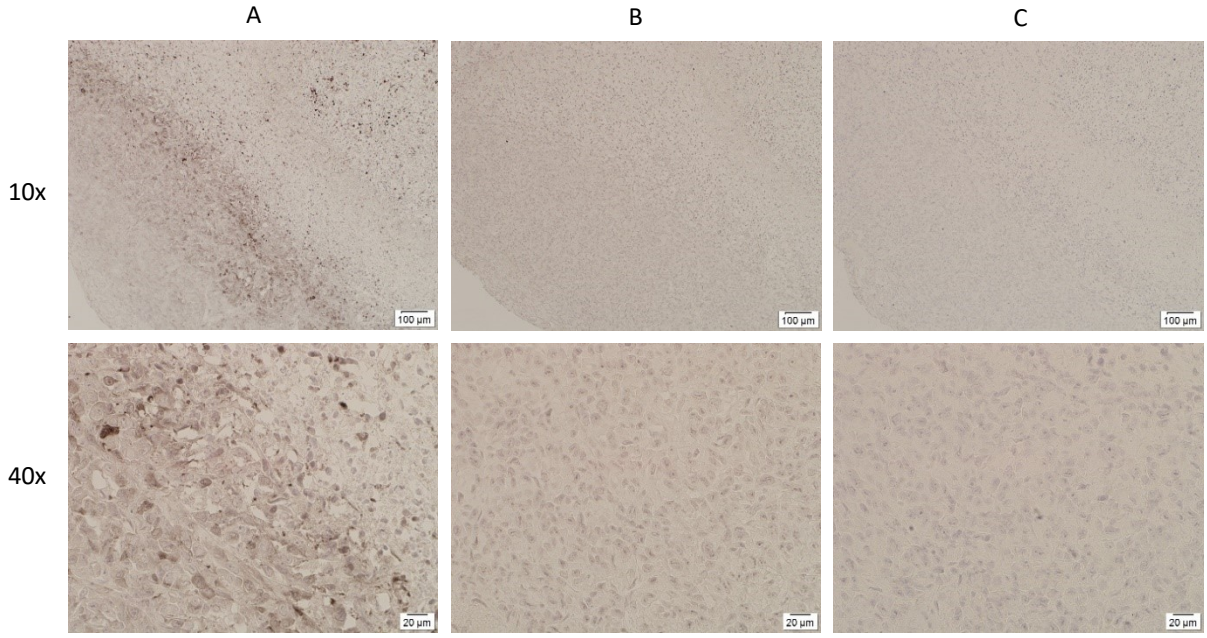

Figure 29 Detection of the enzyme luciferase in bb-mCherry group (AGE-0482 TU RI). *(A) brown staining shows positive luciferase signal (B) isotype control (C) secondary AB control. Scale bar: 100 µm and 20 µm; Magnification: 10x, 40x*

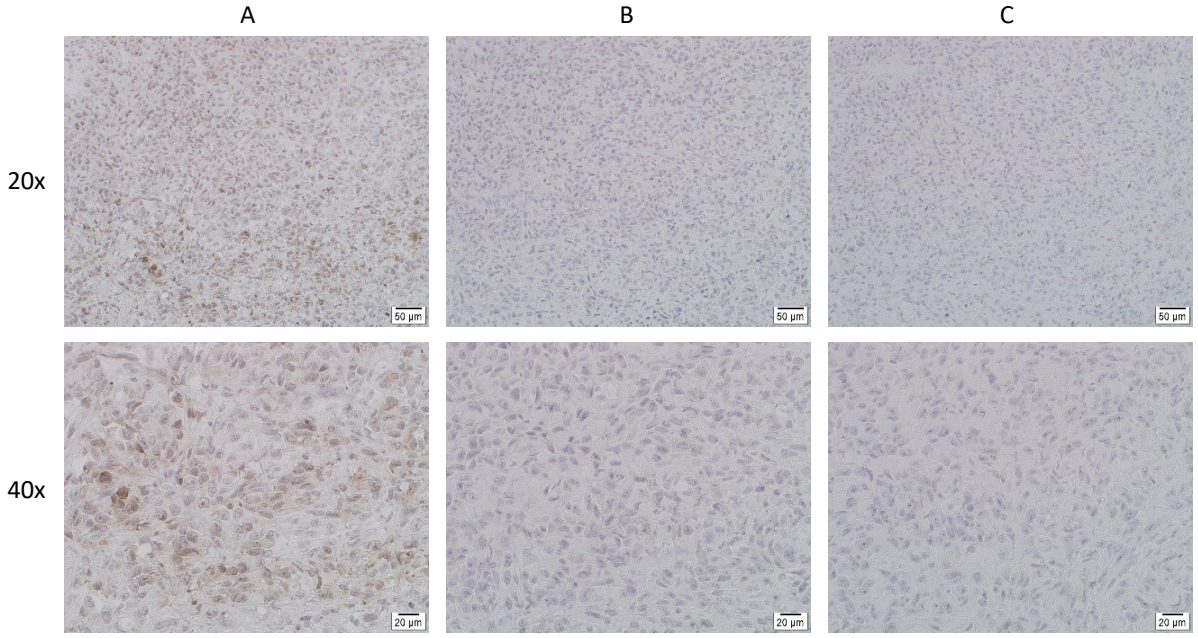

Figure 30 Detection of the enzyme luciferase in untransfected tumor tissue (MCT-0043 TU LE). *(A) positive luciferase signal (B) isotype control (C) secondary AB control. Scale bar: 50 µm and 20 µm; Magnification: 20x, 40x*

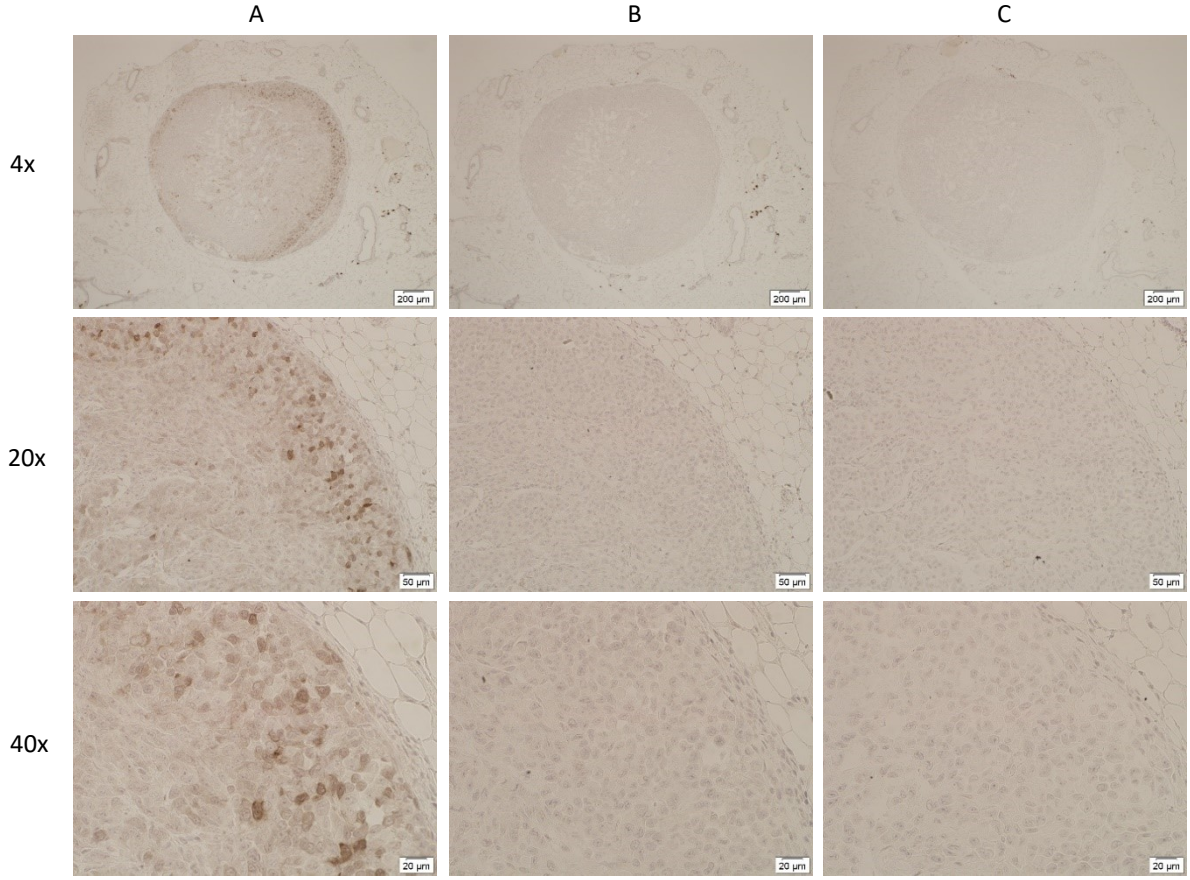

Figure 31 Positive luciferase signal in metastasized lymph node of a mouse from the untransfected group (MCT-0042). *(A) brown staining caused by the reaction of DAB (B) no staining with isotype control (C) secondary control. Scale bar: 200µm, 50 µm and 20 µm; Magnification: 4x, 20x, 40x*

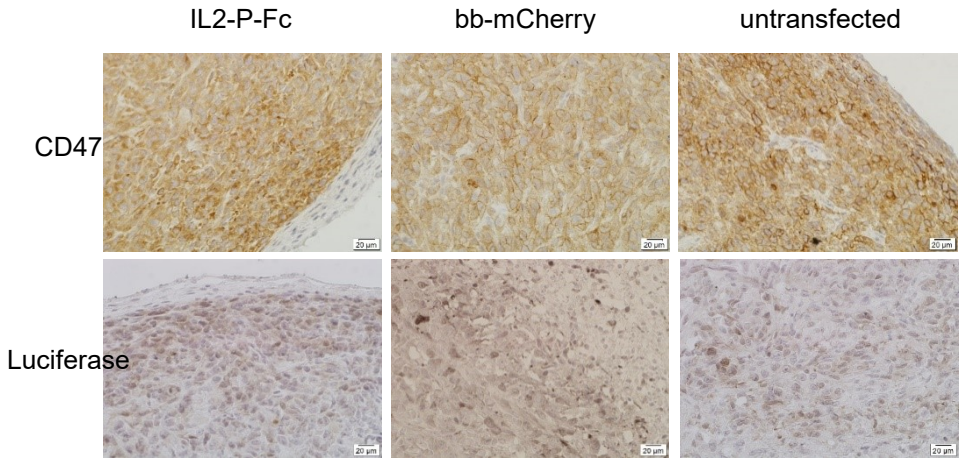

Figure 32 Comparison of CD47 stained areas with luciferase staining *Scale bar: 20 µm; Magnification: 40x*

7.3.3. Staining to detect the Fc-part

For this staining the goat anti-human IgG Fc (HRP) preadsorbed primary antibody (ab98624) at a 1:200 dilution and the goat IgG isotype control (bs-0294P) were consulted. In the first animal experiment, after 34 days of tumor growth, we did not expect any fusion protein left in the tissue. The results (Fig. 33-34) confirm our suggestions. The staining was performed with a sample from the IL2-P-Fc group, where the Fc-part should be detected if there was fusion protein left binding to CD47. As a negative control, the bb-mCherry group was included in the staining procedure. A secondary AB was added onto the anti-Fc AB by mistake, which is not necessary since the anti-Fc AB is already preabsorbed with HRP.

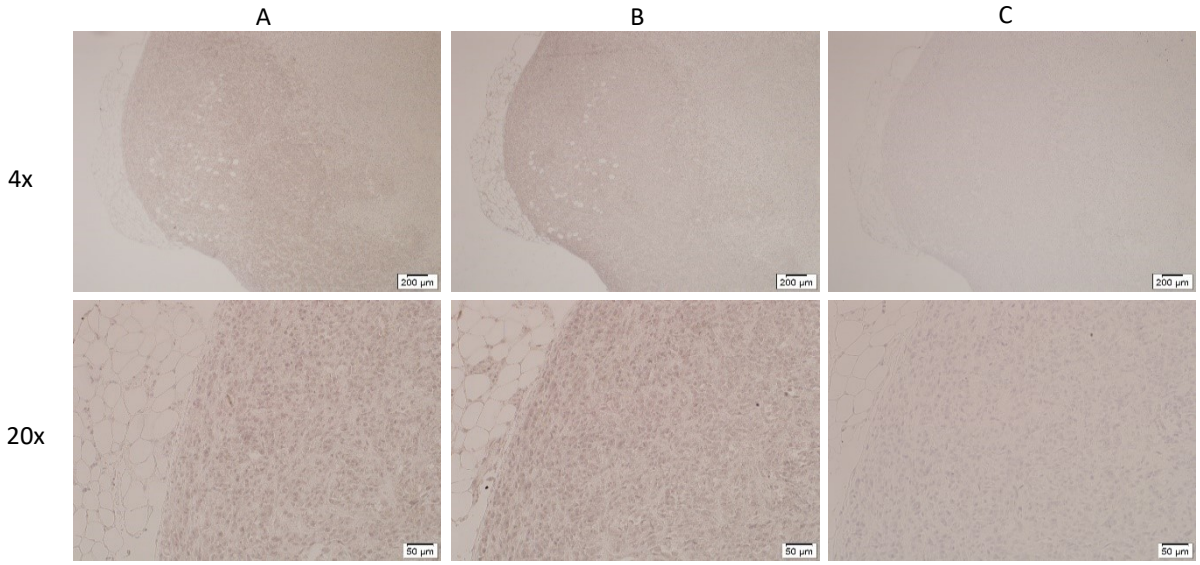

Figure 33 Immunohistochemical detection of the Fc-part of the fusion protein IL2-P-Fc on tumor tissue containing the transfection of IL2-P-Fc (MCT-0046 TU RI). *(A) treatment with AB against Fc-part showed negative staining results (B) isotype control (C) secondary control. Scale bar: 200µm and 50µm; Magnification: 4x, 20x*

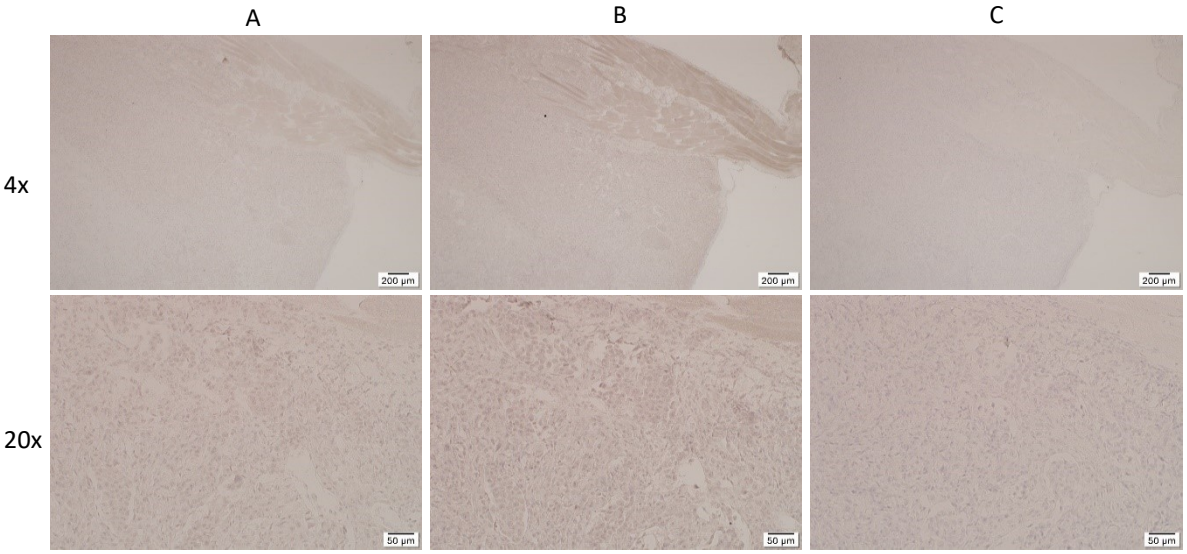

Figure 34 Immunohistochemical detection of the Fc-part on negative control bb-mCherry (AGE-0482 TU RI). *(A) treatment with AB against Fc-part showed negative staining results (B) isotype control (C) secondary control. Scale bar: 200µm and 50µm; Magnification: 4x, 20x*

7.3.4. H&E staining

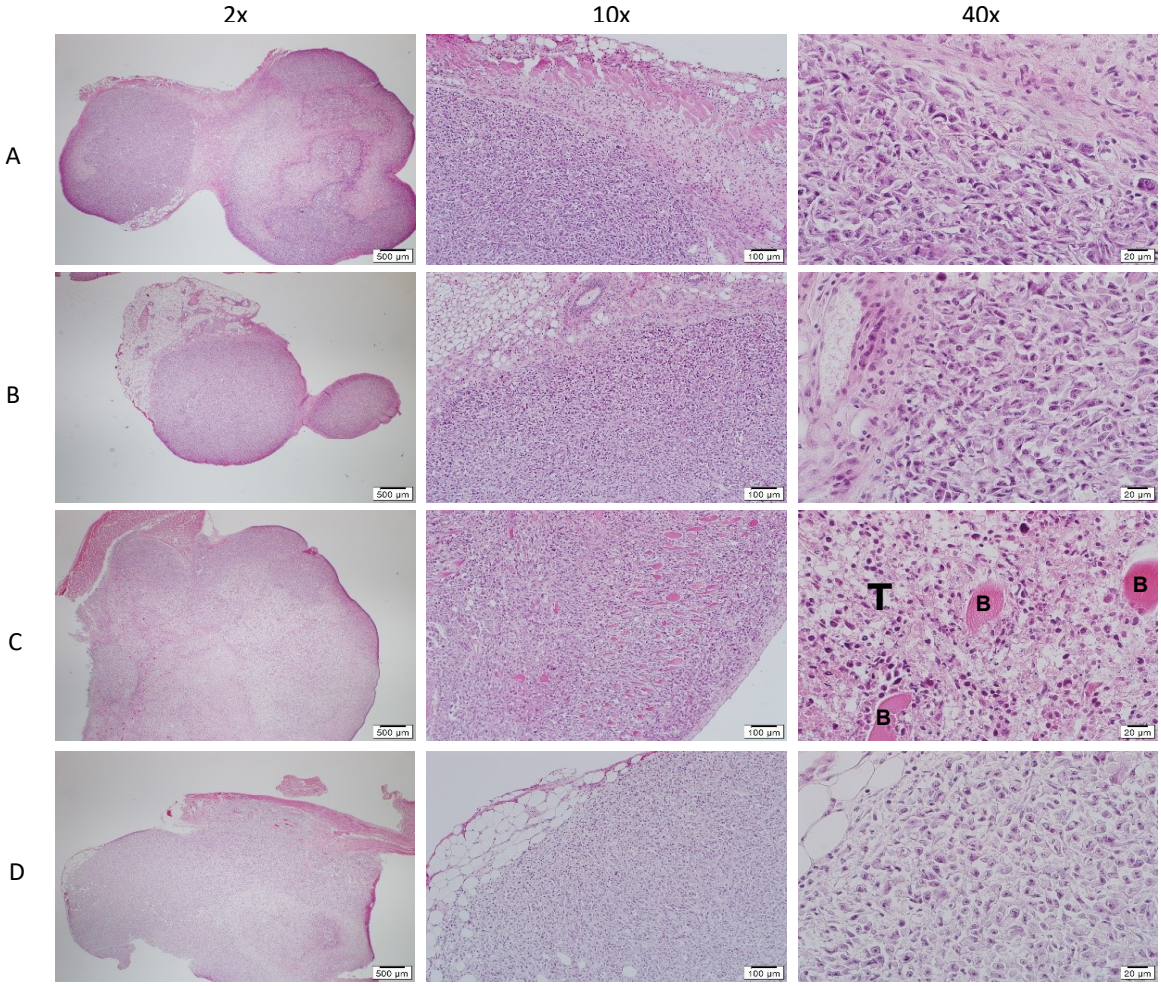

Figure 35 Hematoxylin and Eosin staining of tumor samples from the in vivo experiment 1. *(A+B) tumours from IL2-P-Fc group (C) untransfected group, tumor **(T)** is well supplied with blood (**B**) (D) tumor containing the bb-mCherry plasmid. Scale bar: 500µm, 100µm, 20 µm; Magnification: 2x, 10x, 40x*

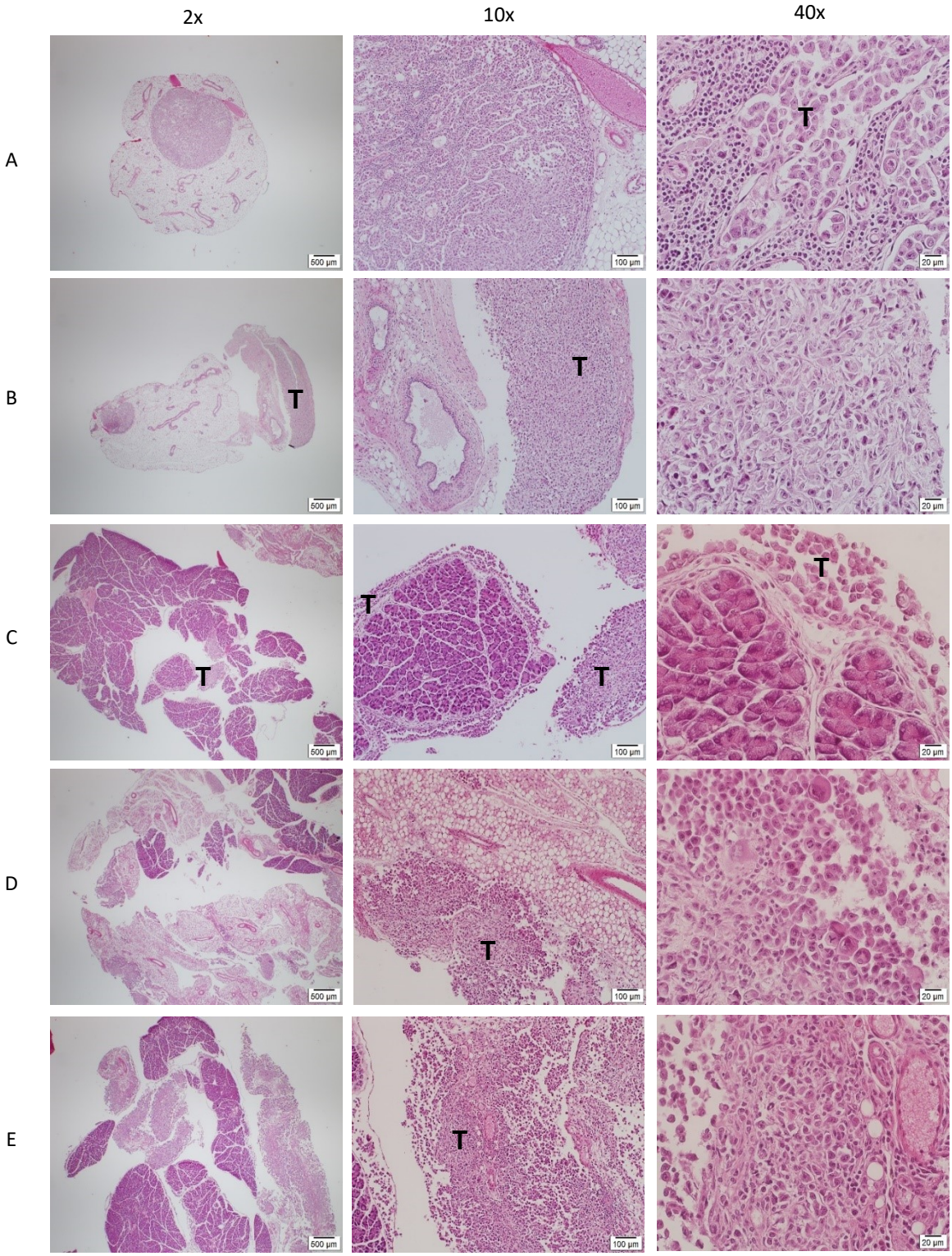

***Figure 36 Hematoxylin and Eosin staining of lymph nodes and pancreas** (**T=metastatic tumor areas**). (A) infiltrated lymph node (B) lymph node with positive tissue beside it (C+D+E) infiltrated pancreas and visceral fat. Scale bar: 500µm, 100µm, 20 µm; Magnification: 2x, 10x, 40x*

7.4. Histological examination of ex vivo transfected tumors 25 days after transfection

7.4.1. CD47 staining

The staining process was the same as in the first experiment and no differences between the groups were visible. Because of the long timeframe between transfection and euthanasia of the mice, no blocking of CD47 was expected in the IL2-P-Fc group.

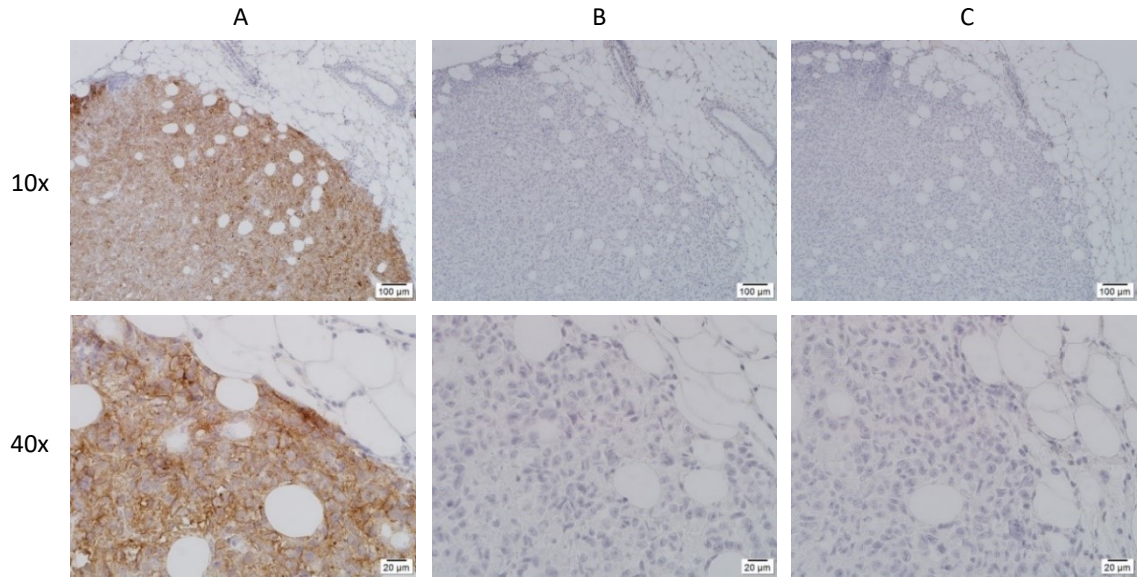

Figure 37 CD47 staining of tumor tissue from the IL2-P-Fc group (MCT-115 TU LE). *(A) strong positive CD47 signal visible (B) isotype control (C) secondary control. Scale bar: 100µm, and 20 µm; Magnification: 10x, 40x*

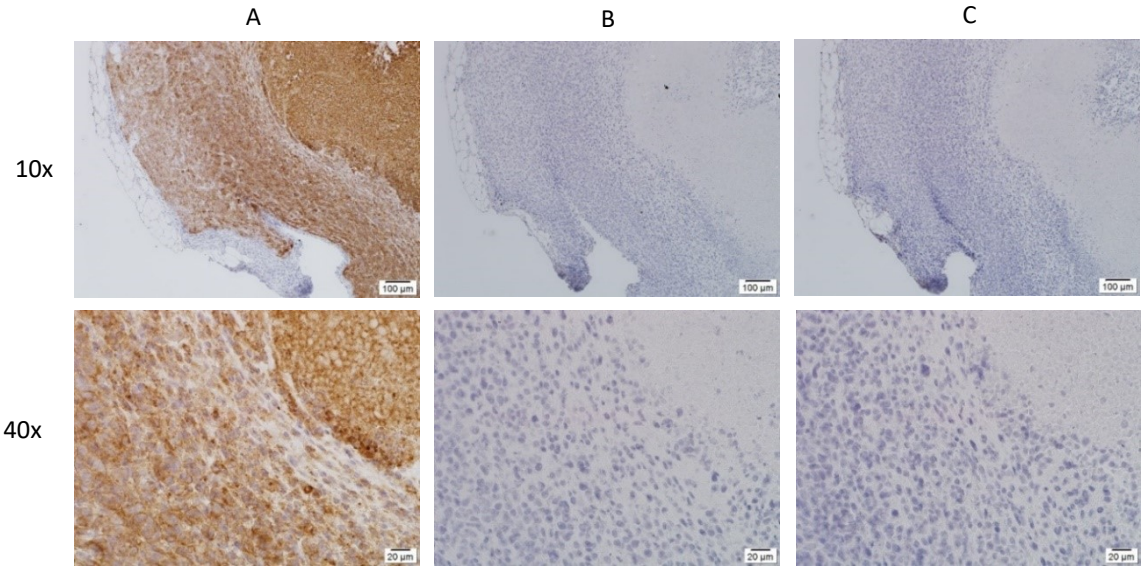

Figure 38 CD47 staining of another IL2-P-Fc sample (MCT-114 TU LE). *(A) brown staining indicates for the overexpression of the CD47 protein (B) isotype control (C) secondary control. Scale bar: 100µm, and 20 µm; Magnification: 10x, 40x*

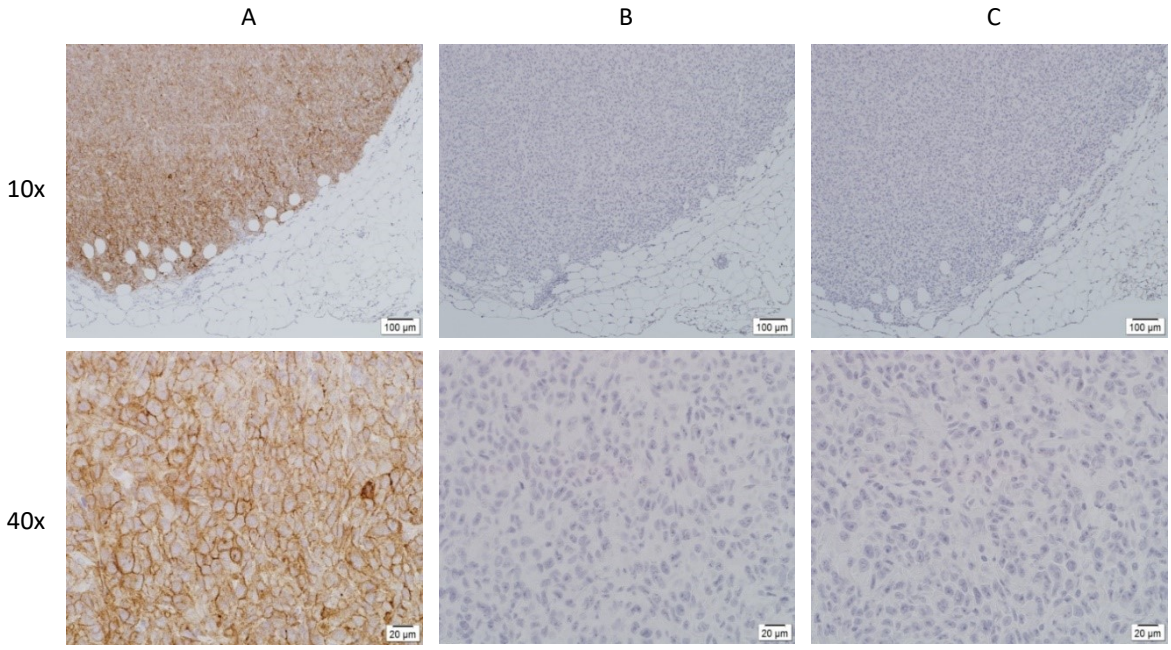

Figure 39 CD47 staining of a tumor from the IL2-P group (MCT-118 TU RI). *(A) brown staining caused by the reaction of DAB (B) isotype control (C) secondary control. Scale bar: 100µm, and 20 µm; Magnification: 10x, 40x*

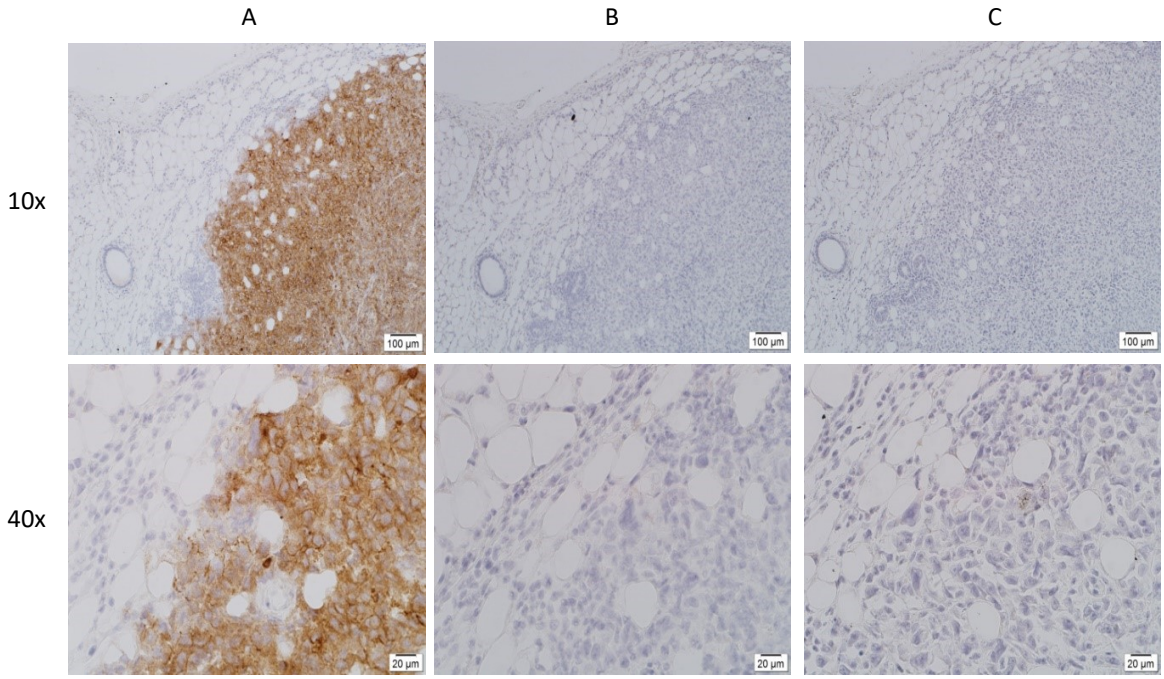

Figure 40 CD47 staining of a tumor from the IL2-P group (MCT-120 TU RI). *(A) positive CD47 signal (B) isotype control (C) secondary control. Scale bar: 100µm, and 20 µm; Magnification: 10x, 40x*

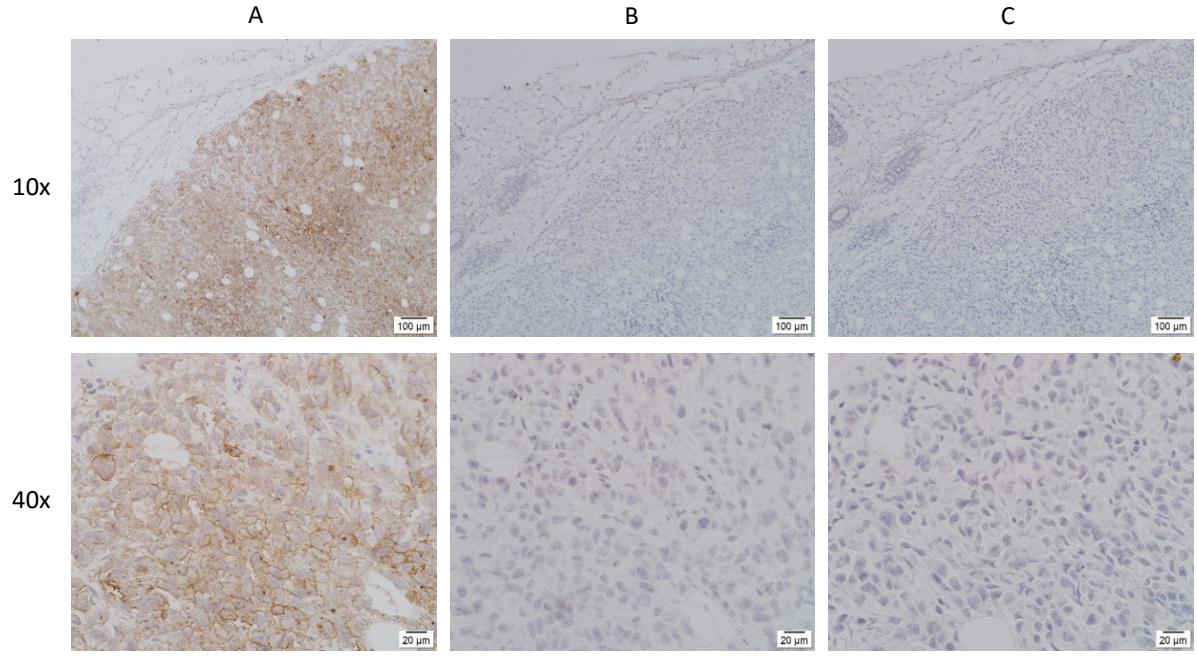

Figure 41 CD47 staining of a sample from the bb-mCherry group (SGE-0051 TU RI). *(A) brown staining shows positive CD47 signal (B) isotype control (C) secondary control. Scale bar: 100µm and 20 µm; Magnification: 10x, 40x*

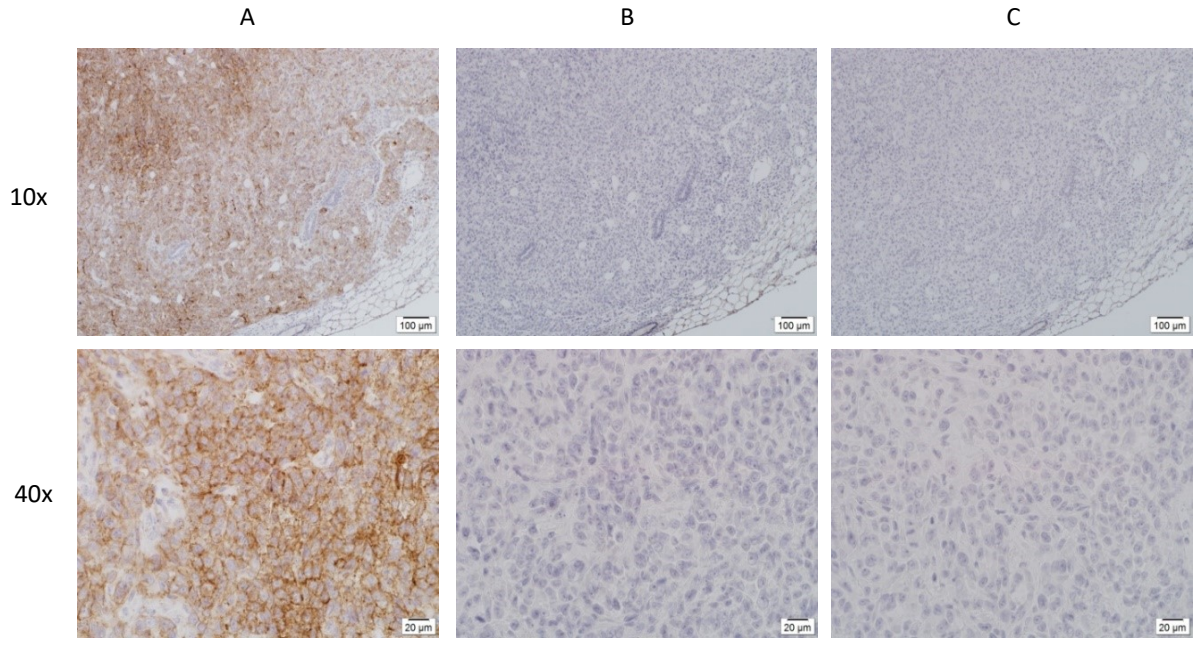

Figure 42 CD47 staining of a tumor from the untransfected group (AGE-0352 TU RI). *(A) positive CD47 signal (B) isotype control (C) secondary control. Scale bar: 100µm, 20 µm; Magnification: 10x, 40x*

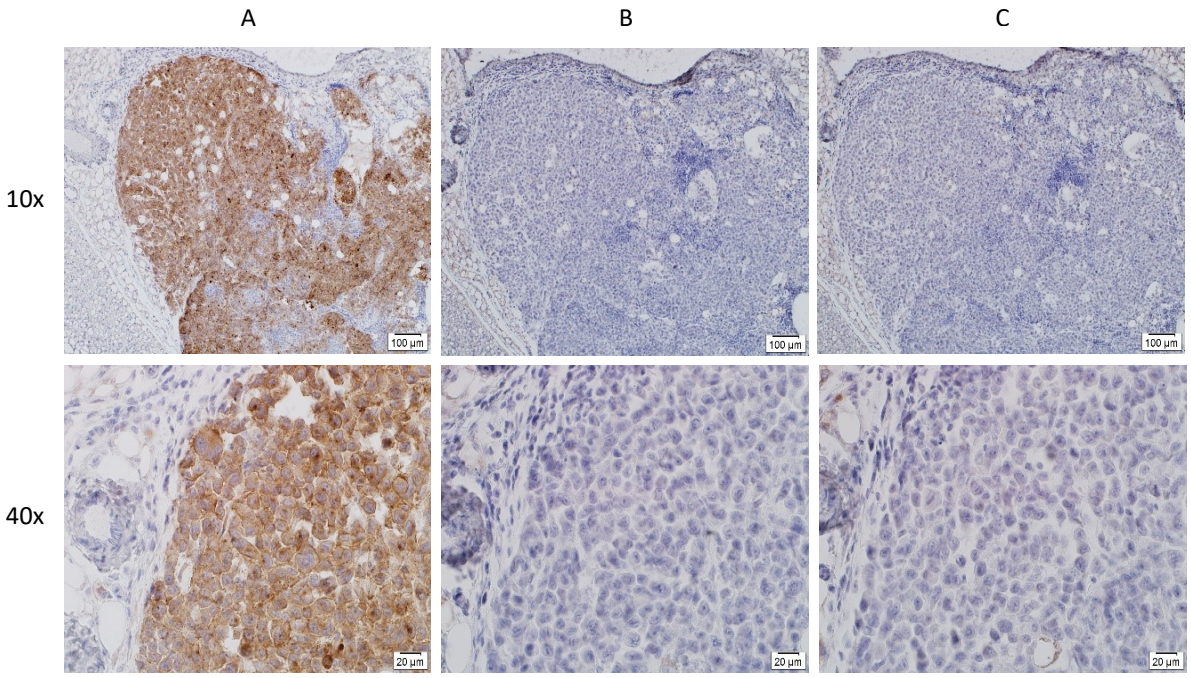

***Figure 43 CD47 staining of an axillary lymph node left side from the untranfected group (AGE-0352**). (A) brown staining shows infiltration of the LN with the injected tumor cells (B) isotype control is negative (C) secondary control. Scale bar: 100µm and 20 µm; Magnification: 10x, 40x*

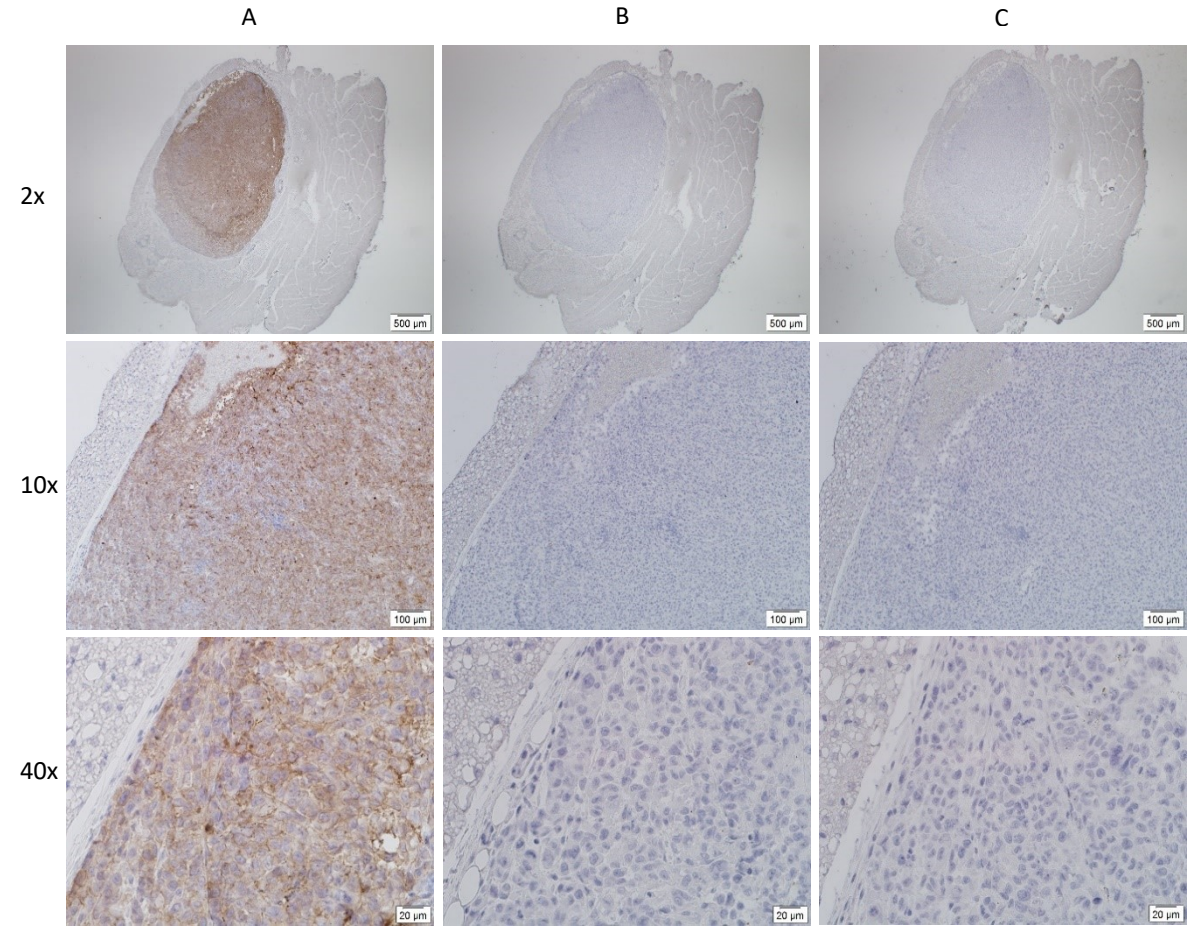

***Figure 44 CD47 staining of an axillary lymph node right side from the bb-mCherry group (SGE-0051).** (A) brown staining shows infiltration of the LN (B) isotype control (C) secondary control. Scale bar: 500µm, 100µm and 20 µm; Magnification: 2x, 10x, 40x*

7.4.2. Luciferase staining

The staining process was the same as in the first experiment. Luciferase-positive areas were found in all the samples.

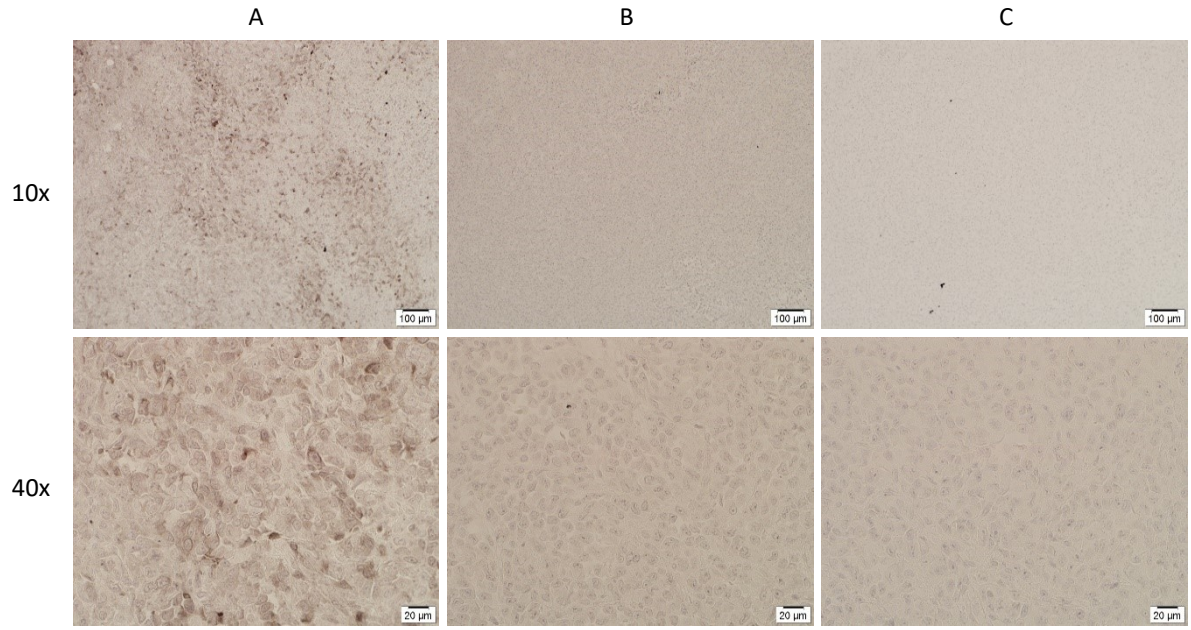

Figure 45 Detection of the enzyme luciferase in the injected MDA-MB-231 LM2-4 cells transfected with the IL2-P-Fc plasmid (MCT-115 TU LE). *(A) brown staining shows positive firefly luciferase signal (B) isotype control is negative (C) no brown staining with secondary AB control. Scale bar: 100µm, 20 µm; Magnification: 10x, 40x*

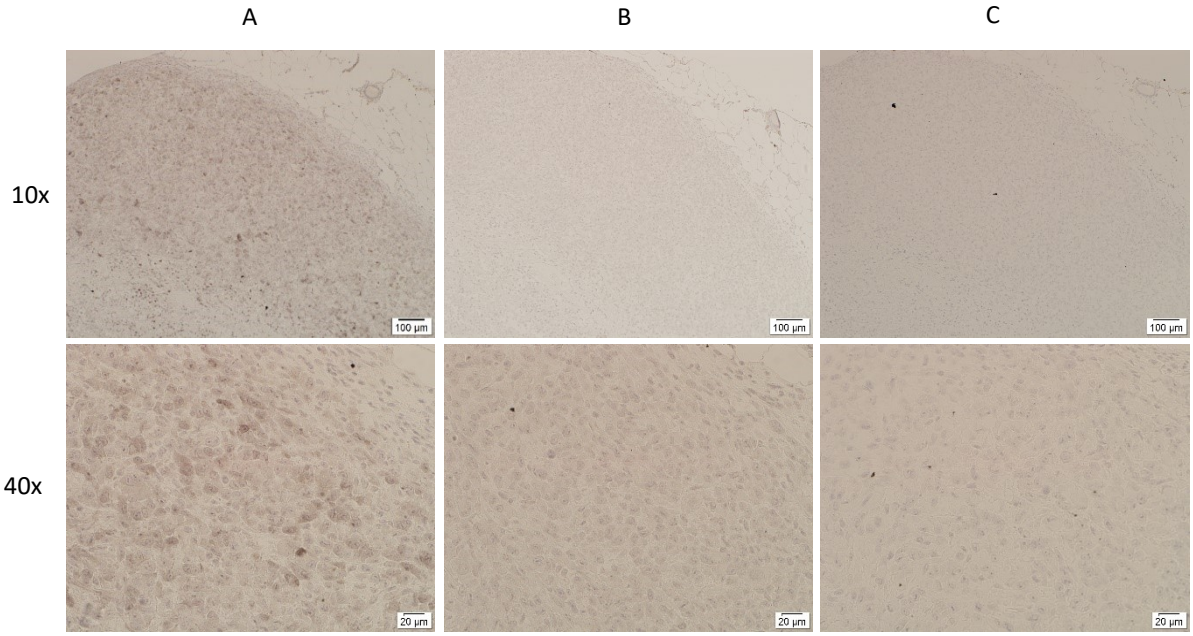

Figure 46 Detection of the enzyme luciferase in the injected MDA-MB-231 LM2-4 cell line transfected with IL2-P plasmid (MCT-118 TU RI). *(A) brown staining caused by the reaction of DAB (B) isotype control (C) secondary AB control. Scale bar: 100µm, 20 µm; Magnification: 10x, 40x*

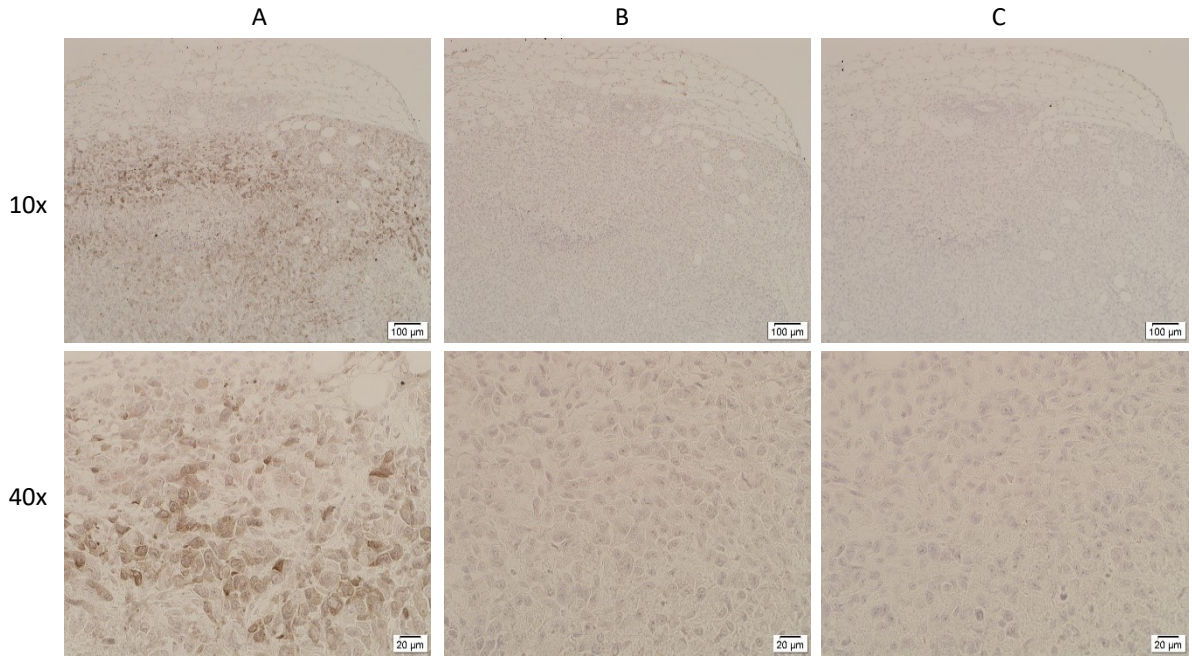

Figure 47 Detection of the enzyme luciferase in MDA-MB-231 LM2-4 cell line transfected with the bb-mCherry plasmid (SGE-0051 TU RI). *(A) brown staining visualizes the enzyme firefly luciferase (B) isotype control (C) 2nd AB control. Scale bar: 100µm, 20 µm; Magnification: 10x, 40x*

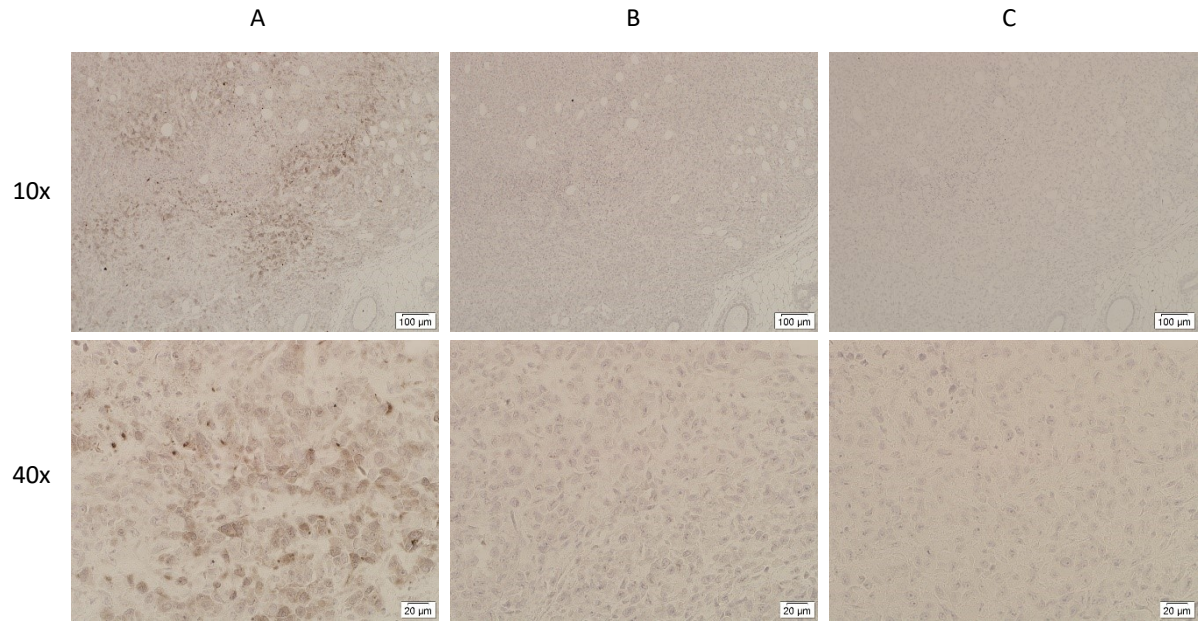

Figure 48 Detection of the enzyme luciferase in the untransfected MDA-MB-231 LM2-4 cells (AGE-0352 TU RI). *(A) positive luciferase staining (B) isotype control (C) secondary AB control. Scale bar: 100µm, 20 µm; Magnification: 10x, 40x*

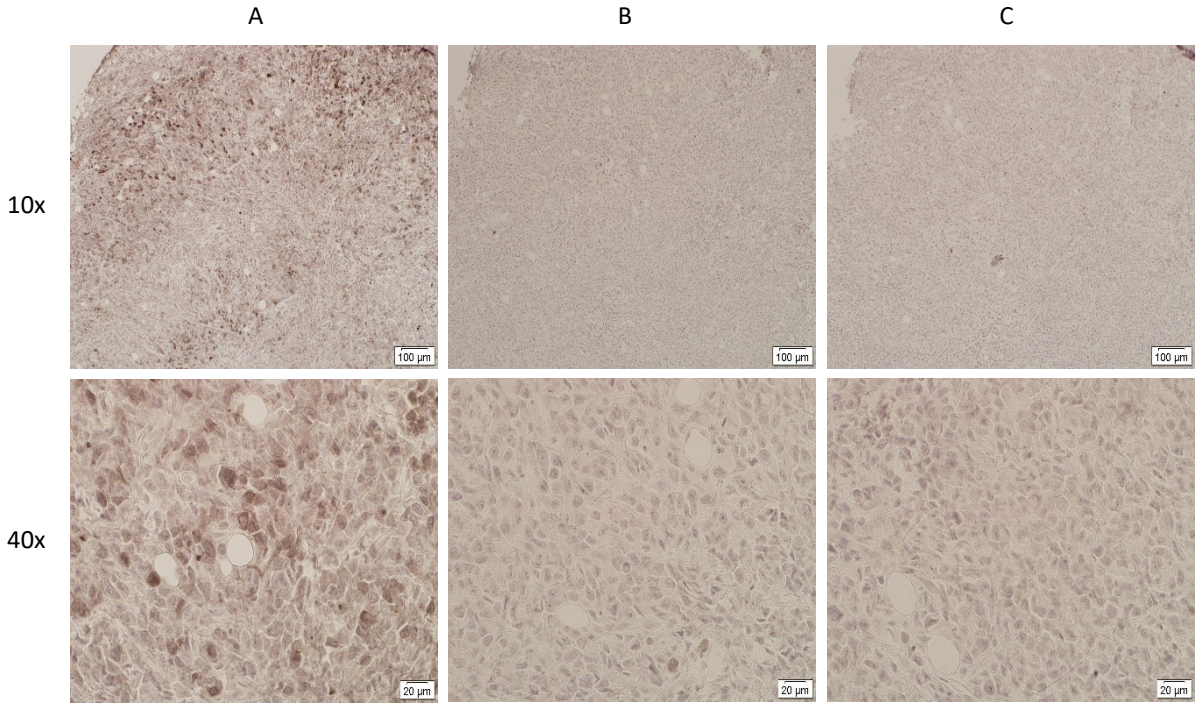

Figure 49 Detection of luciferase in a sentinel LN right side from a mouse which was part of the bb-mCherry group (MCT-121). *(A) positive luciferase staining (B) isotype control (C) secondary AB control. Scale bar: 100µm and 20 µm; Magnification: 10x, 40x*

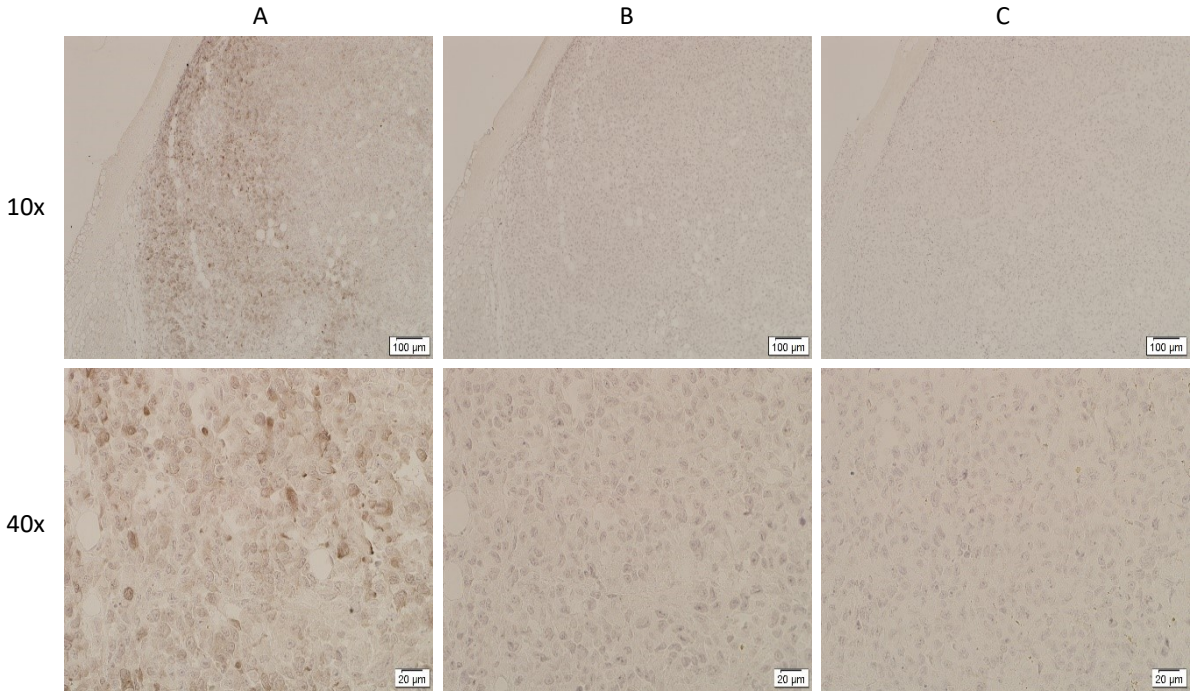

Figure 50 Detection of the enzyme luciferase in an axillary LN right side from a mouse of the bb-mCherry group (SGE-0051). *(A) positive luciferase staining (B) isotype (C) secondary AB control. Scale bar: 100µm and 20 µm; Magnification: 10x, 40x*

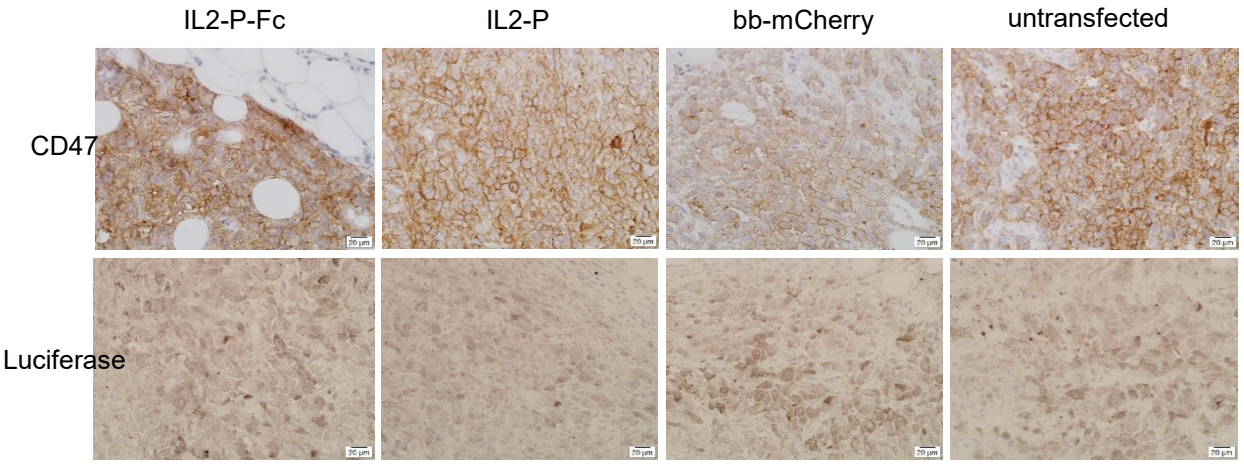

Figure 51 Comparison of CD47 stained areas with luciferase staining *Scale bar: 20 µm; Magnification: 40x*

7.4.3. Staining to detect the Fc-part

As well as in the first animal experiment, no positive signal with an anti-Fc antibody was expected. The staining procedure was the same as in the first experiment and the results looked totally equal (Fig. 52-53).

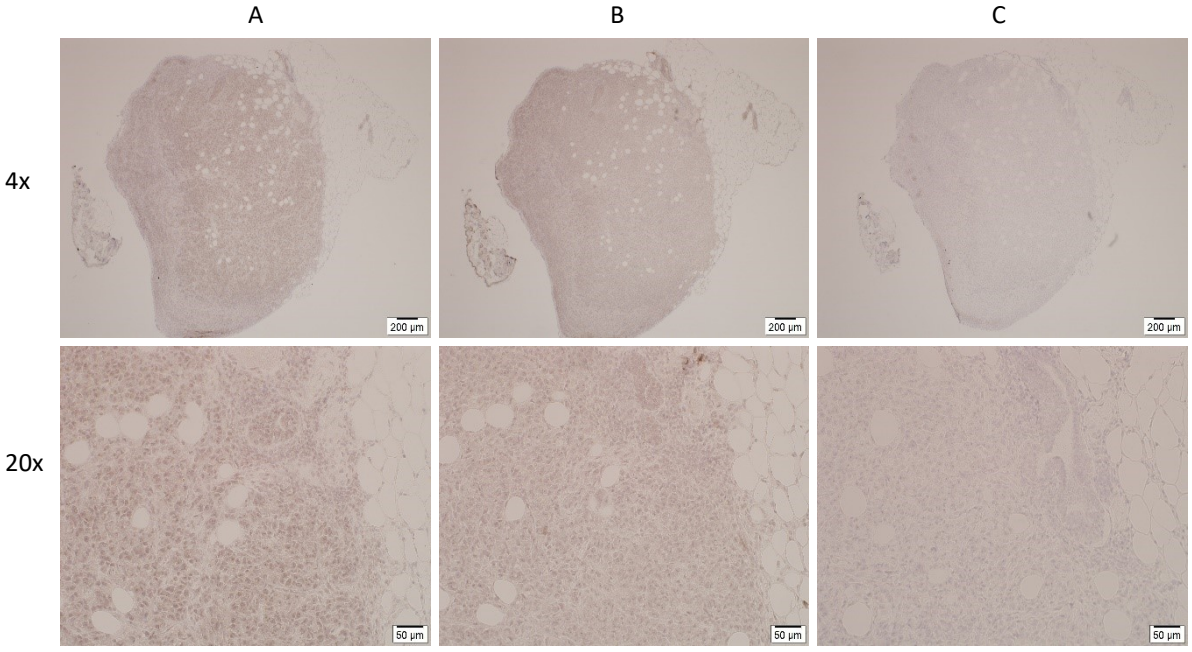

Figure 52 Immunohistochemical detection of the Fc-part of the fusion protein IL2-P-Fc on IL2-P-Fc transfected tumor tissue (MCT-115 TU LE). *(A) treatment with AB against Fc-part was negative (B) isotype control (C) secondary control. Scale bar: 200µm and 50µm; Magnification: 4x, 20x*

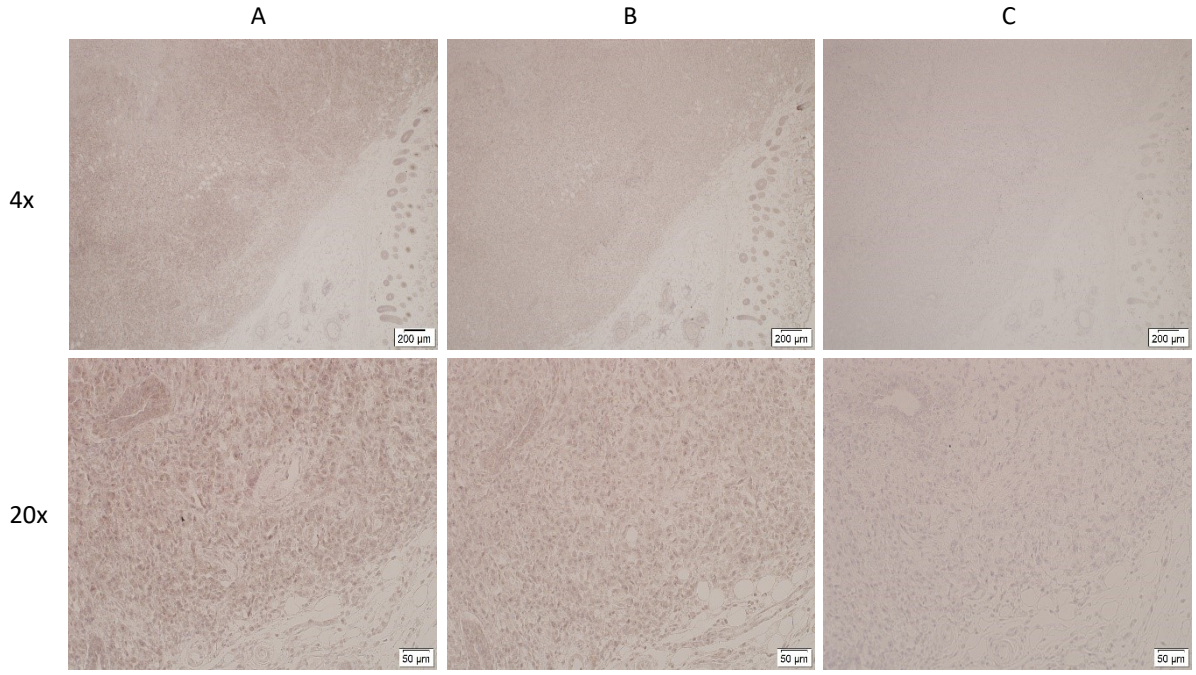

Figure 53 Immunohistochemical detection of the Fc -part on negative control bb-mCherry (SGE-0051 TU LE). *(A) treatment with AB was negative (B) isotype control (C) secondary control. Scale bar: 200µm and 50µm; Magnification: 4x, 20x*

7.4.4. H&E staining

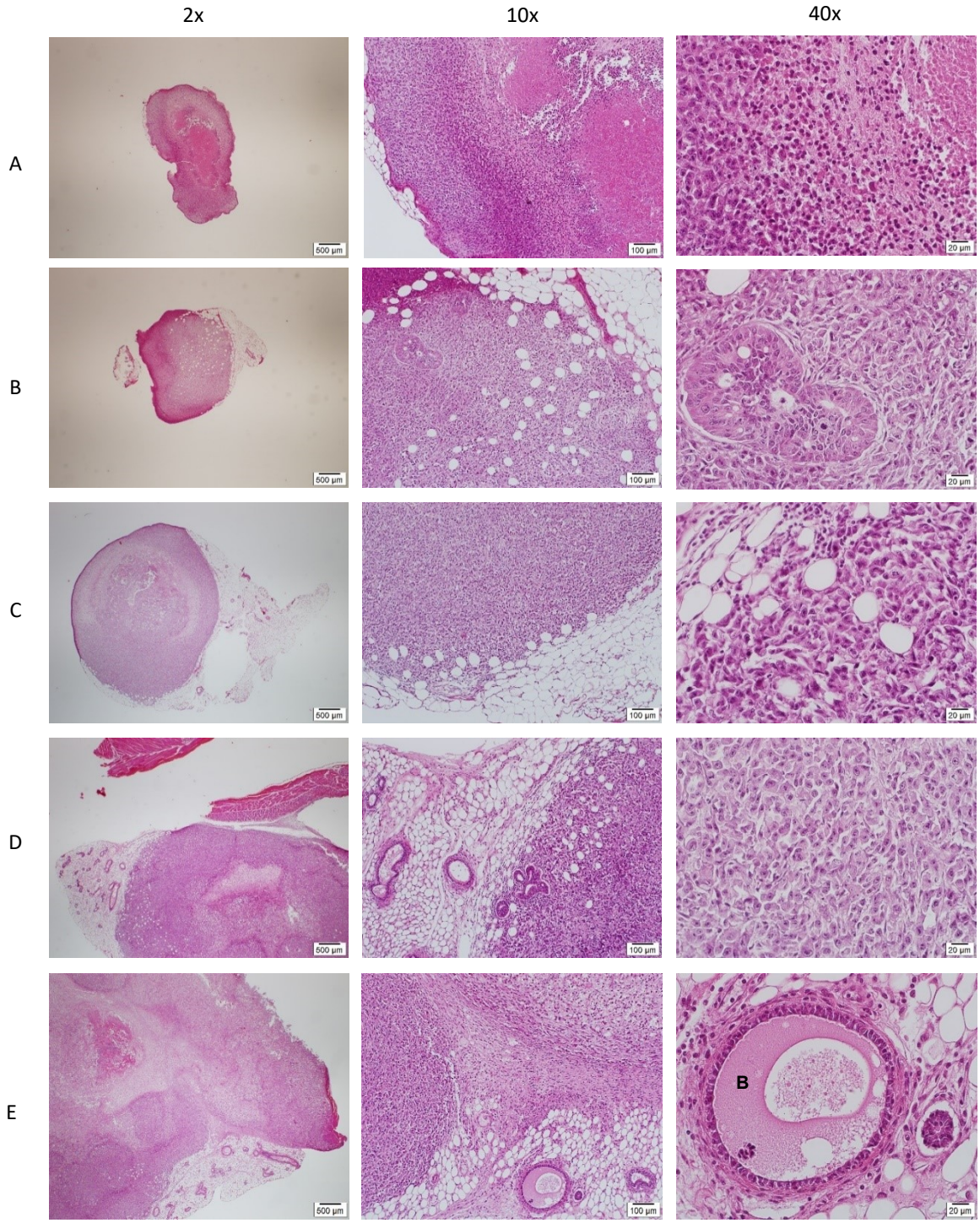

Figure 54 H&E staining of the tumors from the in vivo experiment 2 (B=blood vessel). *(A+B) tumors from the IL2-P-Fc group (C+D) samples from IL2-P group (E) tumor from untransfected group. Scale bar: 500µm, 100µm, 20 µm; Magnification: 2x, 10x, 40x*

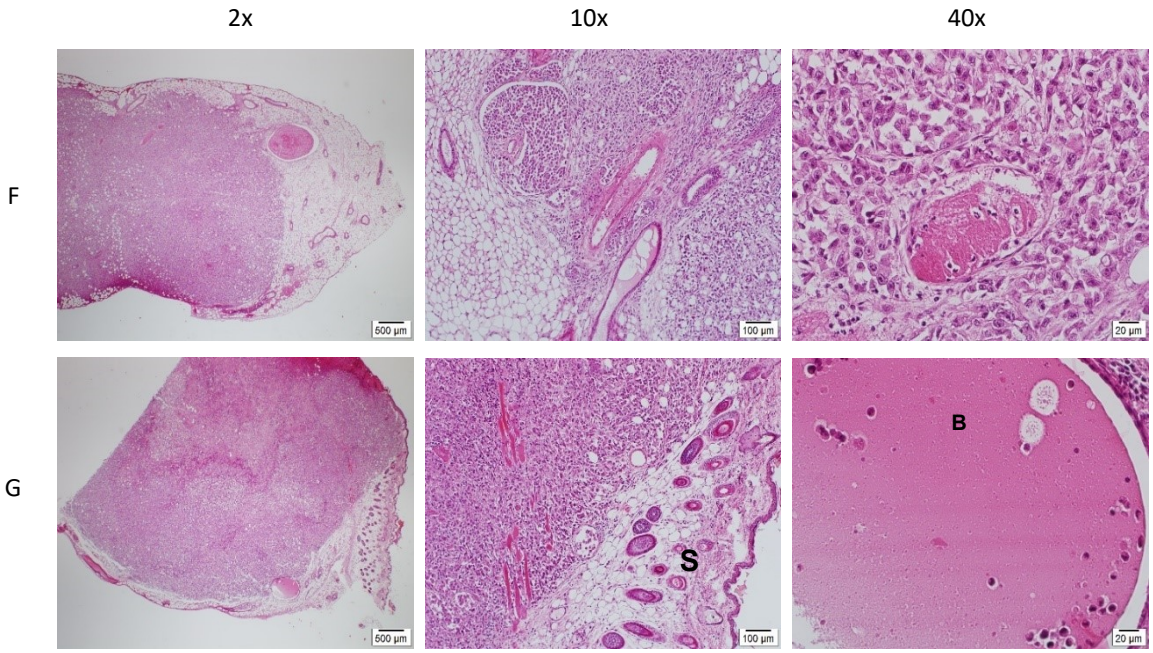

Figure 55 H&E staining of tumors from in vivo experiment 2 (B=blood vessel; S=skin). *(F+G) samples from bb-mCherry group. Scale bar: 500µm, 100µm, 20 µm; Magnification: 2x, 10x, 40x*

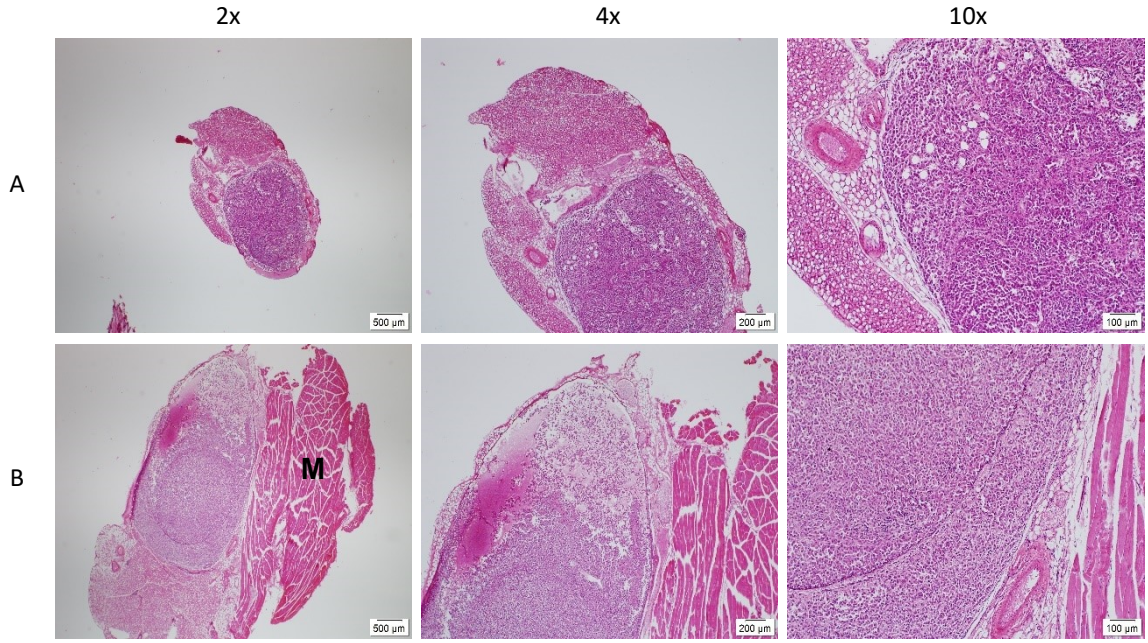

Figure 56 H&E staining of lymph nodes from in vivo experiment 2 (M=muscle tissue). *(A) LN from untransfected group (B) LN from bb-mCherry group. Scale bar: 500µm, 200µm, 100 µm; Magnification: 2x, 4x, 10x*

7.5. Histological examination of in vivo transfected tumors via intratumoral injection of polyplexes

7.5.1. CD47 staining

This time we expected a blockade of CD47, which should be visible in the anti-CD47 staining causing lower staining intensity of the tumor cells, because the CD47 receptor is blocked with the fusion protein. At first, the staining was performed with the left tumors of the three groups, 24 h, 48 h, and 72 h after the injection of the therapeutic polyplexes. One sample of each bb-mCherry group and a buffer control were included in the staining procedure. In fact, in the sample of the left tumor 24 hours after the injection, the CD47 signal was lower comparable to the other groups.

<u>24 hours post injection:</u>

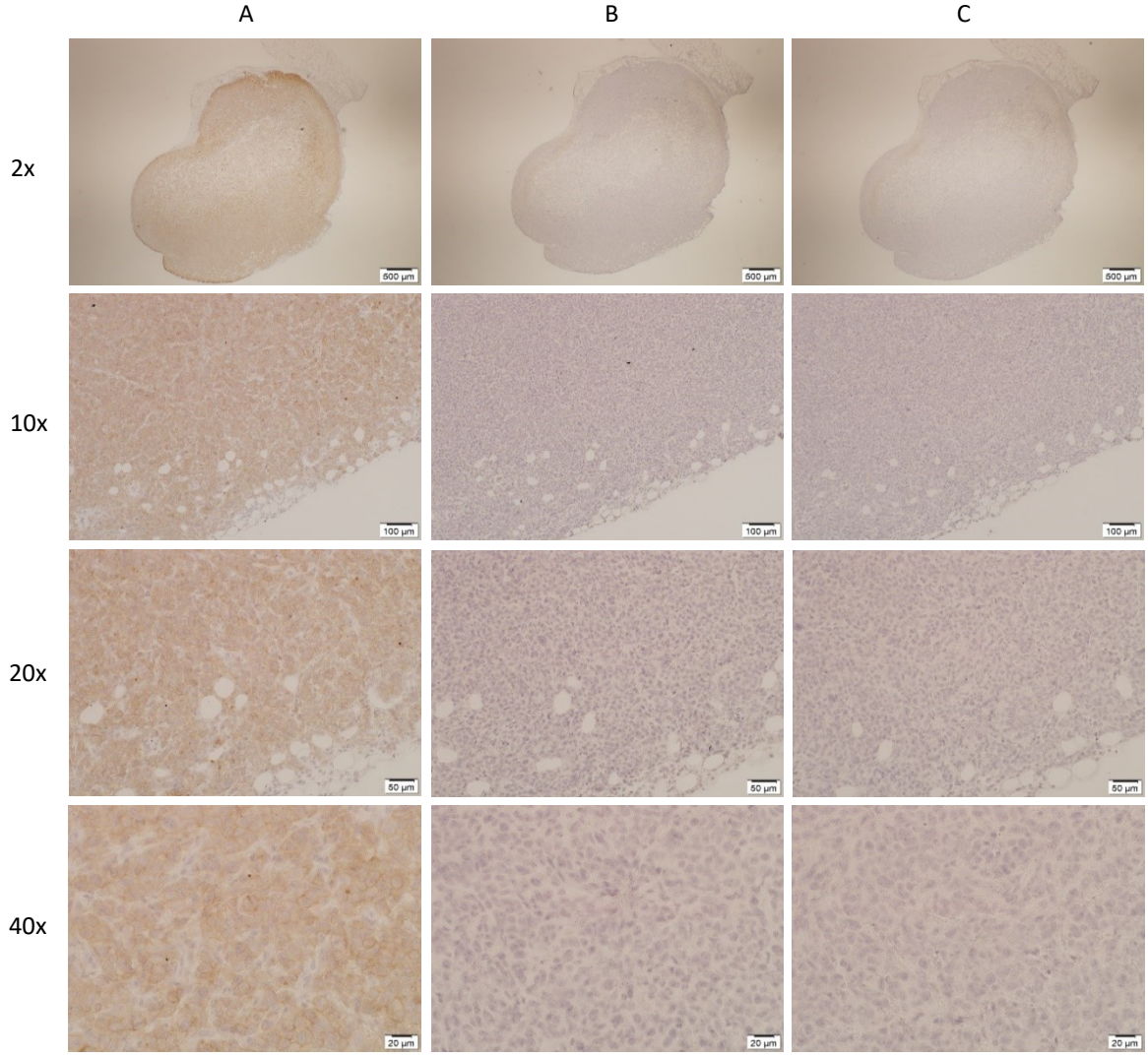

Figure 57 CD47 staining of a tumor from the IL2-P-Fc group <u>24 h</u> post injection (MCT-0209 TU LE). *(A) only low CD47 signal is visible (B) isotype control is negative (C) secondary control is negative. Scale bar: 500µm, 100µm, 50 µm and 20 µm; Magnification: 2x, 10x, 20x, 40x*

48 hours post injection:

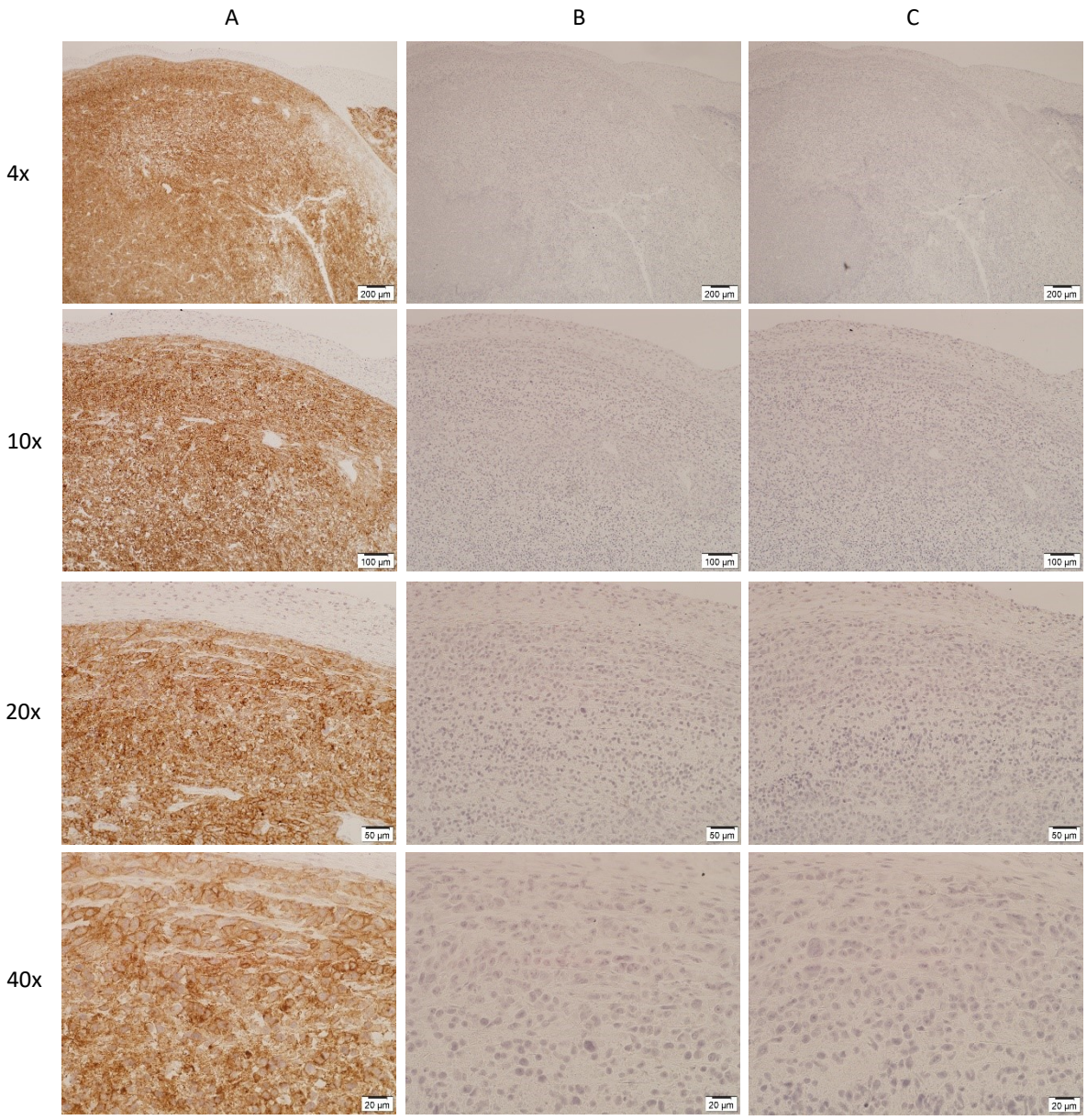

Figure 58 CD47 staining of a tumor from the IL2-P-Fc group 48 h post injection (MCT-0208 TU LE). *(A) higher CD47 signal is visible than after 24 h (B) isotype control (C) secondary control. Scale bar: 200µm, 100µm, 50 µm and 20 µm; Magnification: 4x, 10x, 20x, 40x*

72 hours post injection:

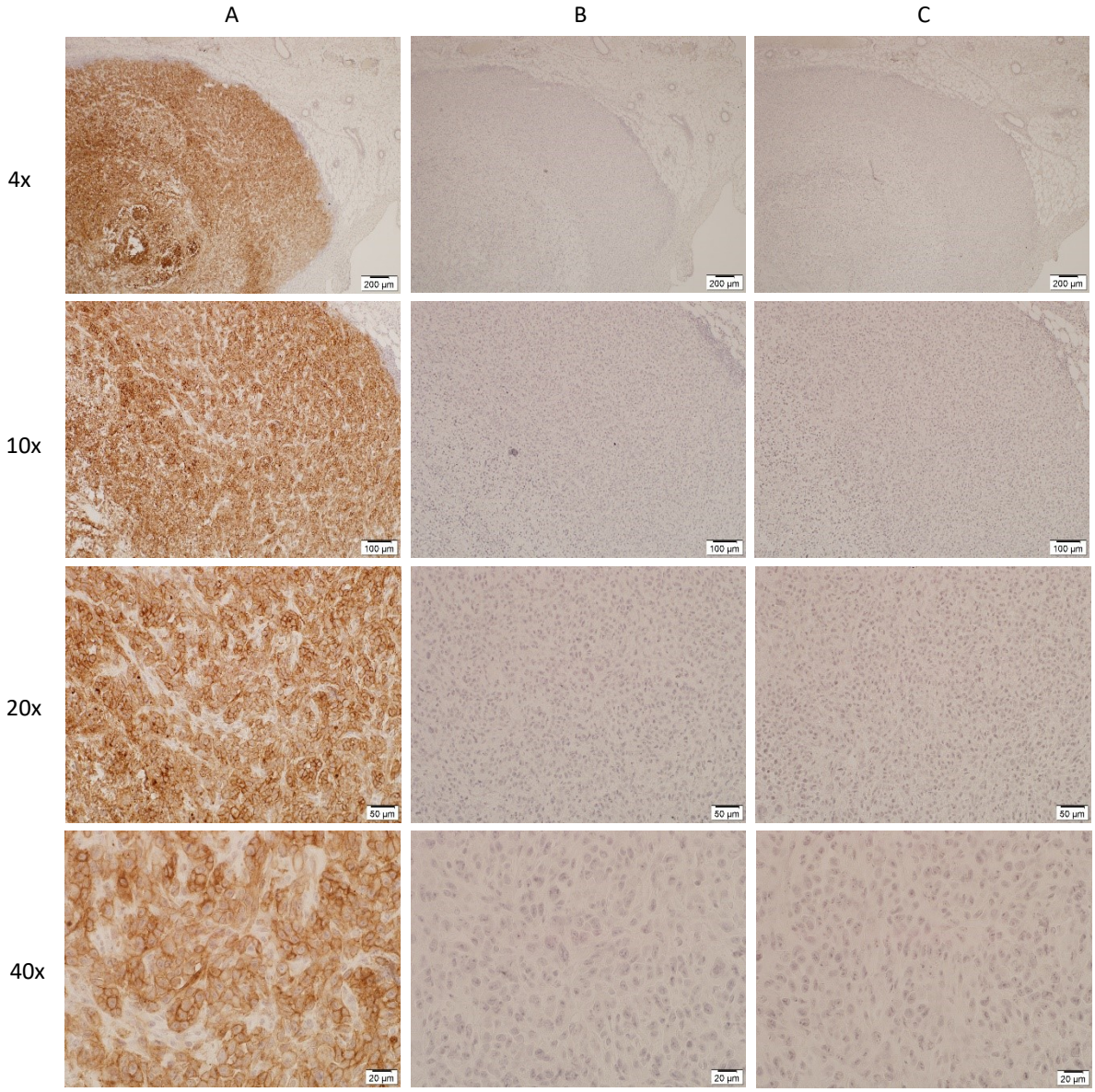

Figure 59 CD47 staining of a tumor from the IL2-P-Fc group 72 h post injection (MCT-0210 TU LE). *(A) brown staining is very intense 72 h after injection (B) isotype control (C) secondary AB control. Scale bar: 200µm, 100µm, 50 µm and 20 µm; Magnification: 4x, 10x, 20x, 40x*

24 hours post injection:

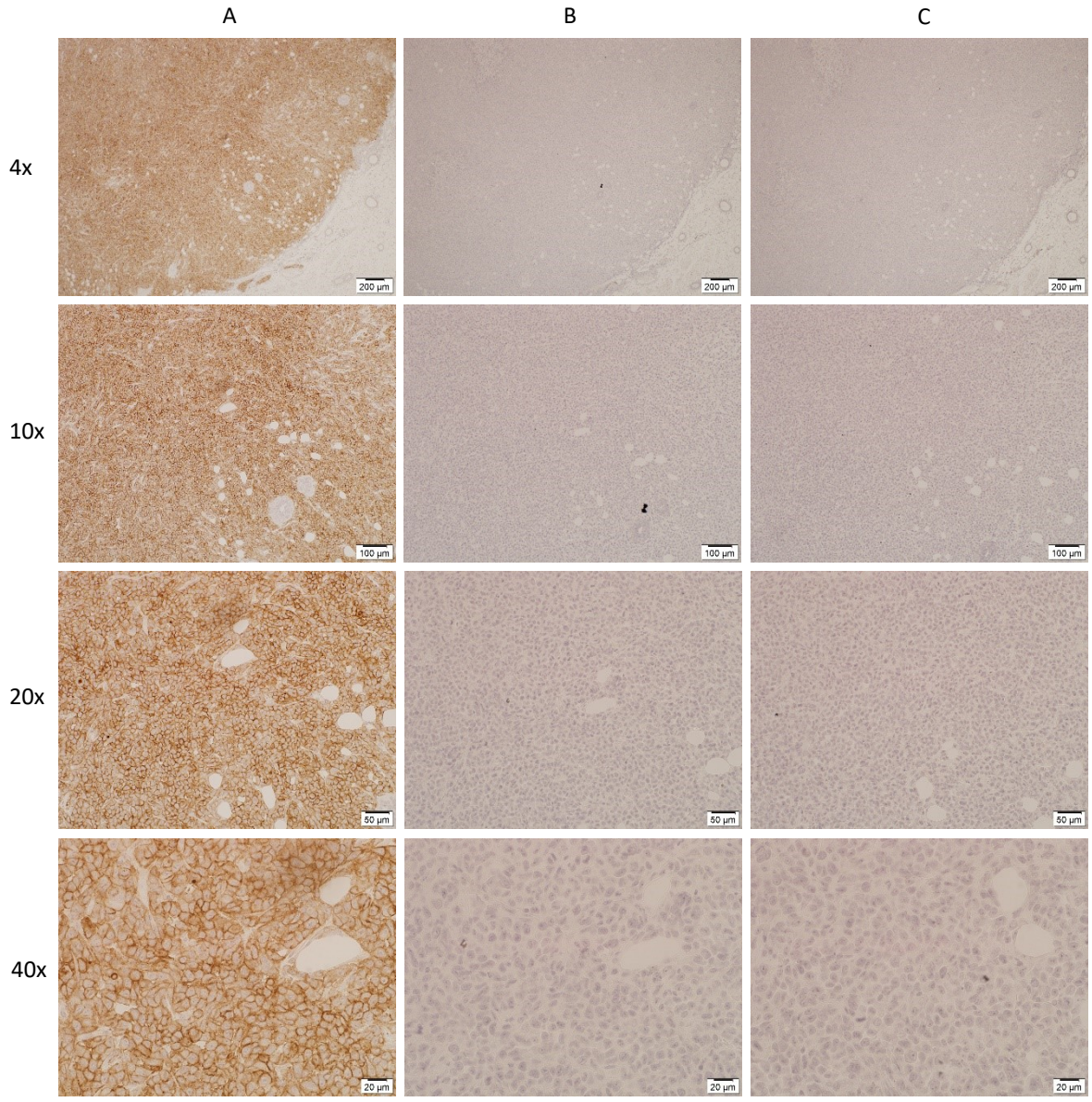

Figure 60 CD47 staining of a tumor from the bb-mCherry group 24 h post injection (MCT-204 TU LE). *(A) intense brown staining compared to the IL2-P-Fc group 24 hours after injection (figure 28) (B) isotype control (C) secondary control. Scale bar: 200µm, 100µm, 50 µm and 20 µm; Magnification: 4x, 10x, 20x, 40x*

48 hours post injection:

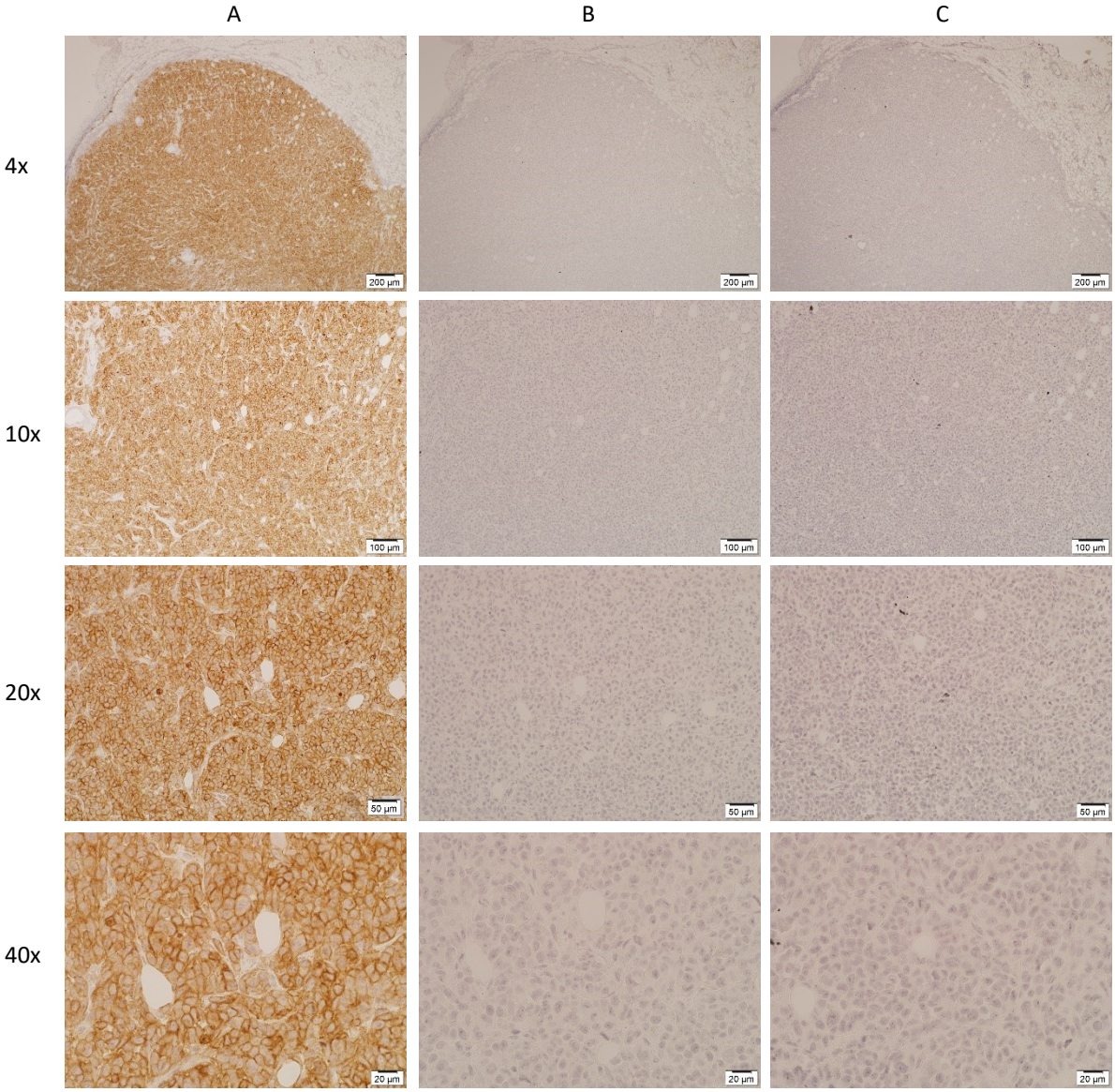

Figure 61 CD47 staining of a tumor from bb-mCherry group 48 h post injection (MCT-113 TU RI). *(A) positive CD47 signal, no difference between 24h and 48 hours post injection (B) isotype control (C) secondary control. Scale bar: 500µm, 100µm, 50 µm and 20 µm; Magnification: 2x, 10x, 20x, 40x*

72 hours post injection:

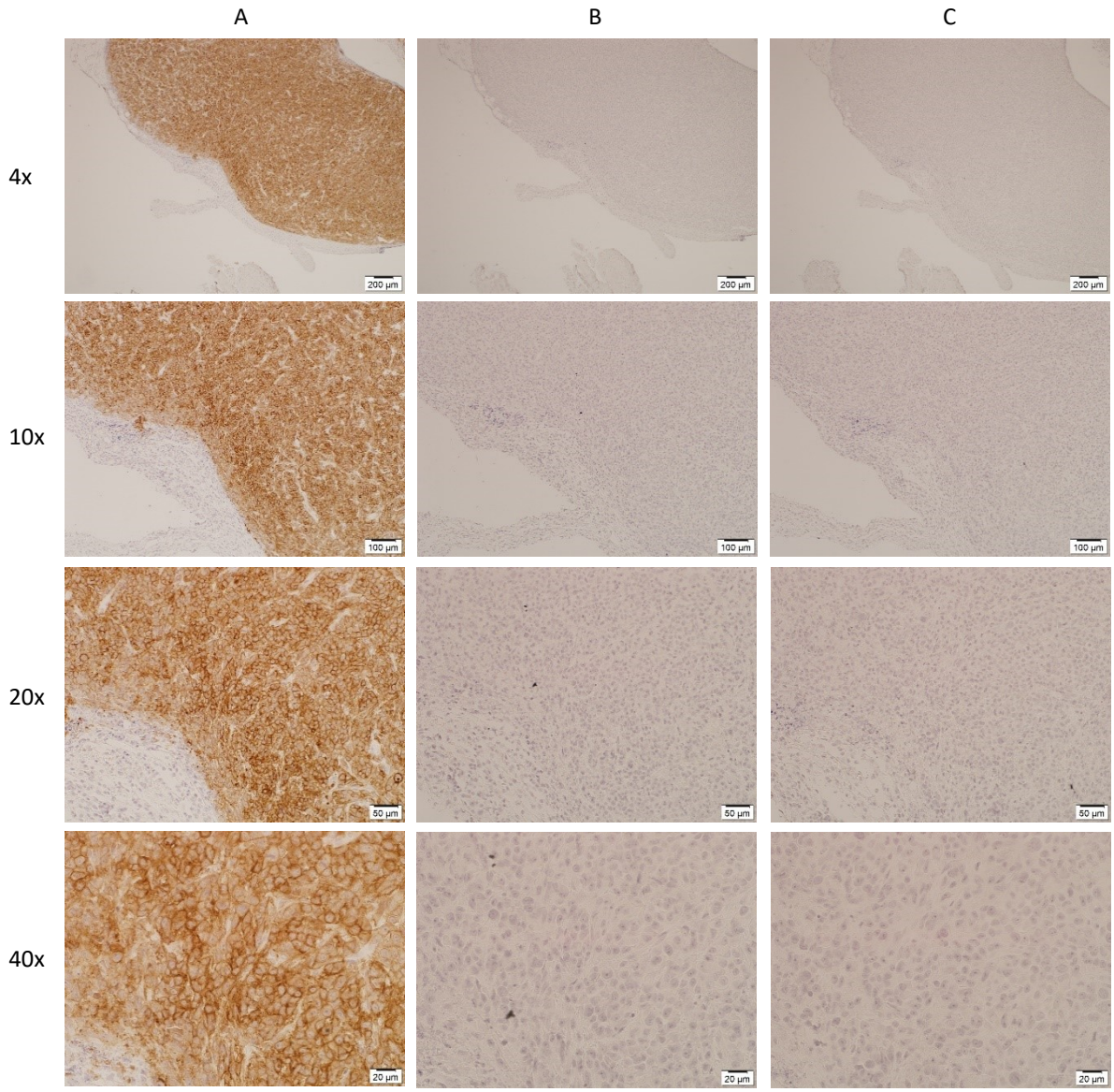

Figure 62 CD47 staining of a tumor from bb-mCherry group 72 h post injection (MCT-203 TU RI). *(A) positive CD47 signal, looks a bit more intense than after 24 and 48 h, may depend on the thickness of the tissue section (B) isotype control (C) secondary control. Scale bar: 200µm, 100µm, 50 µm and 20 µm; Magnification: 4x, 10x, 20x, 40x*

24 hours post injection:

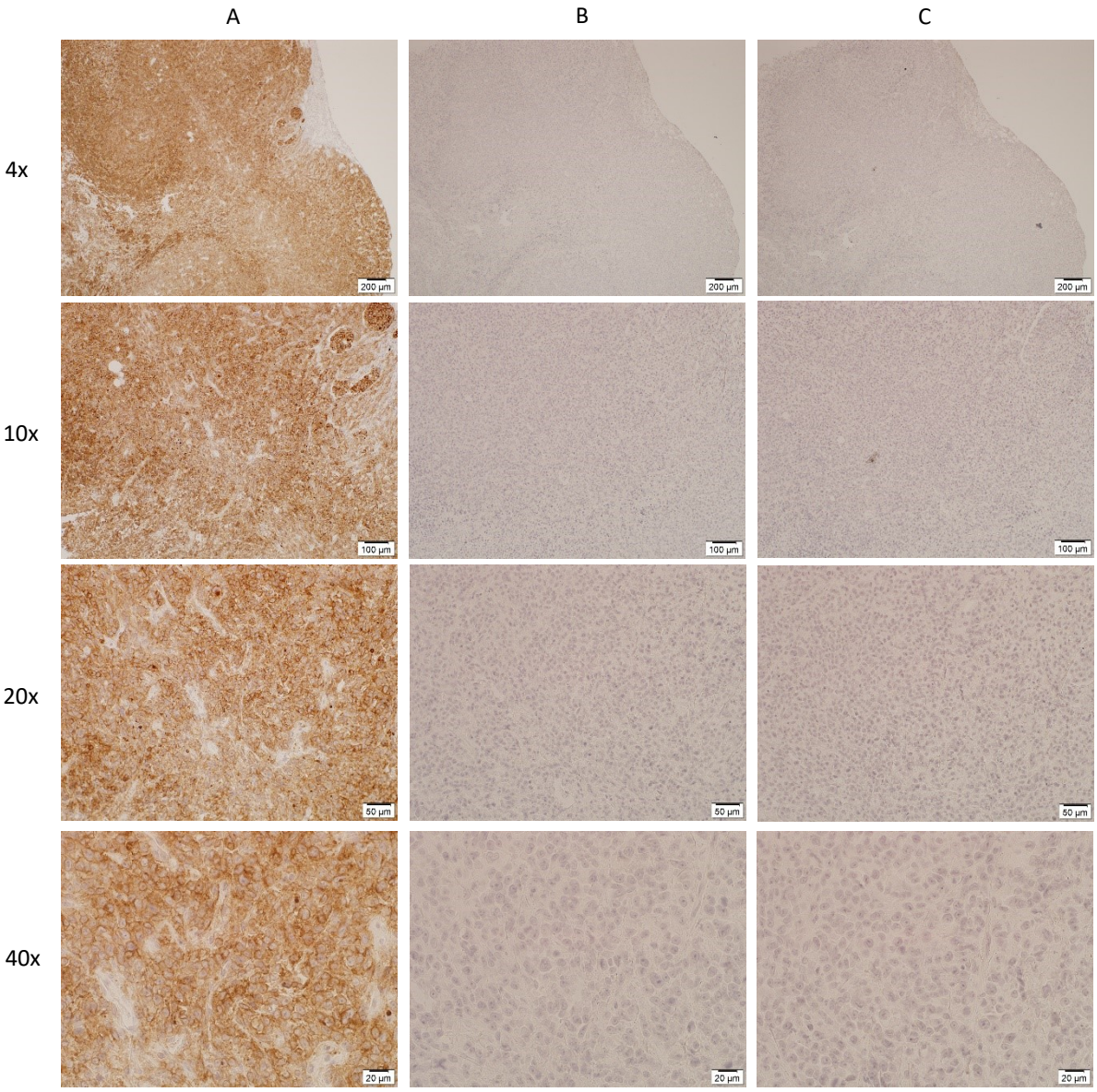

Figure 63 CD47 staining of a tumor from the control group treated only with buffer 24 h post injection (MCT-182 TU RI). *(A) positive CD47 staining (B) isotype control (C) secondary control. Scale bar: 200µm, 100µm, 50 µm and 20 µm; Magnification: 4x, 10x, 20x, 40x*

The staining was revised with the right tumors of the same mice, but this time no blocking of CD47 was visible.

24 h post injection:

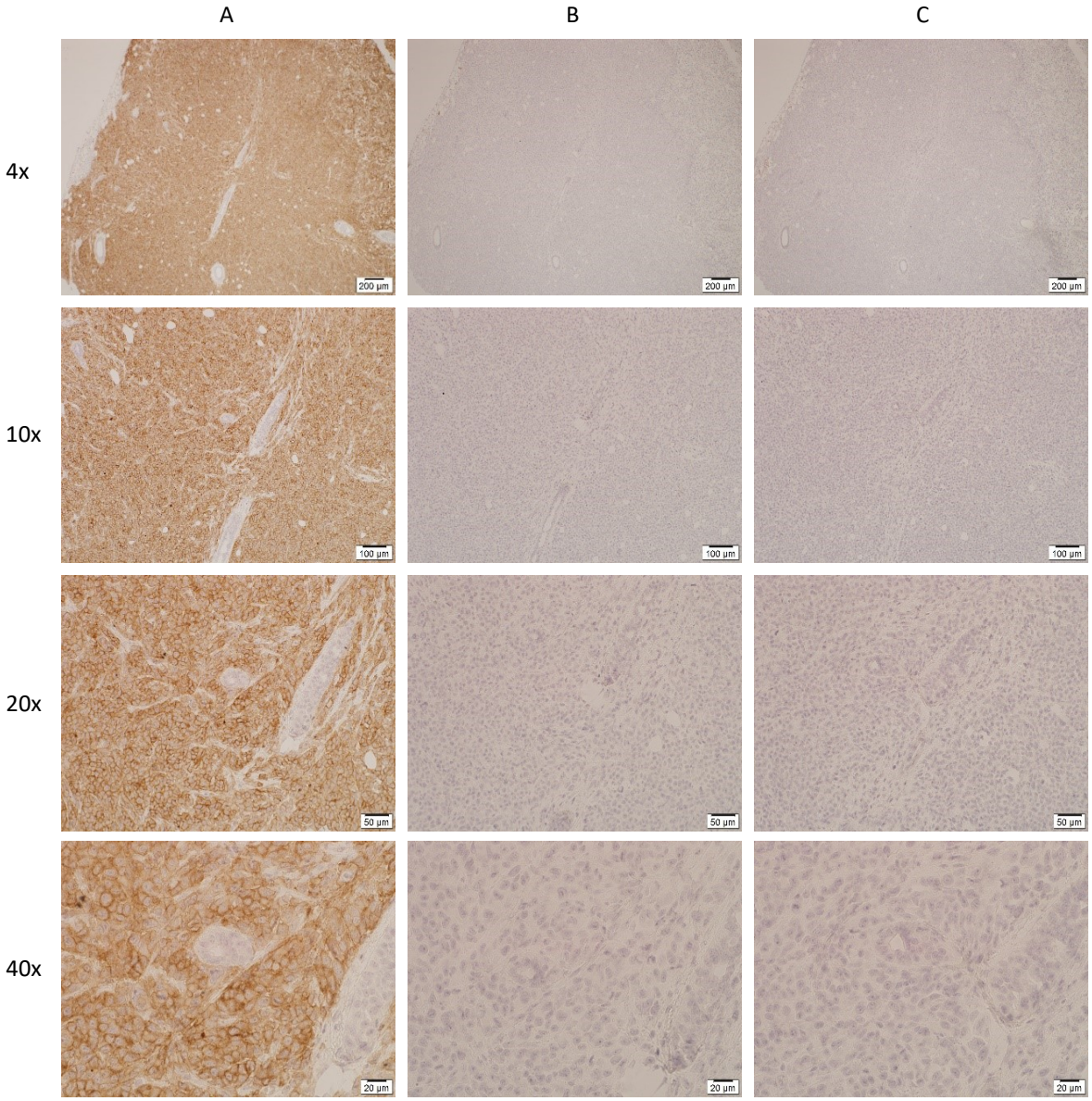

Figure 64 CD47 staining of a tumor from the IL2-P-Fc group 24 h post injection (MCT-0209 TU RI). *(A) CD47 signal is visible (B) isotype control (C) secondary control. Scale bar: 200µm, 100µm, 50 µm and 20 µm; Magnification: 4x, 10x, 20x, 40x*

48 hours post injection:

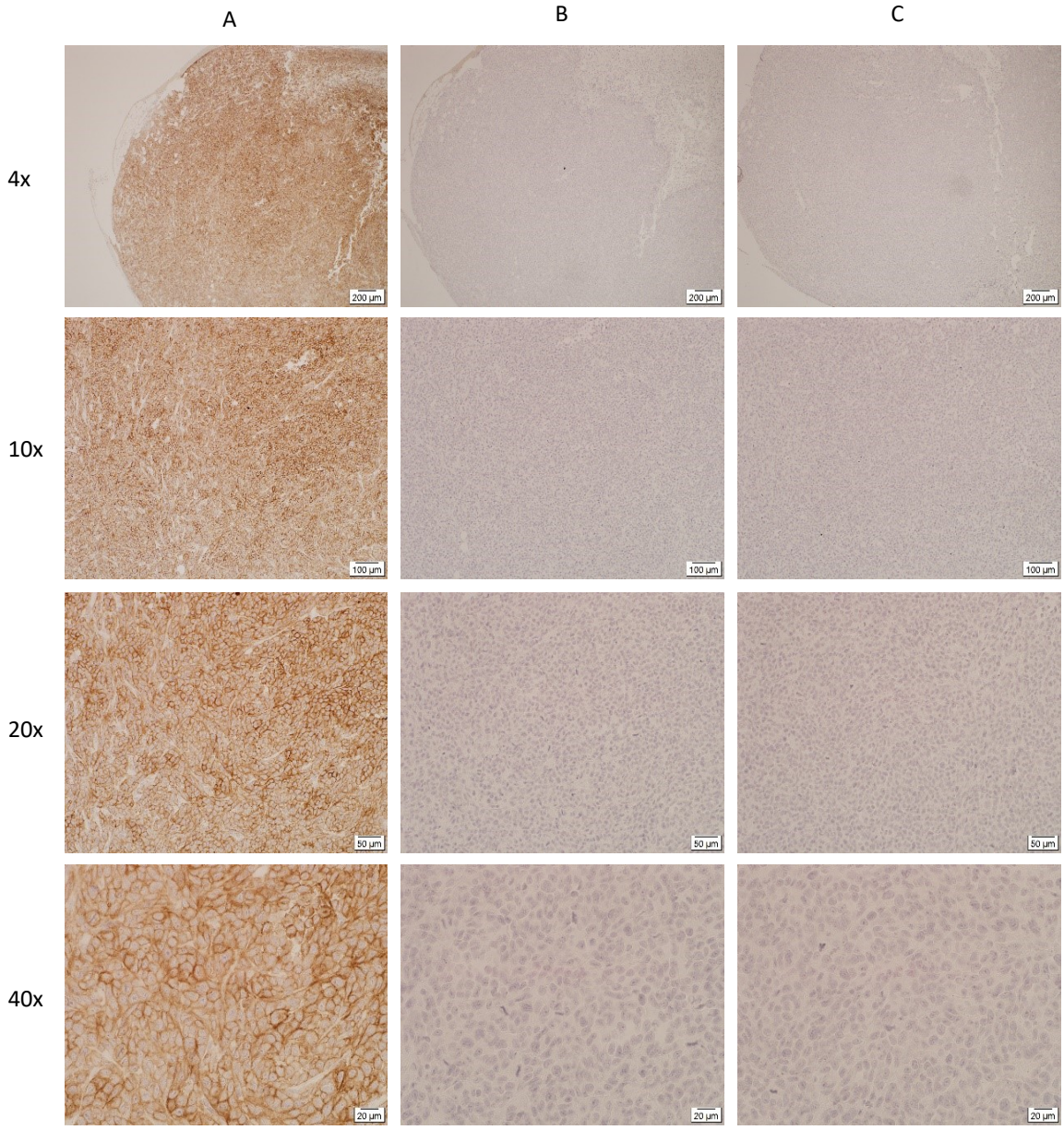

Figure 65 CD47 staining of a tumor from the IL2-P-Fc group 48 h post injection (MCT-0208 TU RI). *(A) strong CD47 signal is visible (B) isotype control (C) secondary control. Scale bar: 200µm, 100µm, 50 µm and 20 µm; Magnification: 4x, 10x, 20x, 40x*

72 hours post injection:

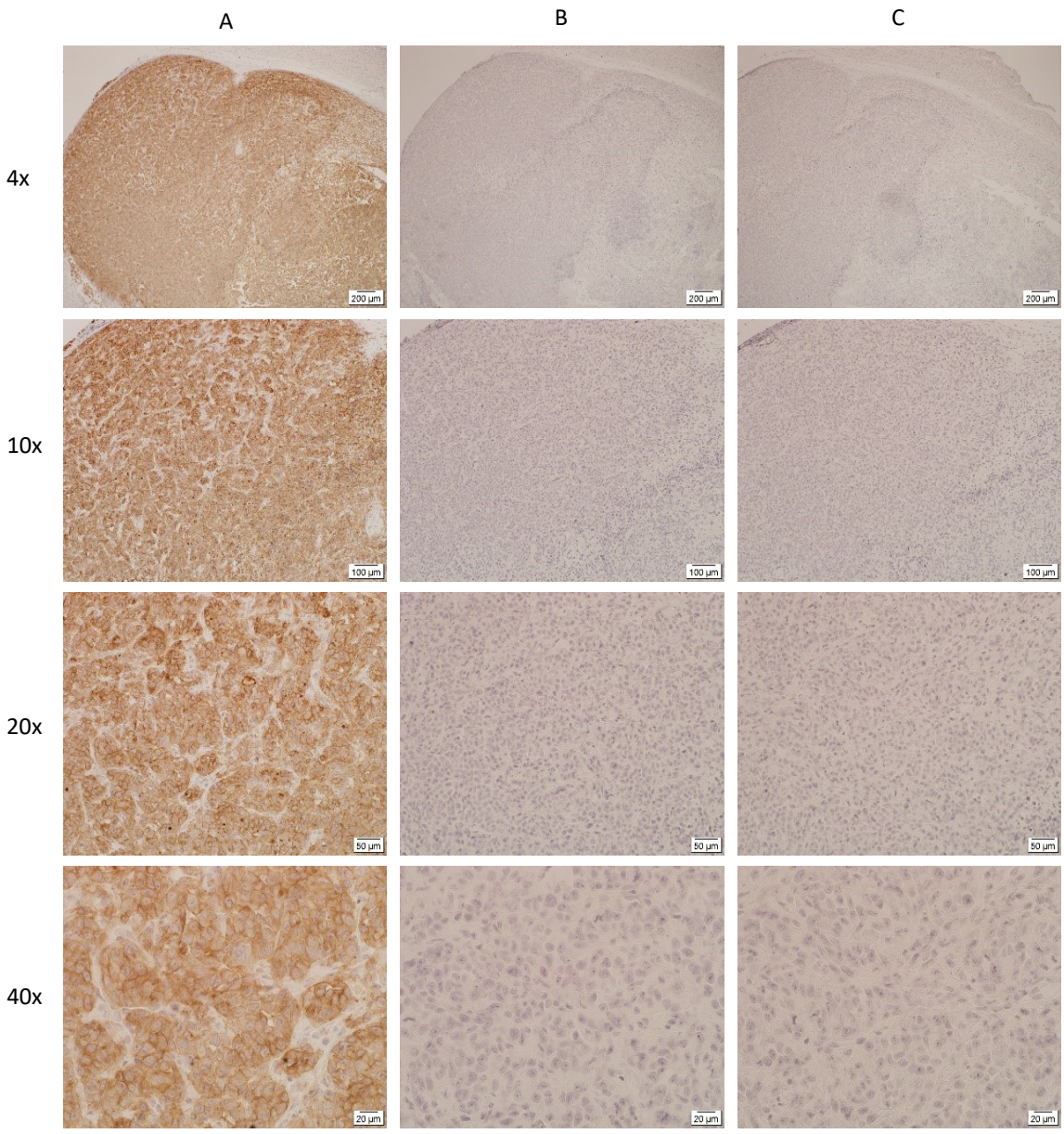

Figure 66 CD47 staining of a tumor from the IL2-P-Fc group 72 h post injection (MCT-0210 TU RI). *(A) strong CD47 signal is visible (B) isotype control (C) secondary control. Scale bar: 200µm, 100µm, 50 µm and 20 µm; Magnification: 4x, 10x, 20x, 40x*

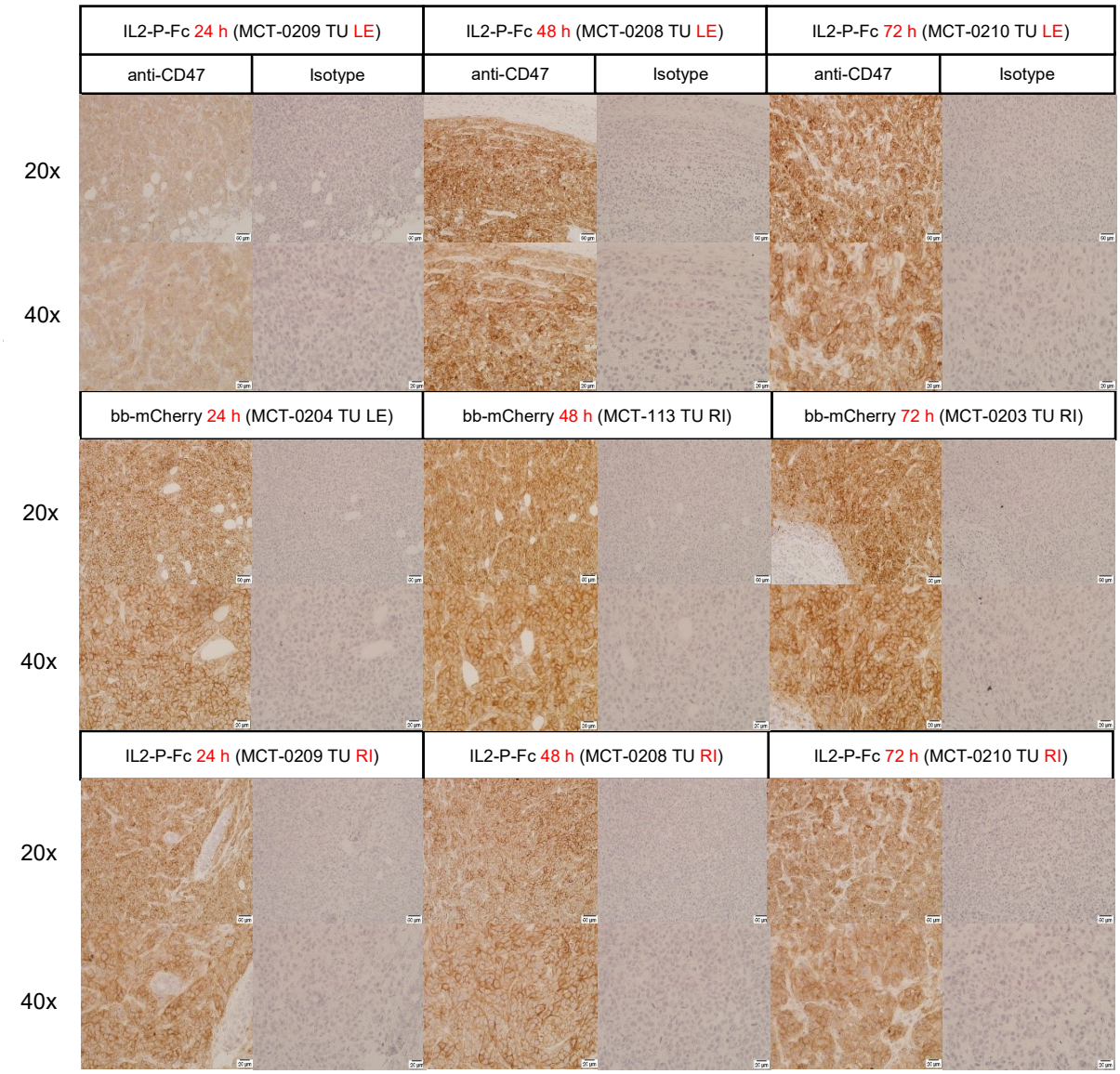

Figure 67 Overview of CD47 stainings with samples from in vivo experiment 3. *Scale bar: 50 µm and 20 µm; Magnification: 20x, 40x*

It is clearly visible in figure 67, that the CD47 signal is less intense in the left tumor of the IL2-P-Fc group (animal MCT-0209) 24 hours after the treatment. This blocking effect is gone 48 hours after the treatment. 72 hours post injection the CD47 signal reaches its highest intensity. The control group bb-mCherry shows a constant brown staining. A second staining was performed with the tumors on the right flank of the IL2-P-Fc treated mice in the same way. This time no difference was visible in staining intensity.

7.5.2. Luciferase staining

The luciferase staining was performed the same way as with the samples from the first and second experiment. Independently from the different groups, brown staining was visible in all the samples.

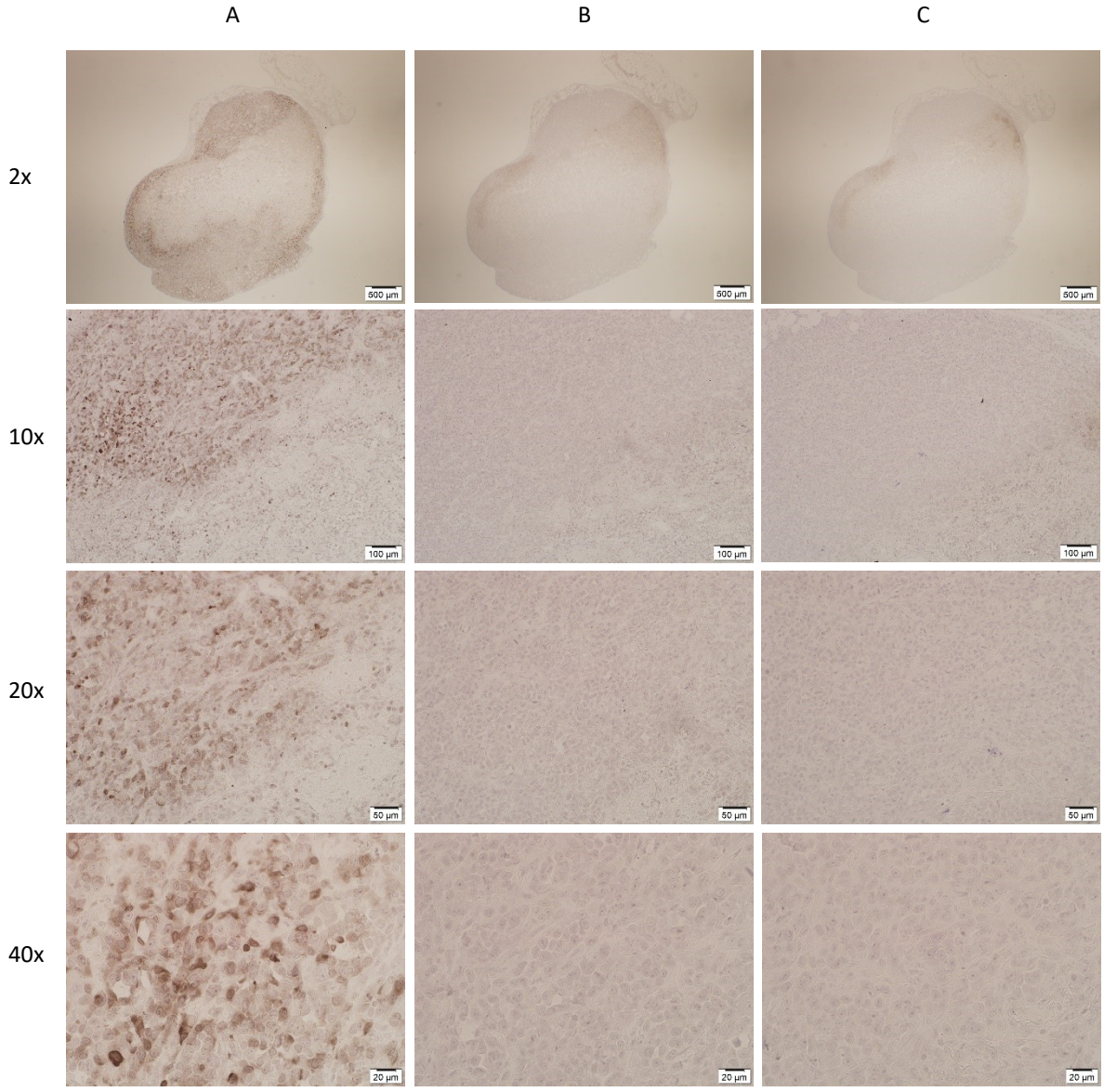

Figure 68 Detection of the enzyme luciferase in tumor tissue 24 h after treatment with IL2-P-Fc fusion protein (MCT-0209 TU LE). *(A) brown staining shows positive luciferase signal (B) isotype control (C) secondary control. Scale bar: 500µm, 100µm, 50µm and 20 µm; Magnification: 2x, 10x, 20x, 40x*

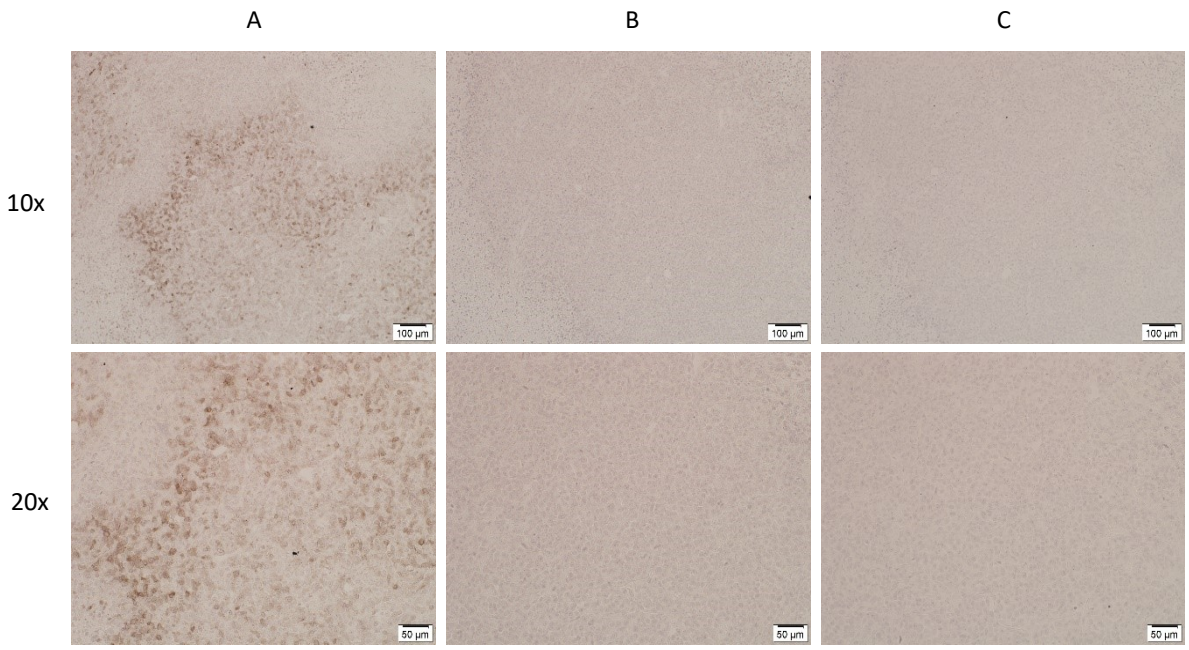

Figure 69 Detection of the enzyme luciferase in tumor tissue 48 h after treatment with IL2-P-Fc fusion protein (MCT-0208 TU LE). *(A) positive luciferase staining (B) isotype control (C) secondary control. Scale bar: 100µm and 50µm; Magnification: 10x, 20x*

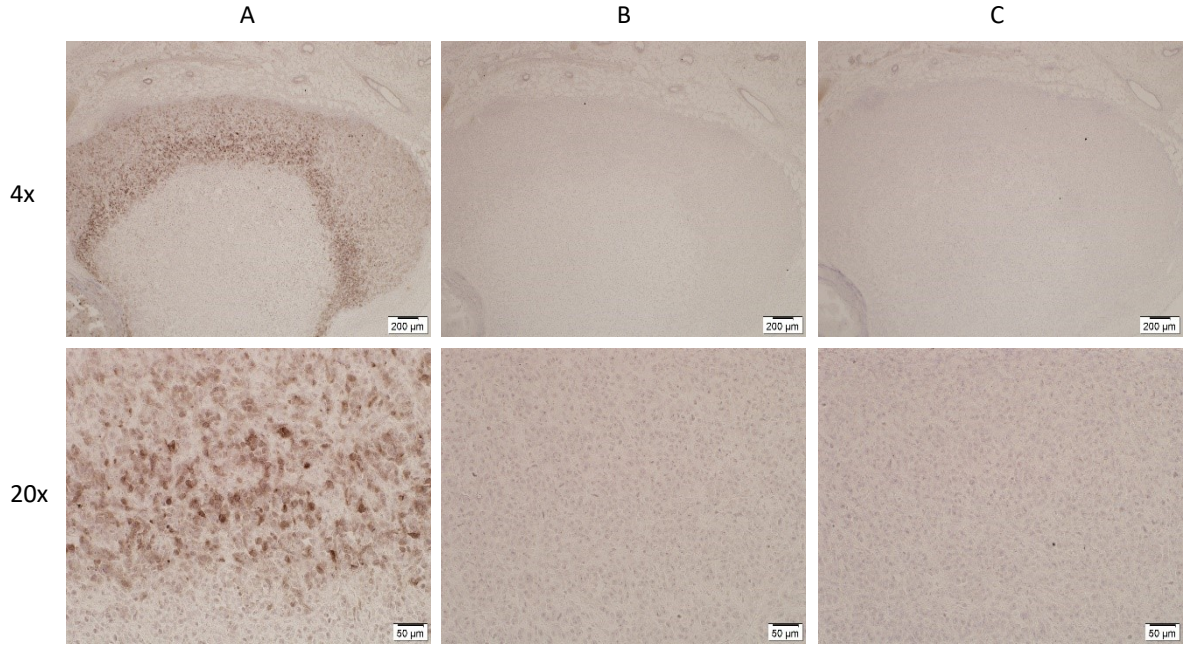

Figure 70 Detection of the enzyme luciferase in tumor tissue 72 h after treatment with IL2-P-Fc fusion protein (MCT-0210 TU LE). *(A) brown staining shows positive Luc signal (B) isotype control (C) secondary control. Scale bar: 200µm and 50µm; Magnification: 4x, 20x*

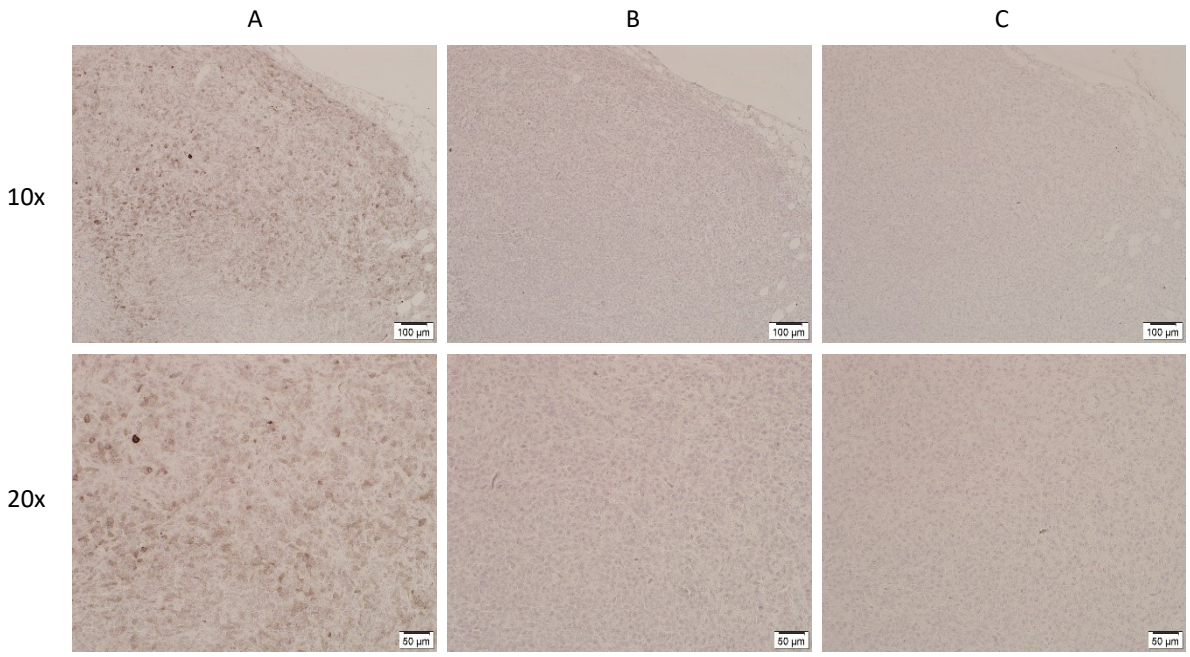

Figure 71 Detection of the enzyme luciferase in tumor tissue 24 h after treatment with polyplexes containing the bb-mCherry plasmid (MCT-204 TU LE). *(A) positive luciferase signal (B) isotype control (C) secondary control. Scale bar: 100µm and 50µm; Magnification: 10x, 20x*

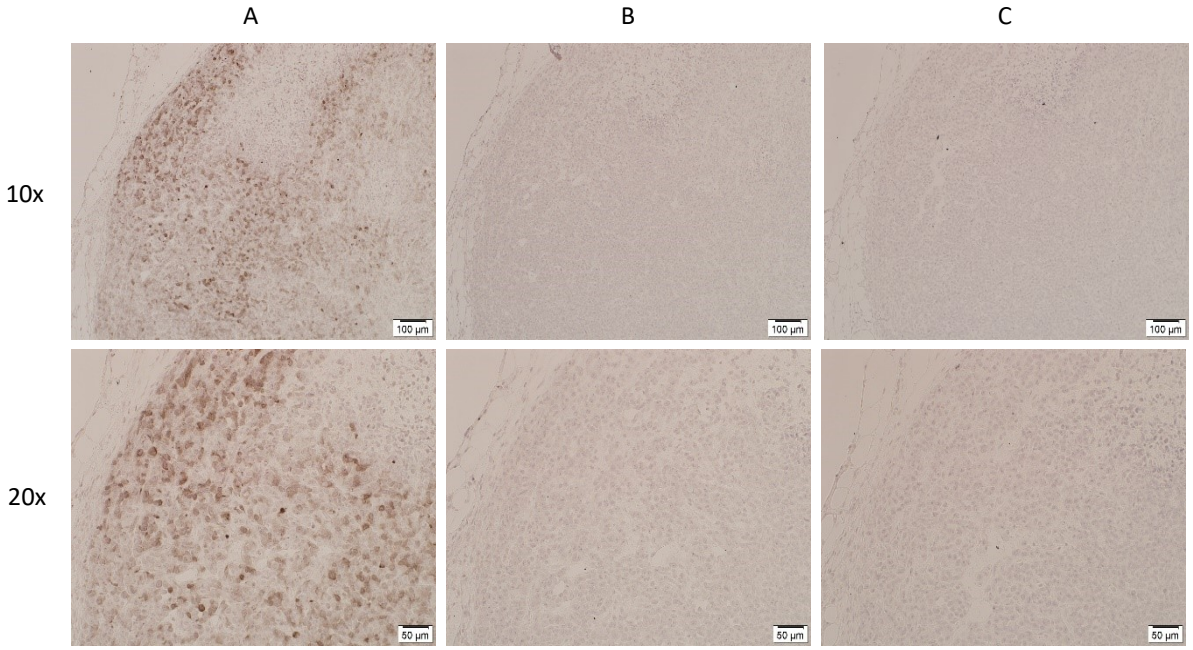

Figure 72 Detection of the enzyme luciferase in tumor tissue 48 h after treatment with polyplexes containing bb-mCherry plasmid (MCT-113 TU RI). *(A) brown staining shows positive luciferase signal (B) isotype control (C) secondary control. Scale bar: 100µm and 50µm; Magnification: 10x, 20x*

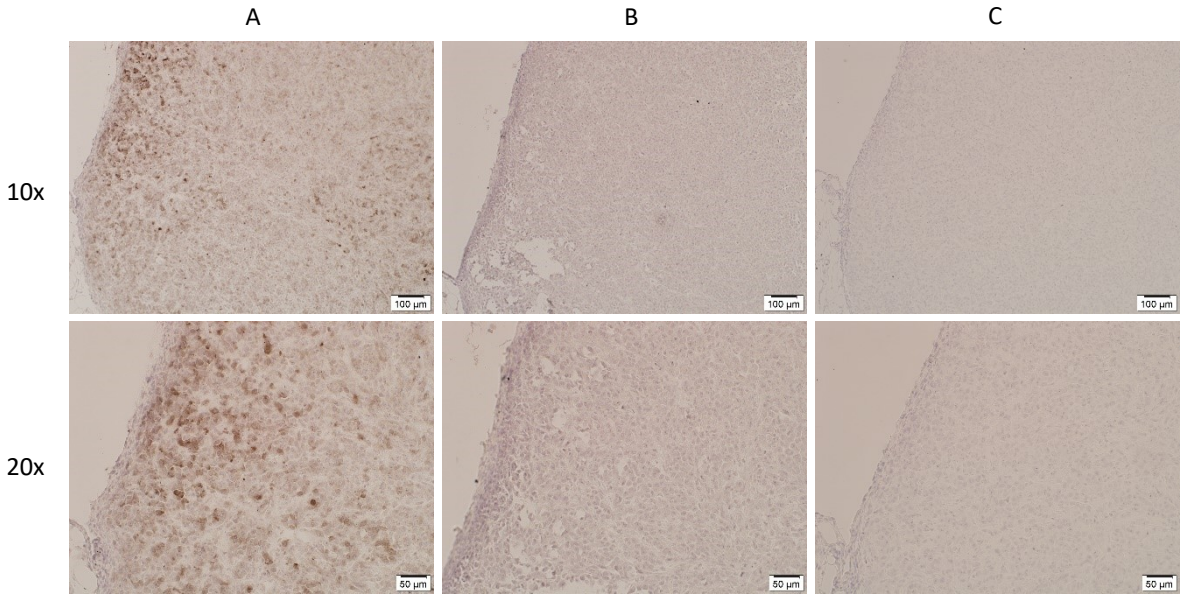

Figure 73 Detection of the enzyme luciferase in tumor tissue 72 h after treatment with polyplexes containing bb-mCherry plasmid (MCT-203 TU RI). *(A) positive luciferase staining (B) isotype control (C) secondary control. Scale bar: 100µm and 50µm; Magnification: 10x, 20x*

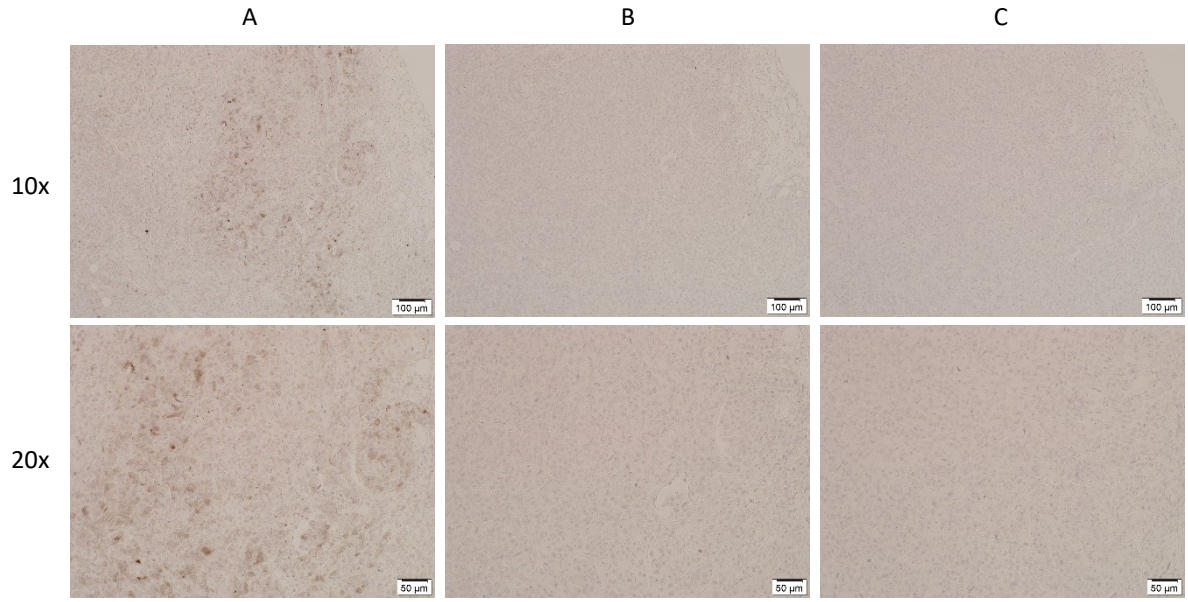

Figure 74 Detection of the enzyme luciferase in tumor tissue treated only with buffer for 24 hours (MCT-182 TU RI). *(A) brown staining shows positive luciferase signal (B) isotype control (C) secondary antibody control. Scale bar: 100µm and 50µm; Magnification: 10x, 20x*

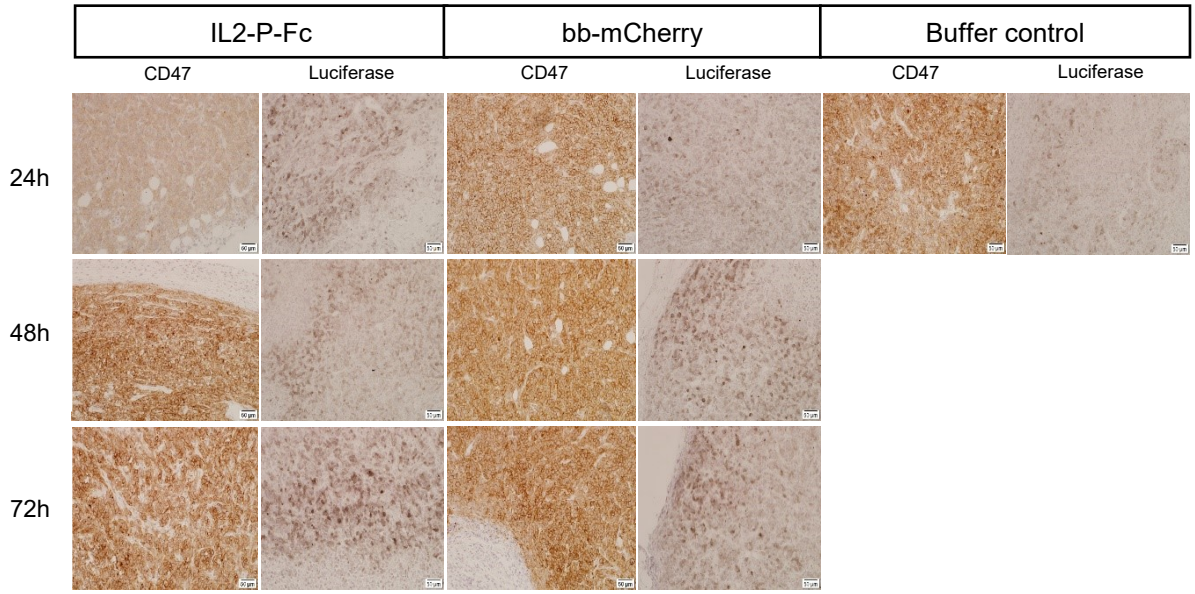

Figure 75 Comparison of CD47 stained areas with luciferase staining. *Lower CD47 signal in the IL2-P-Fc group may be caused by binding of the fusion protein to its receptor CD47. Scale bar: 20 µm; Magnification: 40x*

7.5.3. Staining to detect the Fc-part

In comparison to the first and second in vivo experiment, this time a positive detection of the Fc-part was desirable in the tumor tissue 24 hours after the injection of polyplexes as the CD47 signal was partially blocked. Consequently, we expected a decrease in signal intensity in the tissue 48 hours after treatment with the lowest signal 72 hours post injection. The staining procedure was the same as in the previous experiments, but this time no secondary AB was added by mistake. The detection of the Fc-part with the goat HRP preabsorbed anti-human IgG Fc antibody (ab98624) was performed twice with the samples of the third in vivo experiment. The first time (Fig. 76) the incubation with the anti-Fc AB was done overnight and a dilution of 1:200 was used. As shown in figure 76, all the samples are stained in a light brown color which looks very unspecific. Especially the bb-mCherry group should be negative. Therefore, the staining was repeated, this time with a lower concentration of the antibody (1:500) and the incubation time was 2h (instead of about 17 hours overnight) at room temperature. The staining results illustrated in figure 77 show negative signal in all the samples.

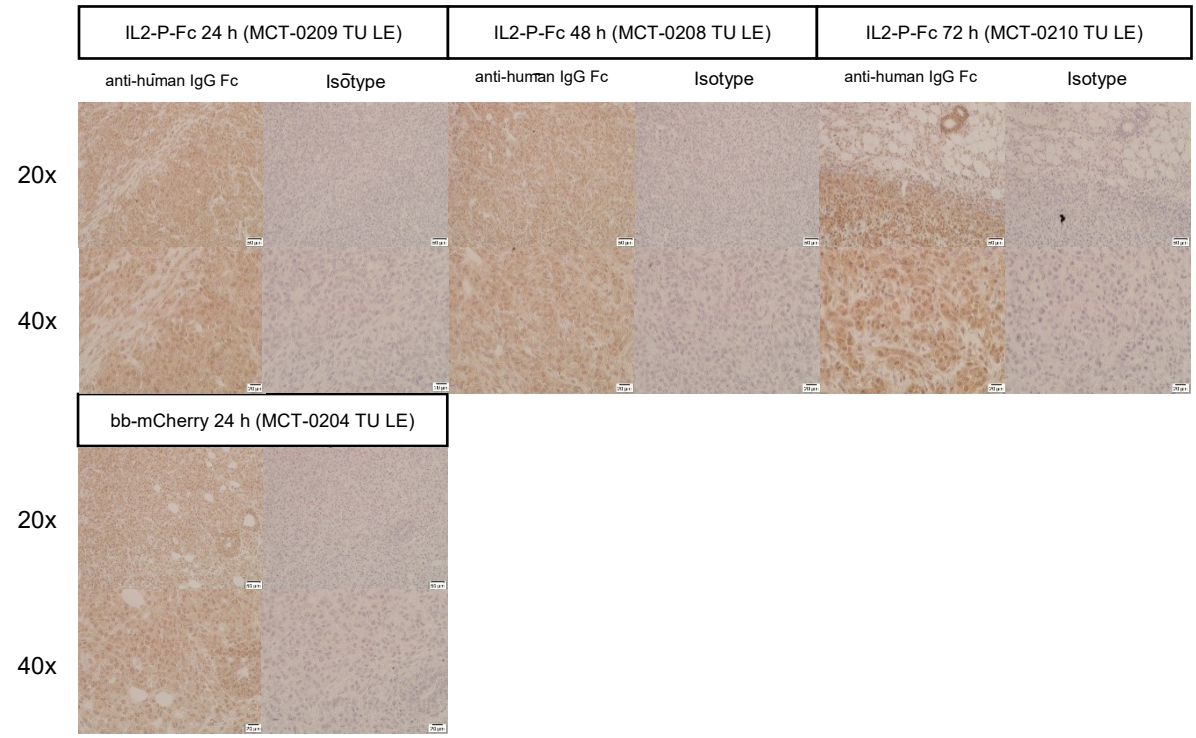

Figure 76 Overview of the staining to detect the Fc-part with 1:200 dilution of the AB and incubation overnight. *Scale bar: 50 µm and 20 µm; Magnification: 20x, 40x*

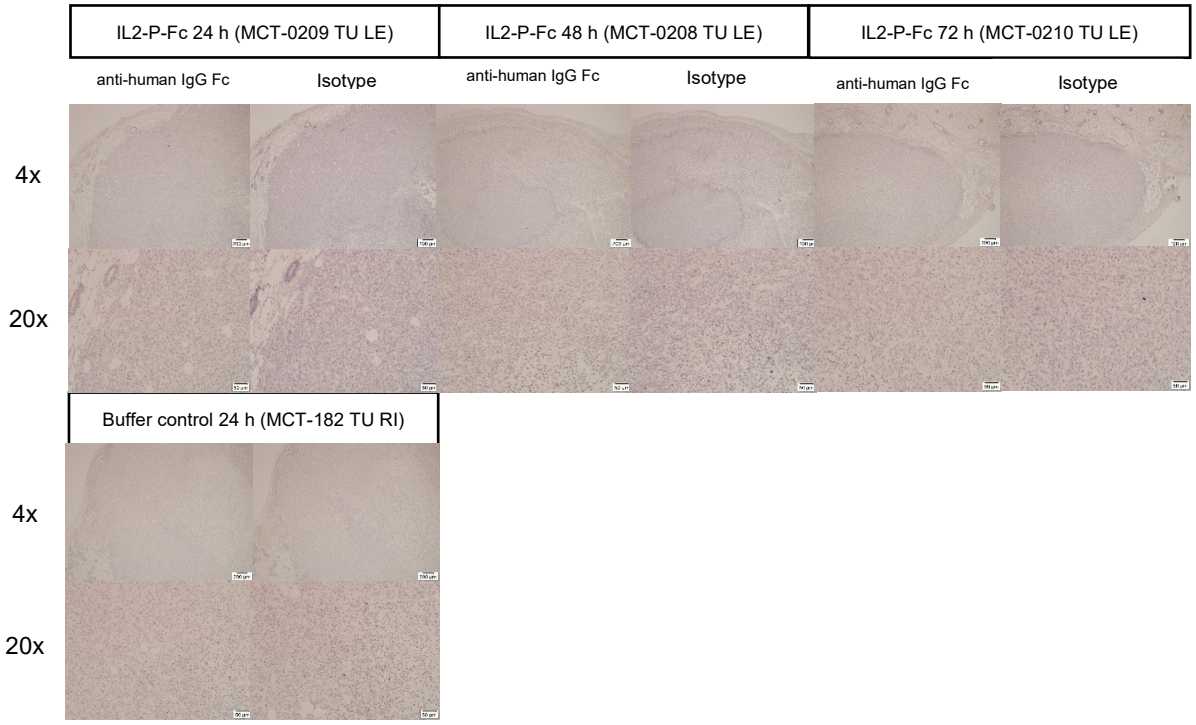

Figure 77 Overview of the staining to detect the Fc-part with 1:500 dilution of the AB and incubation 2 h at RT. *Scale bar: 200 µm and 50 µm; Magnification: 4x, 20x*

7.5.4. H&E staining

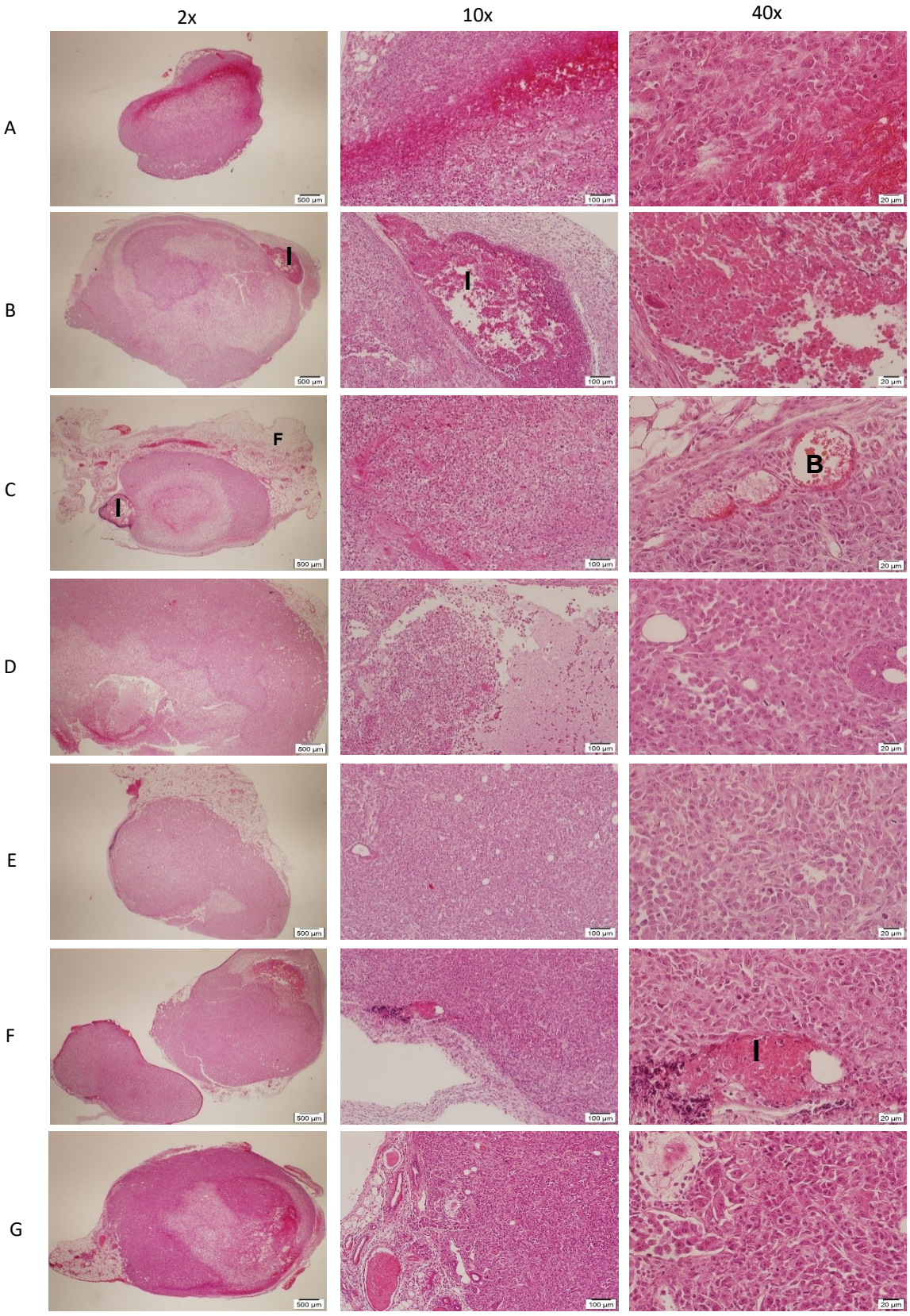

Figure 78 H&E staining of the tumor samples from the in vivo experiment 3 (I= site of injection; B=blood; F=fat tissue) *(A) tumor from IL2-P-Fc group 24 h after treatment (B) tumor from IL2-P-Fc group 48 h after treatment (C) tumor from IL2-P-Fc group 72 h after treatment (D+E+F) tumors containing the bb-mCherry transfection 24h (D), 48 h (E) and 72 h (F) post injection (G) tumor from buffer control group. Scale bar: 500µm, 100µm, 20 µm; Magnification: 2x, 10x, 40x*

8. Discussion

The main goal of this thesis was the optimization of IHC staining protocols for human CD47 and for luciferase in a xenograft tumor model and the histological evaluation of tumors transfected with a plasmid encoding for a secreted, CD47 binding SIPRα-Fc fusion protein.

First, the focus was on the optimization of a CD47 staining protocol. The first results with the polyclonal antibody (ab175388) targeted against CD47 showed a very unspecific and intense brown color development, not only on tumor cells, but also on muscle tissue. As the antibody reacts towards human and murine CD47, staining of murine, non-tumor tissue cannot be excluded. In humans, CD47 expression is found in histological specimens of brain, lymph nodes, urogenital tract and prostate (The human protein atlas). In mice similarly expression is found in brain, lower signal in other areas of the CNS, expression pattern is described, including expression in gut, thymus, but not in muscle (Gene Expression Database 2019). In the stainings presented in this work muscle cells were positive too. In addition, not just the cell membrane, but also the cytoplasm of the cells was stained in brown, which was not expected since CD47 is a transmembrane protein. At this time point we expected this to be a problem of the antibody showing cross reactivity to other antigens.

The next problem that occurred was a positive staining of the isotype showing the same intensity as the primary AB, but without primary antibody or isotype, no background signal was observed. This reduced the probability that background staining is due to unspecific binding/reactivity of the secondary reagents. Nevertheless, we compared two different detection systems, one was based on Avidin-Biotin and the other kit contained a polymer-based detection. We expected that the Avidin-Biotin based kit may enhance high non-specific background, because many tissues contain endogenous biotin (IHC world). However, we did not get more specific results.

We then tested two different monoclonal primary CD47 antibodies next, both specific for human CD47. One of them showed excellent staining results – the rabbit monoclonal anti CD47 primary antibody (ab218810) in the dilution 1:2000, which reacts only with human tissue, whereas the other mouse monoclonal AB (ab213079) showed negative staining. The monoclonal rabbit IgG isotype control and the Vectastain ABC kit as detection system were established in the CD47 protocol. With this monoclonal antibody it was clearly visible that only the membrane of the cell

was stained in an intense brown color. Nearly every tumor cell was stained specifically, which showed us that the CD47 protein is really overexpressed in this cell line also when growing as xenografts. In contrast, the tumor capsule, muscle tissue, collagen fibrils or other murine tissue were negative. Accordingly, the staining was very specific and reproducible, and it was possible to detect metastatic areas with high specificity.

The second part of this thesis was to detect the enzyme luciferase which was transduced into the cell line in vitro using a lentivirus encoding for luciferase-EGFP fusion protein (Su et al. 2013). In a former diploma thesis conducted in the MMCT lab, an optimal luciferase staining protocol characterizing similarly transduced murine 4T1 tumor cells was developed (Manuela Simlinger 2018). There, a polyclonal goat anti firefly luciferase antibody was used, which also showed cross reactivity towards other murine tissues, mainly smooth muscle cells, and it was suggested that it is reasonable to test a monoclonal one. It was difficult to find a suitable antibody targeted against firefly luciferase, because most of the monoclonal antibodies originated from mice. We worked with murine tissue, due to that there was always a problem of unspecific staining. The monoclonal AB testing will be continued in the MMCT further on, using a mouse on mouse detection kit.
We tried out other polyclonal antibodies, but we got high background staining (Fig. 19). That was the reason why we decided to stay with the goat polyclonal AB (ab181640) in the dilution 1:1000. In our case it does not matter that the antibody reacts with muscle tissue, because we stained only tumor tissue and muscle can be distinguished morphologically from tumor cells. With this AB we observed specific staining, which was comparable with the CD47 staining. In the same areas where we observed a positive CD47 signal, luciferase was positive too. Of course, the staining intensity differed distinctly, because luciferase is not that highly expressed as CD47, because only 70-80 % of the implanted cells were luciferase-positive.

Altogether, the CD47 and luciferase stainings from the first and second in vivo experiment showed very similar results since the experimental settings were similar. The results from the third experiment raised some questions. The left tumor of the IL2-P-Fc mouse, which was euthanized 24 hours after the treatment with the polyplexes showed less CD47 signal compared to the tumors harvested 48 h and 72 h after injection of the polyplexes. This could be explained with the circumstance that within

this time frame of 24 h post injection, CD47 is blocked by the SIRPα fusion protein leading to a lower signal of lower CD47 signal. Between the 48 h and 72 h group no significant difference was noticed. It seemed to be logical that after 48 h the effect declined and after approximately 72 h a new injection would be necessary. It is also possible, that the transfection/treatment did not work adequately for example in this tumor tissue 48 hours after transfection. Of note, in this experiment tumors were transfected in vivo by intratumoral injection of the plasmid (as a polyplex), and the transfection efficiency could vary between tumors.
This staining was repeated in the same way with the right tumors and this time there was no difference in the CD47 staining intensity visible. All the samples (24 h, 48 h, 72 h) appeared identical and this result is questionable. A possible reason therefore could be that the injection into the right tumor did not work adequately, which would explain that CD47 is not blocked at all. Otherwise it is possible that something happened during the staining procedure. To strengthen these results, this experiment must be performed again, preferably with all the samples together in one staining procedure to be sure that every step was performed in the same way.

Furthermore, a staining to detect the SIRPα-Fc fusion protein directly by using a primary antibody reactive for human IgG Fc-part of the fusion protein was performed. At first, we tried this experiment with samples from the first and second in vivo experiment where we expected negative staining, because at this stage, after approximately 4 weeks of tumor growth, there should not be a CD47 blockade detectable anymore. In fact, the staining was negative. The problem was, that we even had no positive tissue to compare.
Samples from the third in vivo experiment were tested twice, the first time the result was a positive staining which looked quite unspecific and the second time it was negative. Maybe the dilution 1:200 of the antibody was too low the first time. The second time we chose a higher dilution of 1:500 and did an incubation time of only 2 hours at RT, instead of approximately 17 hours overnight, and got negative staining results. If we expected any positive staining, we would expect it in the tumor tissue harvested 24 hours after the injection of the polyplexes containing the fusion protein, since at this time frame the intensity in the CD47 staining was less assuming blocking and binding of CD47 receptor by the SIRPα-Fc fusion protein.

In summary, we do not have a suitable working protocol yet. In that case a positive control would be necessary, e.g. an analysis of in vitro transfected cells. Moreover, it could be that it is not possible at all to detect the Fc-part using an immunohistochemical working protocol, since the concentration of the fusion protein bound to CD47 might be too low for detection. Another possibility to amplify the signal would be the use of a labeled secondary antibody. The antibody which was utilized was targeted against the Fc-part and already preabsorbed with HRP. This may also be a reason why it did not work, because with a low amount of the antigen it is often recommended to use an indirect detection system to enhance the signal.

H&E stainings were the prerequisite of every IHC staining, because interesting tumor areas and especially metastatic areas could be found easily and further analyzed with IHC. The searching of blood vessels was also possible with this staining.

In conclusion, the staining protocols for the detection of CD47 and luciferase were optimized for the MDA-MB-231 LM2-4 EGFP Luc cell line, but the staining to detect the Fc-part of the fusion protein did not work adequately.

Nevertheless, this work is an important input to the research of CD47, which indeed will be a big topic in cancer therapy in the next years. At least three antagonists of CD47 are currently in a phase I clinical trial tested in patients with hematological malignancies and solid tumors (Huang et al. 2017). Furthermore, the activation of M1 polarized macrophages by a knockdown of SIRPα is an interesting target in cancer therapy too as mentioned in “Tumor microenvironment”. If TAMs polarize to the other subtype of macrophages, the M1 macrophages, phagocytosis of the tumor cells might be enhanced (Lin et al. 2018). Immunotherapy is a promising therapy and will be certainly represented in the future cancer treatment.

9. References

1. abcam: Direct vs indirect immunofluorescence. https://www.abcam.com/secondary-antibodies/direct-vs-indirect-immunofluorescence

2. Ackerman, Margaret; Nimmerjahn, Falk (2013): Antibody Fc. Linking Adaptive and Innate Immunity. Burlington: Elsevier Science. http://gbv.eblib.com/patron/FullRecord.aspx?p=1337490.

3. ACROBiosystems (Hg.) (2017): Leukocyte Surface Antigen CD47. https://www.acrobiosystems.com/A1037-Leukocyte-Surface-Antigen-CD47.html

4. Amer, Magid H. (2014): Gene therapy for cancer: present status and future perspective. In: *Molecular and cellular therapies* 2, S. 27. DOI: 10.1186/2052-8426-2-27.

5. American Cancer Society (Hg.) (2007): Global Cancer Facts & Figures. https://www.cancer.org/content/dam/cancer-org/research/cancer-facts-and-statistics/global-cancer-facts-and-figures/global-cancer-facts-and-figures-2007.pdf

6. Aminah Kassem (2017): Evaluation of mCherry tagged SIRPα fusion protein in vitro, S. 19–20.

7. Biocompare (2014): FFPE or Frozen? Working with Human Clinical Samples. https://www.biocompare.com/Editorial-Articles/168948-FFPE-or-Frozen-Working-with-Human-Clinical-Samples/

8. Bray, Freddie; Ferlay, Jacques; Soerjomataram, Isabelle; Siegel, Rebecca L.; Torre, Lindsey A.; Jemal, Ahmedin (2018): Global cancer statistics 2018: GLOBOCAN estimates of incidence and mortality worldwide for 36 cancers in 185 countries. In: *CA: a cancer journal for clinicians*. DOI: 10.3322/caac.21492.

9. Breastcancer.org (Hg.) (2018): What Is Triple-Negative Breast Cancer? https://www.breastcancer.org/symptoms/diagnosis/trip_neg/behavior

10. Brown, E. (1990): Integrin-associated protein: a 50-kD plasma membrane antigen physically and functionally associated with integrins. In: *The Journal of Cell Biology* 111 (6), S. 2785–2794. DOI: 10.1083/jcb.111.6.2785.

11. Brown, E. (2001): Integrin-associated protein (CD47) and its ligands. In: *Trends in Cell Biology* 11 (3), S. 130–135. DOI: 10.1016/S0962-8924(00)01906-1.

12. Dana-Farber Cancer Institute (Hg.) (2018): How is Gene Therapy Being Used to Treat Cancer? https://blog.dana-farber.org/insight/2018/04/gene-therapy-used-treat-cancer/

13. Deutsches Ärzteblatt: Aktueller Stand der Gentherapie: Konzepte, klinische Studien und Zukunftsperspektiven. In: Deutsches Ärzteblatt, 93: A-2620–2628 1996 (41).

14. Eltoum, Isam; Fredenburgh, Jerry; Myers, Russell B.; Grizzle, William E. (2001): Introduction to the Theory and Practice of Fixation of Tissues. In: *Journal of Histotechnology* 24 (3), S. 173–190. DOI: 10.1179/his.2001.24.3.173.

15. Fredrick Griffith: Griffith's Mouse Experiment. Hg. v. Slide Player. https://slideplayer.com/slide/3495492/

16. Gene Expression Database (2019): CD47 antigen (Rh-related antigen, integrin-associated signal transducer). http://www.informatics.jax.org/gxd/marker/MGI:96617?tab=imagestab#gxd=markerMgiId%3DMGI:96617%26theilerStage%3D%26assayType%3D%26results%3D100%26startIndex%3D0%26sort%3D%26dir%3Dasc%26tab%3Dstagegridtab

17. Grivennikov, Sergei I.; Greten, Florian R.; Karin, Michael (2010): Immunity, inflammation, and cancer. In: *Cell* 140 (6), S. 883–899. DOI: 10.1016/j.cell.2010.01.025.

18. Holliday, Deborah L.; Speirs, Valerie (2011): Choosing the right cell line for breast cancer research. In: *Breast cancer research: BCR* 13 (4), S. 215. DOI: 10.1186/bcr2889.

19. Huang, Yuting; Ma, Yuchi; Gao, Peng; Yao, Zhi (2017): Targeting CD47: the achievements and concerns of current studies on cancer immunotherapy. In: *Journal of thoracic disease* 9 (2), E168-E174. DOI: 10.21037/jtd.2017.02.30.

20. a) IHC world: Blocking Endogenous Biotin. http://www.ihcworld.com/_technical_tips/biotin_tips.htm
    b) IHC world: Citrate Buffer Antigen Retrieval Protocol. http://www.ihcworld.com/_protocols/epitope_retrieval/citrate_buffer.htm
    c) IHC world: Introduction to Immunohistochemistry. http://www.ihcworld.com/_intro/tissue-prep.htm
    d) IHC world: Tris-EDTA Buffer Antigen Retrieval Protocol. http://www.ihcworld.com/_protocols/epitope_retrieval/tris_edta.htm

21. Jaiswal, Siddhartha; Jamieson, Catriona H. M.; Pang, Wendy W.; Park, Christopher Y.; Chao, Mark P.; Majeti, Ravindra et al. (2009): CD47 is upregulated on circulating hematopoietic stem cells and leukemia cells to avoid phagocytosis. In: *Cell* 138 (2), S. 271–285. DOI: 10.1016/j.cell.2009.05.046.

22. Kang, Yibin; Siegel, Peter M.; Shu, Weiping; Drobnjak, Maria; Kakonen, Sanna M.; Cordón-Cardo, Carlos et al. (2003): A multigenic program mediating breast cancer metastasis to bone. In: *Cancer cell* 3 (6), S. 537–549.

23. Kauder, Steven E.; Kuo, Tracy C.; Harrabi, Ons; Chen, Amy; Sangalang, Emma; Doyle, Laura et al. (2018): ALX148 blocks CD47 and enhances innate and adaptive antitumor immunity with a favorable safety profile. In: *PloS one* 13 (8), e0201832. DOI: 10.1371/journal.pone.0201832.

24. Krebsinformationsdienst (2017): Immuntherapien bei Krebs.. https://www.krebsinformationsdienst.de/behandlung/monoklonale-antikoerper.php

25. Krebsinformationsdienst (2018): Immuntherapie gegen Krebs: Die körpereigene Abwehr nutzen.. https://www.krebsinformationsdienst.de/wegweiser/iblatt/iblatt-immuntherapie.pdf

26. Lin, Yan; Zhao, Jun-Long; Zheng, Qi-Jun; Jiang, Xun; Tian, Jiao; Liang, Shi-Qian et al. (2018): Notch Signaling Modulates Macrophage Polarization and Phagocytosis Through Direct Suppression of Signal Regulatory Protein α Expression. In: Frontiers in immunology 9, S. 1744. DOI: 10.3389/fimmu.2018.01744.

27. Lindberg, F. P. (1993): Molecular cloning of integrin-associated protein: an immunoglobulin family member with multiple membrane-spanning domains implicated in alpha v beta 3-dependent ligand binding. In: *The Journal of Cell Biology* 123 (2), S. 485–496. DOI: 10.1083/jcb.123.2.485.

28. Lindberg, F. P.; Lublin, D. M.; Telen, M. J.; Veile, R. A.; Miller, Y. E.; Donis-Keller, H.; Brown, E. J. (1994): Rh-related antigen CD47 is the signal-transducer integrin-associated protein. In: *The Journal of biological chemistry* 269 (3), S. 1567–1570.

29. Liu, Xiaojuan; Kwon, Hyunwoo; Li, Zihai; Fu, Yang-Xin (2017): Is CD47 an innate immune checkpoint for tumor evasion? In: *Journal of hematology & oncology* 10 (1), S. 12. DOI: 10.1186/s13045-016-0381-z.

30. Maile, Laura A.; DeMambro, Victoria E.; Wai, Christine; Lotinun, Sutada; Aday, Ariel W.; Capps, Byron E. et al. (2011): An essential role for the association of CD47 to SHPS-1 in skeletal remodeling. In: *Journal of bone and mineral research: the official journal of the American Society for Bone and Mineral Research* 26 (9), S. 2068–2081. DOI: 10.1002/jbmr.441.

31. Manuela Simlinger (2018): In vitro, in vivo and ex vivo evaluation of a syngeneic murine lung cancer model 2018, S. 23–24; 57

32. Mescher, Anthony L. (Hg.) (2018): Junqueira's Basic Histology. pp 11-12. Indiana University School of Medicine. Fifteenth Edition. 15 Bände.

33. Morton, Christopher L.; Houghton, Peter J. (2007): Establishment of human tumor xenografts in immunodeficient mice. In: *Nature protocols* 2 (2), S. 247–250. DOI: 10.1038/nprot.2007.25.

34. Murata, Yoji; Saito, Yasuyuki; Kotani, Takenori; Matozaki, Takashi (2018): CD47-signal regulatory protein α signaling system and its application to cancer immunotherapy. In: *Cancer science* 109 (8), S. 2349–2357. DOI: 10.1111/cas.13663.

35. Nikiel, Barbara; Chekan, Mykola; Jarząb, Michal; Lange, Dariusz (2009): Endogenous avidin biotin activity (EABA) in thyroid pathology: immunohistochemical study. In: *Thyroid research* 2 (1), S. 5. DOI: 10.1186/1756-6614-2-5.

36. Oldenborg, P.-A. (2000): Role of CD47 as a Marker of Self on Red Blood Cells. In: *Science* 288 (5473), S. 2051–2054. DOI: 10.1126/science.288.5473.2051.

37. Oldenborg, Per-Arne (2013): CD47: A Cell Surface Glycoprotein Which Regulates Multiple Functions of Hematopoietic Cells in Health and Disease. In: *ISRN hematology* 2013, S. 614619. DOI: 10.1155/2013/614619.

38. Richards, John O.; Karki, Sher; Lazar, Greg A.; Chen, Hsing; Dang, Wei; Desjarlais, John R. (2008): Optimization of antibody binding to FcgammaRIIa enhances macrophage phagocytosis of tumor cells. In: *Molecular cancer therapeutics* 7 (8), S. 2517–2527. DOI: 10.1158/1535-7163.MCT-08-0201.

39. Richmond, Ann; Su, Yingjun (2008): Mouse xenograft models vs GEM models for human cancer therapeutics. In: *Disease models & mechanisms* 1 (2-3), S. 78–82. DOI: 10.1242/dmm.000976.

40. Rogers, Natasha M.; Sharifi-Sanjani, Maryam; Csányi, Gábor; Pagano, Patrick J.; Isenberg, Jeffrey S. (2014): Thrombospondin-1 and CD47 regulation of cardiac, pulmonary and vascular responses in health and disease. In: *Matrix biology: journal of the International Society for Matrix Biology* 37, S. 92–101. DOI: 10.1016/j.matbio.2014.01.002.

41. Stanford Medicine News center (2017): Fibrosis reversed when 'don't eat me' signal blocked. https://med.stanford.edu/news/all-news/2017/04/fibrosis-reversed-when-dont-eat-me-signal-blocked.html

42. Su, Baowei; Cengizeroglu, Arzu; Farkasova, Katarina; Viola, Joana R.; Anton, Martina; Ellwart, Joachim W. et al. (2013): Systemic TNFα gene therapy synergizes with liposomal doxorubicine in the treatment of metastatic cancer. In: Molecular therapy: the journal of the American Society of Gene Therapy 21 (2), S. 300–308. DOI: 10.1038/mt.2012.229.

43. Teng, Fei; Tian, Wen-Yan; Wang, Ying-Mei; Zhang, Yan-Fang; Guo, Fei; Zhao, Jing et al. (2016): Cancer-associated fibroblasts promote the progression of endometrial cancer via the SDF-1/CXCR4 axis. In: *Journal of hematology & oncology* 9, S. 8. DOI: 10.1186/s13045-015-0231-4.

44. Thavarajah, Rooban; Mudimbaimannar, Vidya Kazhiyur; Elizabeth, Joshua; Rao, Umadevi Krishnamohan; Ranganathan, Kannan (2012): Chemical and physical basics of routine formaldehyde fixation. In: *Journal of oral and maxillofacial pathology: JOMFP* 16 (3), S. 400–405. DOI: 10.4103/0973-029X.102496.

45. The human protein atlas: CD47 expression overview. https://www.proteinatlas.org/ENSG00000196776-CD47/tissue

46. Thermo Fisher Scientific: Cell culture flasks | Tissue culture flasks. [Web] https://www.thermofisher.com/uk/en/home/life-science/cell-culture/cell-culture-plastics/cell-culture-flasks.html

47. Tournoy, K. G.; Depraetere, S.; Pauwels, R. A.; Leroux-Roels, G. G. (2000): Mouse strain and conditioning regimen determine survival and function of human leucocytes in immunodeficient mice. In: *Clin Exp Immunol* 119 (1), S. 231–239. DOI: 10.1046/j.1365-2249.2000.01099.x.

48. VitroVivo Biotech (Hg.): Polymer Based 1-Step IHC System. https://vitrovivo.com/product-category/immunostain-detection-system/polymer-based-1-step-ihc-system/

49. Willingham, Stephen B.; Volkmer, Jens-Peter; Gentles, Andrew J.; Sahoo, Debashis; Dalerba, Piero; Mitra, Siddhartha S. et al. (2012): The CD47-signal regulatory protein alpha (SIRPa) interaction is a therapeutic target for human solid tumors. In: *Proceedings of the National Academy of Sciences of the United States of America* 109 (17), S. 6662–6667. DOI: 10.1073/pnas.1121623109.

50. World Cancer Research Fund International (Hg.) (2018): Breast cancer statistics. https://www.wcrf.org/dietandcancer/cancer-trends/breast-cancer-statistics

51. Yang, Li; Zhang, Yi (2017): Tumor-associated macrophages: from basic research to clinical application. In: *Journal of hematology & oncology* 10 (1), S. 58. DOI: 10.1186/s13045-017-0430-2.